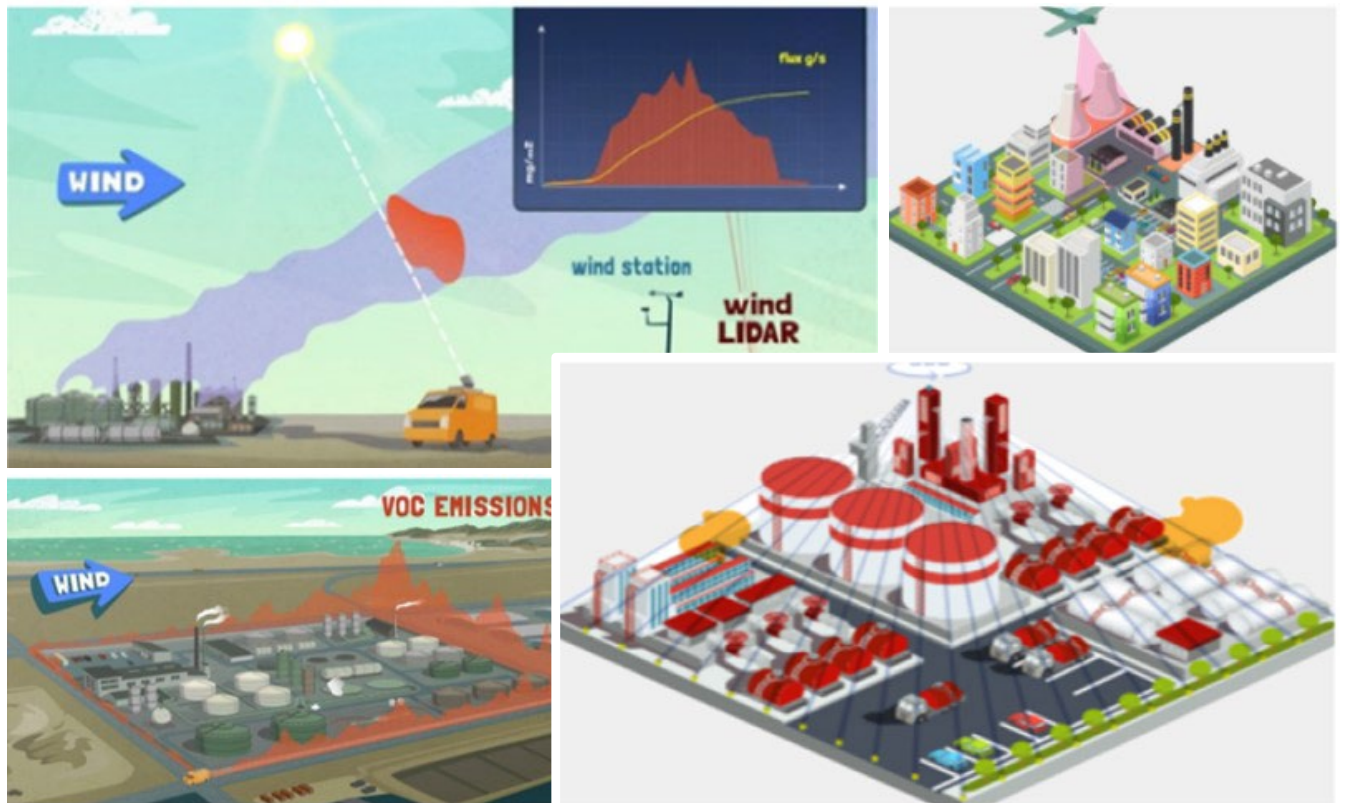

MULTIPLE AIR TOXICS EXPOSURE STUDY V: ADVANCED MONITORING OF REFINERIES



Contents

1.	Executive Summary.....	4
2.	Introduction and Overview of the MATES V Advanced Monitoring Project.....	6
3.	Optical Remote Sensing Mobile Laboratory	8
3.1.	Instrumentation and Setup.....	8
3.2.	2015 Pilot Study	11
3.3.	Performance Evaluation of ORS ML.....	12
3.3.1.	ORS ML Intercomparison	12
3.3.2.	Stability Testing of Onboard Instruments.....	13
3.4.	Refinery Emission Estimates	15
3.5.	Refinery Fenceline and Community Monitoring.....	17
4.	Optical Tent.....	20
4.1.	Instrumentation and Setup.....	20
4.2.	Optical Tent Performance Evaluation.....	25
4.3.	Results.....	26
4.3.1.	Characteristics of BTEX Detections	26
4.3.2.	Statistical Analysis of BTEX Detections	30
4.3.3.	Influence of Local Meteorology on BTEX Observations.....	31
4.4.	Advantages of the Optical Tent Compared to Fenceline Monitoring.....	32
5.	Hyperspectral Aerial Measurements	34
5.1.	Instrumentation and Setup.....	34
5.2.	Detection Limits of Aerial Hyperspectral Imaging	36
5.3.	Re-analysis of Historical Archive	37
5.4.	Coordinated Flight Series.....	39
5.4.1.	LAX/El Segundo/Manhattan Beach Domain	41
5.4.2.	San Bernardino Area	43
5.4.3.	Carson/Wilmington/Long Beach Area	44
5.4.4.	Central and East Los Angeles Area.....	47
5.5.	Vehicular Emissions.....	49
6.	Conclusions	50
7.	References	52
8.	Appendices.....	55

8.1.	Histograms of Optical Tent BTEX Retrieval Errors.....	55
8.2.	COIs and Associated Mako MDQs.....	57
8.3.	Summary of Historical Data Over L.A. Refineries and Related Sites.....	58
8.4.	Summary of Data Collected During MATES V Flights.....	62
8.5.	Technical Reports Addendum Asset Summaries (TRAAS)	64
8.6.	Controlled Release	76
8.6.1.	Toluene Test Release	76
8.6.2.	Benzene Test Release	77

1. Executive Summary

Overview

The Multiple Air Toxics Exposure Study V (MATES V) is a monitoring and analysis study conducted in the South Coast Air Basin (Basin). The study is a follow up to previous air toxics studies in the Basin and is part of the South Coast Air Quality Management District (South Coast AQMD) Governing Board Environmental Justice Initiative. During the Advanced Monitoring portion of the MATES V study, multiple advanced optical remote sensing (ORS) techniques were evaluated for their capabilities to monitor air toxic emissions from refineries, and assess the potential community impact of these emissions. ORS measurements were conducted at and near refineries, and in communities of Carson, Wilmington, and Long Beach using three different methods and approaches, namely: 1) mobile monitoring using ORS technologies installed aboard South Coast AQMD's ORS Mobile Laboratory (ORS ML); 2) refinery fenceline monitoring using an optical tent based on Open Path Differential Optical Absorption Spectroscopy (DOAS); and 3) aerial hyperspectral thermal-infrared imaging. The motivation behind these enhanced monitoring efforts is to better characterize air toxics levels in highly impacted areas, to provide higher resolution air quality data, and to better understand emissions from petroleum refineries.

Mobile Monitoring Surveys Using ORS Technologies

In July of 2019, an optical remote sensing mobile laboratory (ORS ML) was purchased by South Coast Air Quality Management District (South Coast AQMD) for the purpose of conducting mobile monitoring surveys. The ORS ML can be used to estimate refinery emissions of volatile organic compounds (VOCs) and other pollutants from industrial sources in real-time, and for measurements of ground level concentrations of total alkanes, benzene, and other selected air toxics. During this study, ground level concentration measurements of total alkanes and benzene near refinery fencelines, and within adjacent communities, were analyzed to identify locations with recurring air pollution levels above background levels. The mobile monitoring surveys showed that the areas of enhanced VOC concentrations were located primarily at refinery fencelines, and near other local sources of air pollution such as tank farms and gas stations. Enhancements above background levels were less common away from refinery fencelines and other local sources of air pollution. In addition to concentration mapping, the emission estimation capability of ORS ML was also demonstrated by conducting a total of 59 refinery emission estimates at six refineries in the Basin between July 3, 2019 and May 5, 2020, with five of those facilities located in Carson, Wilmington, and Long Beach environmental justice communities. The emission estimates collected during this study are consistent with other similar measurements conducted by South Coast AQMD and identify the ORS ML as a powerful leak detection tool at and near refinery fencelines, and for understanding the spatial distribution of these pollutants within adjacent communities. These unique capabilities make ORS ML a valuable asset for a variety of applications ranging from community air monitoring, emission investigations, and compliance projects.

Refinery Air Monitoring Using an Optical Tent

An optical tent based on multiple open path DOAS instruments was installed at one of the major refineries in the Basin, and has been in continuous operation since August 2020. The "optical tent" concept utilizes open path ORS technology, extending inward toward the center of the refinery, for near real-time monitoring of pollutants not only along the fenceline, but also in the air over the refinery. The

optical tent configuration consists of 10 open paths, with an average path length of about 600 meters. This arrangement offers spatially denser coverage of the refinery in comparison to a more “traditional” fenceline air monitoring approach, where open path systems are installed only along the refinery fenceline. An analysis of the optical tent data showed increased concentrations of air toxics such as benzene, toluene, ethylbenzene, and xylenes (BTEX) over the tank farm portion of the refinery; with enhanced BTEX levels detected more frequently than at the refinery fenceline. The results suggest that an optical tent system is a very effective tool for identifying the processes and location(s) within the refinery where fugitive emissions originate, sometimes before the pollution plumes reach the facility fenceline. Although challenging to quantify directly, this study also suggests that the real-time measurements provided by the optical tent helped decrease the time required by the refinery operator to address and resolve unintended releases of BTEX. These observations underscore the optical tent’s effectiveness in managing unwanted releases within a facility.

Aerial Measurements Using Hyperspectral Thermal-Infrared Imaging

An airborne hyperspectral thermal infrared whiskbroom imaging spectrometer, named Mako, designed and built by The Aerospace Corporation, mounted aboard a Twin Otter aircraft, was used to conduct aerial measurement surveys over selected regions of the Basin. Four flight surveys were conducted from July 9th to July 12th, 2019, over refineries and neighboring communities in Carson, Wilmington, Long Beach, El Segundo, and over other industrial emission sources in Los Angeles and San Bernadino. An analysis of the spectral images taken over the refineries showed that gas detection was dominated by ammonia and methane plumes, and also a hydrogen sulfide plume was detected over one of the refineries. BTEX plumes were generally not detected, likely due to lower concentrations of these compounds in emission plumes, relative to other commonly emitted pollutants (e.g., methane or ammonia). These aerial measurements demonstrated the capabilities of aircraft-based hyperspectral imaging to detect emissions from various industrial activities (e.g., port of LA/Long Beach, multiple refineries, and oil wells).

Lessons Learned

The ORS techniques used in this project offer different advantages that make them attractive options for various air monitoring applications. Aerial based hyperspectral measurements have the ability to quickly survey large geographical areas with high spatial resolution in a relatively short period of time (i.e., days), and measurements can be made in areas that are not accessible with ground-based monitoring. However, the results from this study indicate that hyperspectral imaging may not provide the sensitivity required to detect BTEX at concentrations typically measured near refineries. In addition, these measurements are usually too expensive for routine air monitoring.

When compared to the aircraft-based measurements, the two ground-based ORS approaches were more effective at detecting refinery BTEX and other air toxic plumes. Furthermore, the ORS ML is a feasible and cost-effective approach for conducting routine surveys at facility fencelines and within nearby communities. The optical tent approach allows for continuous measurements of BTEX and other air toxics in real-time, however, measurements are limited to the fenceline and within the refinery perimeter. Measurements of this type are useful for informing refinery operators, air quality agencies, and communities of potential leaks.

2. Introduction and Overview of the MATES V Advanced Monitoring Project

This report presents the results of the Advanced Monitoring portion of the 5th MATES project (MATES V) conducted between summer 2019 through summer 2022, aimed at assessing the capabilities of optical remote sensing (ORS) technologies for air toxics monitoring applications. The South Coast AQMD's MATES studies are designed to evaluate health risk associated with exposure to toxic air pollution within communities in the Basin (South Coast AQMD, 2021). This report focuses on the deployment and implementation of three advanced air monitoring technologies for monitoring VOCs and selected air toxics in or near petroleum refineries (see Figure 1), namely: 1) ORS measurements on a mobile platform; 2) an optical tent based on open path Differential Optical Absorption Spectroscopy (DOAS) covering a single petroleum refinery; and 3) aircraft-based hyperspectral thermal-infrared imaging measurements above petroleum refineries. This report discusses the methodology, measurement approaches, and major findings of these three novel technologies.

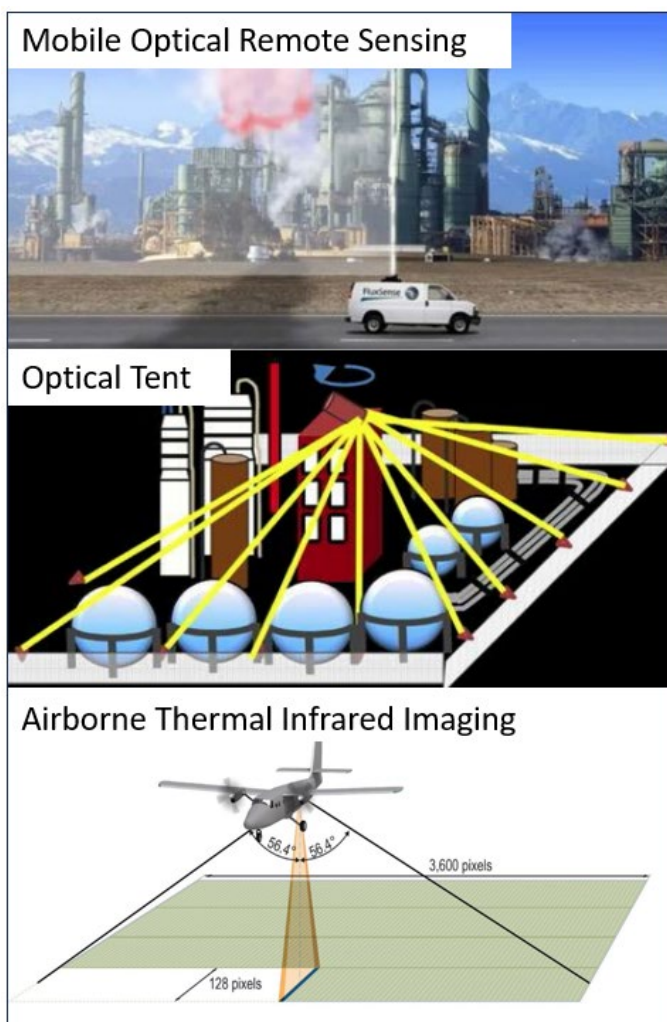


Figure 1. Schematics of the three advanced air monitoring technologies employed in this study.

Mobile ORS is a novel vehicle-based approach using ultraviolet (UV) and infrared (IR) spectrometers mounted inside a vehicle to measure vertical columns (i.e. abundance of a given pollutant in the air above ground) and ground level concentrations (i.e., concentrations of pollutants near the ground) of multiple gases including total alkanes, sulfur dioxide, nitrogen dioxide, BTEX (benzene, toluene, ethylbenzene, and xylenes), and other air pollutants. This measurement approach can be used to conduct air pollutants concentration mapping, enhanced leak detection, and to obtain emission estimates from petroleum refineries or other industrial facilities in real-time. The data can be used to identify pollution hotspots, better understand the levels of pollution in areas adjacent to industrial facilities, and improve the overall understanding of sources and magnitudes of industrial emissions.

The “optical tent” concept utilizes open path ORS technology for near real-time monitoring of BTEX emissions from a stationary area source. This unique technology operates continuously (24 hours a day, seven days a week) and allows for the characterization of long-term emissions from a source. It also provides near real-time data to evaluate emissions during different times of the day and can also help the facility operator identify leaks quickly. The data provided by the optical tent, in conjunction with flight measurements, mobile measurements, and meteorological data, can help identify potential air toxics impacts in communities surrounding the facility of interest. For the purpose of this Advanced Monitoring Project for MATES V, an optical tent system was developed and implemented by University of California Los Angeles (UCLA) at one of the seven major refineries in the Basin. Here we examine the data generated from this system to assess the major strengths, weaknesses, and feasibility for long term monitoring.

The Aerospace Corporation (El Segundo, CA) uses a state of the art hyperspectral thermal-infrared imaging system mounted inside an aircraft to conduct air pollution measurements including BTEX, SO₂, and NO₂, over large areas. One of its main advantages is its ability to identify potential emission sources and pollution hot-spots that otherwise would take a longer time to discover with ground-based measurements. Aerospace Corporation has been conducting flight-based measurements in the Los Angeles Air Basin since 2010, including the region containing seven major petroleum refineries and other industrial facilities within the Basin. These flight measurements also assisted in the selection of locations for enhanced ground-based monitoring and mobile measurements using South Coast AQMD’s ORS mobile laboratory. Overall, the data obtained from flight-based measurements can enhance the analysis of traditional air toxics monitoring and emissions estimates in the Basin.

3. Optical Remote Sensing Mobile Laboratory

3.1. Instrumentation and Setup

Based on the encouraging results from previous technology demonstration studies (South Coast AQMD, 2017), South Coast AQMD commissioned the construction of an optical remote sensing mobile lab (ORS ML), which was delivered in June 2019. The ORS ML (designed and built by FluxSense, Inc.) is equipped with four optical instruments (detailed in Table 1, Figure 2). Two of these instruments are configured as closed cell systems whereby ambient air is continuously pumped through a closed glass cell. In this configuration, when air passes through the cell, Differential Optical Absorption Spectroscopy (DOAS) and Fourier Transform Infrared Spectroscopy (FTIR) are performed with active light sources using an ultraviolet (UV) spectrometer and a FTIR spectrometer, respectively, to obtain concentrations of pollutants in the air. This approach and configuration produce concentration measurements at approximately 0.1 Hz and 0.25 Hz time resolution for the FTIR and UV optical cells, respectively. These measurements are referred to as Mobile Extractive DOAS (MeDOAS) and Mobile Extractive FTIR (MeFTIR). Additional FTIR and UV-DOAS spectrometers onboard the ORS ML are configured to perform spectroscopy on IR and UV radiation from sunlight referred to as Solar Occultation Flux (SOF) and Sky DOAS measurements, respectively. These optical remote sensing configurations result in vertical column measurements (i.e., abundance of a given pollutant in the air above ground through the top of the atmosphere) at ~ 0.5 Hz time resolution. Additional details of the configuration and operation of the four spectrometers and data processing is given in Table 1.

Table 1. Technical Summary of the Four Spectroscopic Methods Used in the ORS ML

Measurement Name	Spectrometer Type	Remote/Extractive	Resulting Measurements	Gases Measured	Detection Level
Solar Occultation Flux	FTIR	Remote	Emission estimates	Total Alkanes	0.1-5 mg/m ²
Mobile Extractive FTIR	FTIR	Extractive	Ground level concentrations	Total Alkanes, Methane, Propane, Butane...	1-10 ppb
Sky DOAS	UVDOAS	Remote	Emission estimates	SO ₂ , NO ₂ , HCHO	0.1-5 mg/m ²
Mobile Extractive DOAS	UVDOAS	Extractive	Ground Level concentrations	Benzene, Ethylbenzene, Toluene, Xylenes	0.5-3 ppb

The SOF can estimate the flux of total alkanes from industrial facilities, including petroleum refineries (e.g., Mellqvist et al., 1999; 2008 a and b; 2009; 2010). Measurements are conducted by directing sunlight into an FTIR spectrometer via a solar tracker and a series of mirrors (Figure 3). Path integrated vertical columns of total alkanes are analyzed by fitting theoretical spectra to the collected solar spectra via an algorithm utilizing the wavelength dependent cross sections of specific gases (Rothman et al. 2003; Sharpe et al. 2004). Details of the spectral retrieval and fitting method can be found in Mellqvist et al. (2010) and Griffith (1996). The data collected is geotagged via an onboard GPS and displayed on a digital map in real-time.

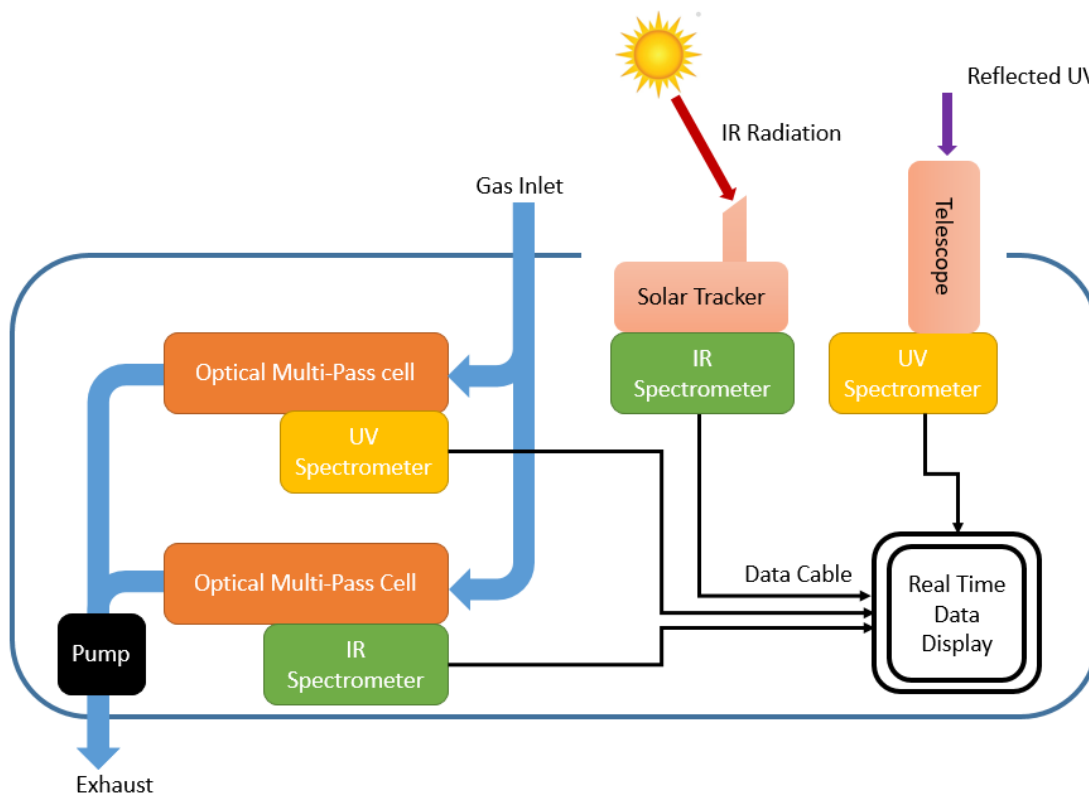


Figure 2. Schematic of ORS ML.



Figure 3. Picture of the solar occultation flux (SOF) instrument mounted inside the ORS ML.

The Sky DOAS operates by collecting scattered ultraviolet-visible (UV-Vis) light to measure vertical columns of NO_2 , SO_2 , and formaldehyde. UV-Vis light is collected with an upward looking telescope directed through a fiber optic cable to a grating spectrometer where the spectral analysis occurs between 290 and 470 nm (Figure 4). An algorithm fits theoretical spectra to the measured spectra using wavelength dependent cross sections using the DOAS technique (Platt and Stutz, 2008).



Figure 4. Picture of the SkyDOAS telescope mounted inside the ORS ML.

A MeFTIR (Figure 5) instrument (Galle et al., 2001; Börjesson et al., 2009) is used to measure ground level concentrations of alkanes. Ambient air is drawn through a closed cell at 50-80 liters per minute (lpm) while IR light is passed through the sample volume via curved mirrors resulting in a total path length of 100 meters. The light beam is then directed into an FTIR spectrometer where light is detected with Indium-Antimonide (InSb) and Mercury-Cadmium-Telluride (MCT) detectors. Light is detected in the 2.5-5.5 μm region via the InSb detector and the 8.3-13.3 μm region via the MCT detector. The spectral analysis uses wavelength dependent absorption cross sections published in the high-resolution transmission molecular absorption database (HITRAN) and Pacific Northwest National Laboratory (PNNL) database (Rothman et al. 2003; Sharpe et al. 2004) of atmospheric constituents. These cross sections are combined in spectral fitting to calculate pollutant concentrations. See Griffith (1996) for a detailed discussion of the gas phase infrared spectral analysis.

The spectral analysis is conducted in real-time and the resulting gas concentrations are displayed on a digital map which is visible to the operators of the ORS ML.

The instrument is capable of measuring ppb level concentrations of total VOC as total alkanes and selected speciated VOCs. In addition, the ratios of individual gases (propane, butane, etc.) to total VOC ($C_{gas}/C_{total\ voc}$) is also used in combination with SOF measurements to estimate the flux of individual gases (Equation 1).

$$Q_{gas} = \frac{C_{gas}}{C_{Total\ VOC}} \cdot Q_{total\ VOC\ SOF} \quad \text{Equation 1}$$

In Equation 1, Q_{gas} is the flux of a gas, C_{gas} and $C_{total\ VOC}$ are the ground level concentrations of a gas and total VOCs measured by the MeFTIR, and $Q_{total\ VOC\ SOF}$ is the flux of total alkanes measured by the SOF.

A MeDOAS is used to measure ground level concentrations of BTEX compounds. Ambient air is pumped continuously through a 25 L closed cell at \sim 50-80 liters per minute. UV light is generated by a xenon

lamp and directed to the sample volume via an optical fiber. The light beam is passed through the sample via a curved mirror system resulting in a path length of 100 meters. The light exits the cell and is brought to an UV spectrometer via fiber optic cable. The spectrometer uses a grating surface and a charged-coupled device (CCD) camera (1024 x 1024 pixel array) to disperse and detect light. The spectral analysis occurs in the 255-285 nm region and the compounds fitted include O₃, SO₂, O₂, toluene, benzene, 1,3,5-trimethylbenzene, 1,2,4-trimethylbenzene, styrene, phenol, p-xylene, m-xylene, and ethylbenzene (Burrows et al. 1999; Bogumil et al. 2003; Fally et al. 2009; Etkorn et al. 1999) using the DOAS technique (Platt and Stutz, 2008). The spectral analysis occurs in real-time and the resulting gas measurements are displayed on a digital map which is viewable by the operators of the ORS ML.

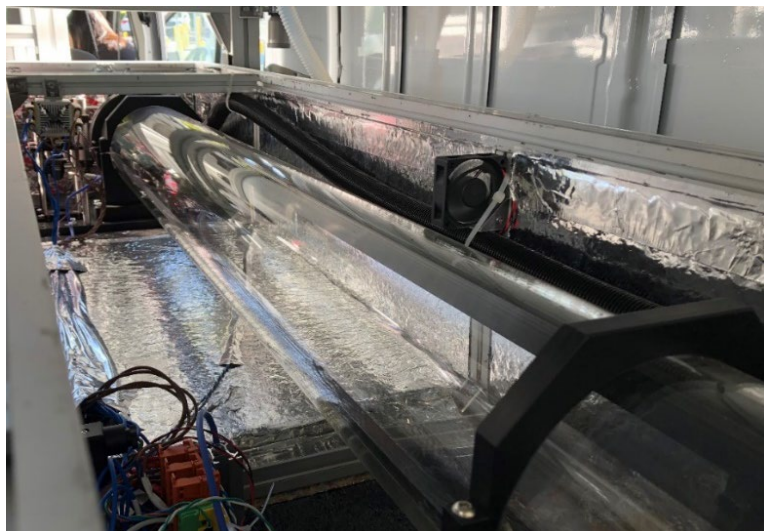


Figure 5. Picture of the extractive cell associated with the MeFTIR mounted inside the ORS ML.

The measurements from the MeDOAS are also used in combination with MeFTIR measurements of total alkanes and SOF flux measurements of total alkanes to calculate inferred fluxes of BTEX in the same way as described for the MeFTIR (Equation 1).

3.2. 2015 Pilot Study

In the Fall of 2015, South Coast AQMD conducted a comprehensive technology demonstration study evaluating several ORS monitoring approaches for a variety of air quality applications, including fenceline monitoring, leak detection, and emission quantification (<http://www.aqmd.gov/ors-study>). During this study Mobile ORS was identified as a useful, versatile, and feasible tool for a variety of air quality, community impact, and emission monitoring applications. However, the dataset from this pilot study was small and significantly more measurements are necessary for a more meaningful evaluation of the Mobile ORS measurement technique. The Advanced Monitoring portion of MATES V builds on this pilot study by using and comparing (when appropriate) the strengths and limitations of three ORS air monitoring techniques (i.e., mobile ORS measurements, an open path optical tent, and aerial based hyperspectral thermal-infrared imaging) for monitoring of air toxic emissions from refineries and assessing their potential community impact.

3.3. Performance Evaluation of ORS ML

3.3.1. ORS ML Intercomparison

The performance of the new ORS ML (built for South Coast AQMD by FluxSense, Inc.) was evaluated through an intercomparison with another established ORS ML operated by FluxSense, Inc. The ORS ML operated by FluxSense, Inc. was used during the 2015 pilot study, where it demonstrated the ability to produce data of sufficient accuracy, precision and overall quality. These measurements were made in a real-world scenario by simultaneously sampling an emission plume from an oil well located in Long Beach, CA. This location was chosen because VOCs emissions could be easily sampled from a publicly accessible road, given the prevailing southerly winds (Figure 6). Minimal vehicle traffic on that isolated street also allowed the two ORS-MLs to sample the emission plume while driving as slow as possible.



Figure 6. Satellite Image of the well site used for field acceptance testing of ORS ML.

Measurements were conducted on July 2, 2019. The two mobile laboratories were driven together at a slow and steady pace multiple times through the emission plume while the onboard instrumentation was in operation. Data from both mobile laboratories was used to qualitatively compare each instrument contained in South Coast AQMD's ORS ML to its corresponding instrument in FluxSense's ORS ML.

The two ORS MLs made seven transects across the emission plume from the oil well (Figure 6). The data from the MeDOAS, MeFTIR, and SOF instruments indicate that the emission plume was successfully sampled by both ORS ML vehicles (Figure 7). In general, the concentrations and columns measured in the plume between the two vans were in reasonable agreement. However, there were a few instances where the two vans measured different concentrations in the plume, specifically with the MeFTIR and MeDOAS instruments. We note that the emission plume was sampled very close to the emission source (~10 m) where small variations in wind direction and speed will have a large impact on the plume trajectory and dilution rate. This, combined with sequential sampling done by the mobile laboratories, are the likely cause for the few instances of disagreement between the two ORS-MLs. For benzene measurements, the difference was possibly also influenced by inherent differences in the sampling method of the MeDOAS instruments aboard the two ORS MLs. The FluxSense ORS ML DOAS system is mounted on the roof of the vehicle, resulting in an immediate response to changes in ambient

concentrations. The South Coast AQMD MeDOAS instrument is installed inside the van and thus air is sampled via a roof-mounted inlet, resulting in a step response time of a few seconds. Sampling a spatially confined plume close to the source, as in the test site, combined with a slower response instrument can attenuate the peak concentrations if the sample period is smaller than the intrinsic response of the instrument.

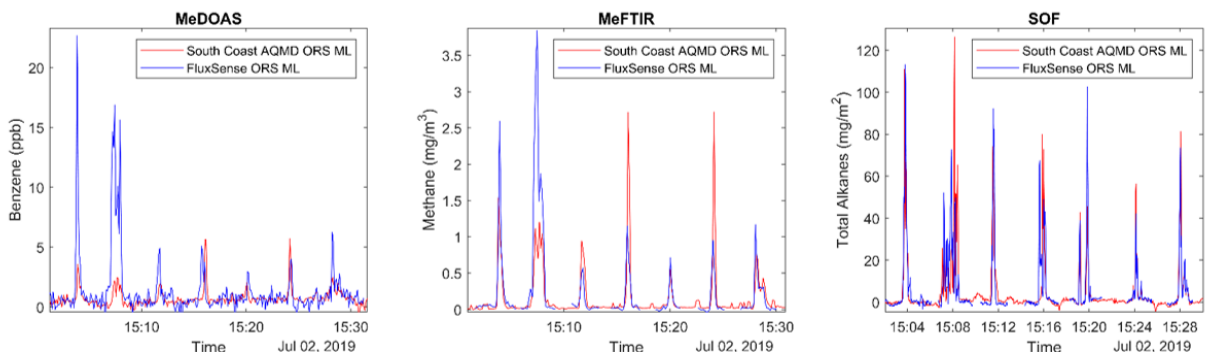


Figure 7. Time series plots showing benzene measured by MeDOAS (left panel), Methane measured by MeFTIR (middle panel), and Total Alkanes measured by SOF (right panel) for the South Coast AQMD ORS ML (red lines) and the FLuxSense ORS ML (blue lines).

3.3.2. Stability Testing of Onboard Instruments

Stability tests for instruments onboard the South Coast AQMD ORS ML were performed on December 7, 2019, for the MeDOAS and MeFTIR instruments; and on December 9, 2019, for the SkyDOAS and SOF instruments at the north-west parking lot of Summitridge Park in Diamond Bar, CA, under “clean air” conditions. For this test, standard deviations (SD) of “clean air” measurements collected over several time periods, each lasting 10-15 minutes, were compared with the test acceptance criteria recommended by the equipment manufacturer. The results of this test are summarized in Table 2, demonstrating that all instruments met the acceptable standard deviation criteria.

Table 2. Standard Deviation (SD) of measurements conducted by South Coast AQMD ORS ML for stability test. Acceptable SC values are based on manufacturer's specifications.

Instrument	Test series #	1	2	3	4	5	6	Test mean SD	Acceptable SD
SOF	<i>Time:</i>	<i>Dec 9, 13:04</i>	<i>Dec 9, 13:17</i>	<i>Dec 9, 13:28</i>	<i>Dec 9, 13:54</i>	<i>Dec 9, 14:05</i>	<i>Dec 9, 14:19</i>		
	Alkanes SD (mg/m²)	0.28	0.34	0.36	0.3	0.45	0.44	0.4	4
SkyDOAS	<i>Time:</i>	<i>Dec 9, 13:12</i>	<i>Dec 9, 13:28</i>	<i>Dec 9, 13:43</i>	<i>Dec 9, 13:54</i>	<i>Dec 9, 14:05</i>	<i>Dec 9, 14:19</i>		
	NO₂ SD (mg/m²)	0.52	0.53	0.45	0.47	0.47	0.51	0.5	2
	SO₂ SD (mg/m²)	1.49	1.45	1.67	1.77	1.85	1.93	1.7	4
	HCHO SD (mg/m²)	0.53	0.46	0.5	0.45	0.48	0.48	0.5	2
MeFTIR	<i>Time:</i>	<i>Dec 7, 15:19</i>	<i>Dec 7, 15:33</i>	<i>Dec 7, 15:45</i>	<i>Dec 7, 15:57</i>				
	Alkanes SD (µg/m³)	3.78	7.02	4.82	4.66			5.1	19
MeDOAS	<i>Time:</i>	<i>Dec 7, 13:21</i>	<i>Dec 7, 14:10</i>	<i>Dec 7, 14:22</i>					
	Benzene SD (µg/m³)	4.2	4.05	4.56				4.3	5
	Toluene SD (µg/m³)	5.61	18.11	16.94				13.6	17
	p-Xylene SD (µg/m³)	4.13	5.12	6.2				5.2	7

3.4. Refinery Emission Estimates

Between July 3rd, 2019, and May 5th, 2020, SOF instrumentation was utilized to complete 59 total alkane emission estimates around six of the seven major Basin refineries. A satellite image containing the six refineries sampled in this report is displayed in Figure 8, and an example of an individual transect is displayed in Figure 9. The resulting emission estimates of total alkanes conducted during this study are summarized in Table 3. These estimates were comparable with those previously conducted during the earlier technology demonstration study (South Coast AQMD, 2017).

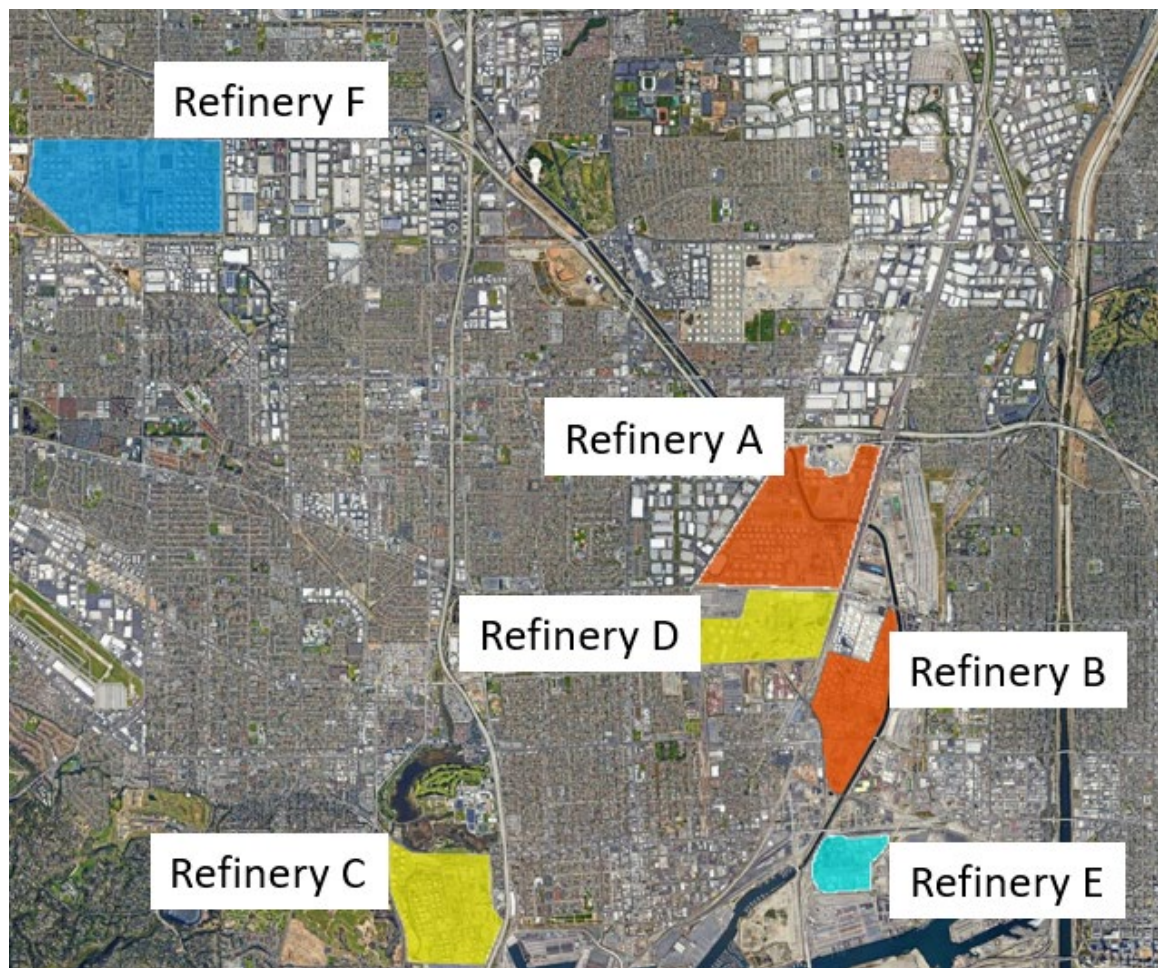


Figure 8. Satellite image of the area containing the six refineries sampled in this report.

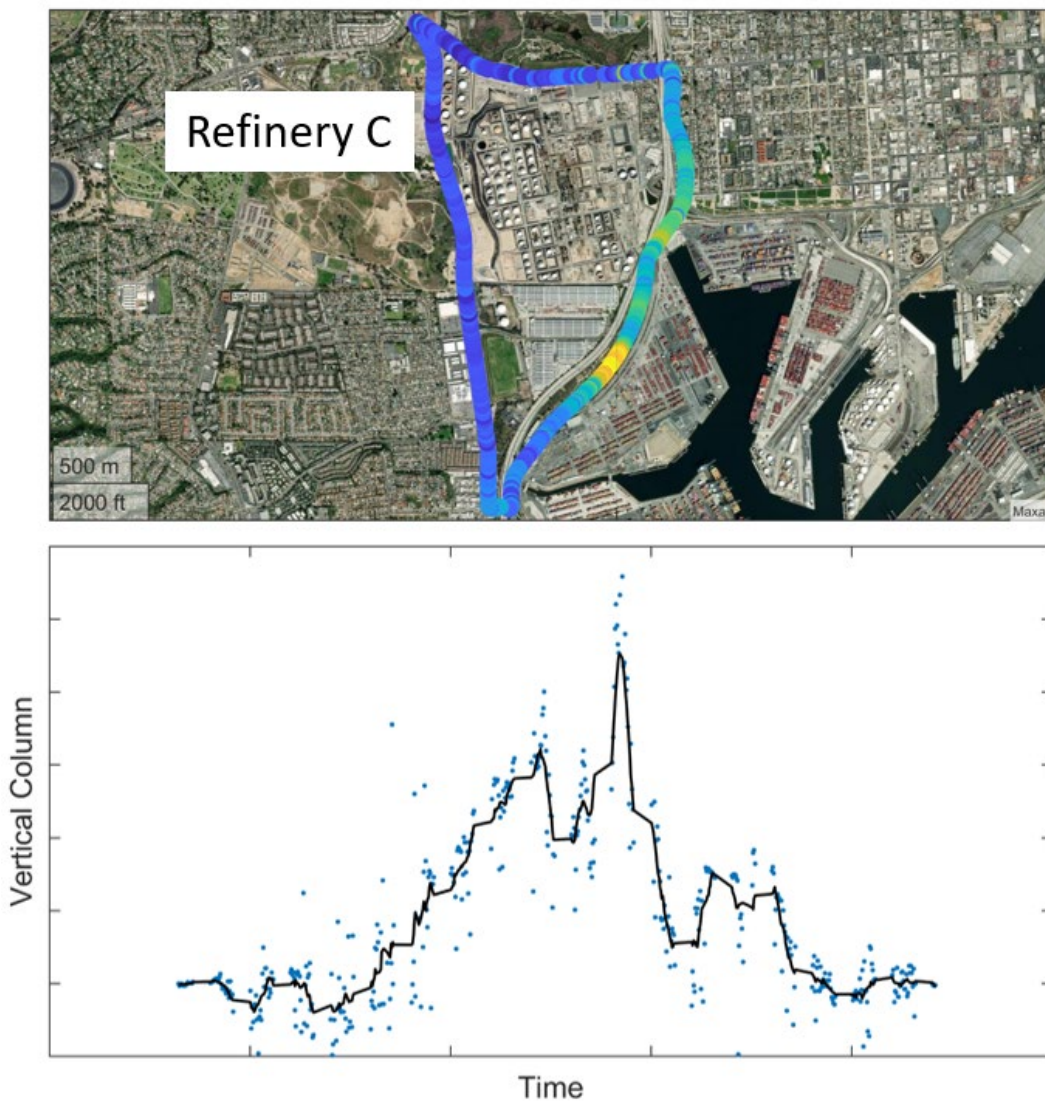


Figure 9. Example of an emission estimate transect around Refinery C conducted on July 11, 2019. The top panel shows measured total alkanes vertical columns (in mg/m^2) collected during a transect overlaid on satellite imagery. The bottom panel shows the total alkanes vertical columns displayed as a time series, with the raw data shown in blue scatter, and a 30 second rolling average shown with a black solid line.

Table 3. Summary of total alkanes refinery emission estimates conducted with the ORS ML in this study.

Refinery	Estimated Mean (kg hr^{-1})	Estimated Median (kg hr^{-1})	Standard Deviation (kg hr^{-1})	Number of Measurements
Refinery A	239	139	257	11
Refinery B	172	187	69	15
Refinery C	149	154	102	13
Refinery D	62	62	38	2
Refinery E	101	98	77	16
Refinery F	604	604	135	2

3.5. Refinery Fenceline and Community Monitoring

In order to evaluate the utility and usefulness of ORS ML for fenceline and community air monitoring, ground level concentration measurements of total alkanes and benzene were conducted between July 2, 2019, and March 19, 2021. Figures 10 and 11 show the combined measurement paths driven during this study for total alkanes and benzene, respectively. For the purpose of this study, alkane enhancements above background levels were defined as any data that is larger than the 97.5% quantile of the entire dataset. Similarly, benzene enhancements above background levels were defined as data larger the 97.5% quantile, and greater than three times the standard deviation above the mean for the given transect (see Equations 2 and 3). The additional criteria for benzene was added to account for variations in the instrumental noise over the course of the study.

$$\text{Enhancement} > \bar{X} + 3 * \sigma_x \quad \text{Equation 2}$$

$$\text{Enhancement} > 97.5\% (\text{quantile}) \quad \text{Equation 3}$$

Where \bar{X} is the mean of the data for the transect and σ_x is the standard deviation of the data for the same transect.

To visualize the frequency of enhancements above background levels, the geographic area around each respective refinery was binned into a square grid of 140 m x 140 m cells. The percent of data identified as an enhancement above background levels within each grid cell was calculated and the grid was colored according to this data (Figure 10 and Figure 11).

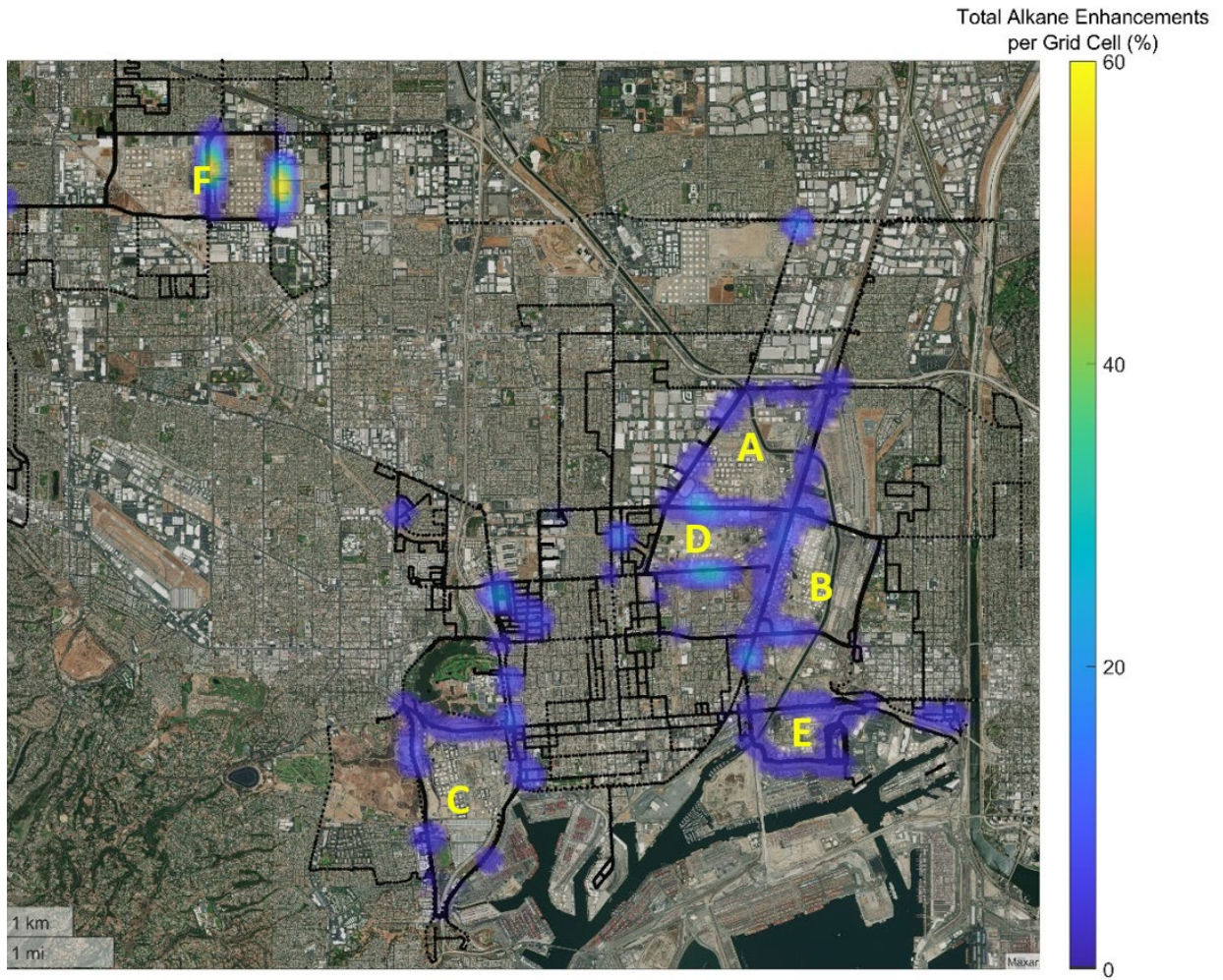


Figure 10. Satellite image of the area containing the six refineries surveyed during this study (identified by letters A through F) with the cumulative measurement path taken by ORS ML during the study shown as black lines. The colored shading represents the percent of observed total alkanes enhancements above background.

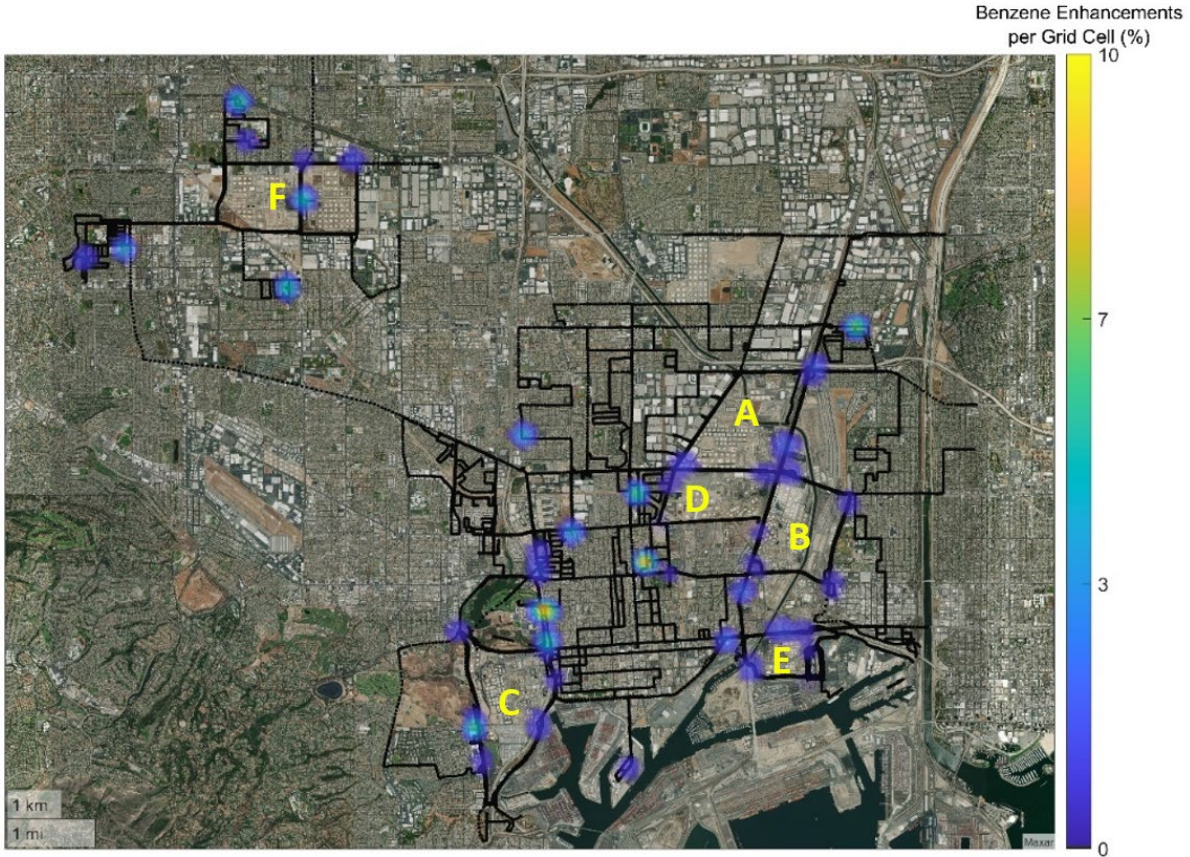


Figure 11. Satellite image of the area containing the six refineries surveyed during this study (identified by letters A through F) with the cumulative measurement path taken during the study shown as black lines. The colored shading represents the percent of observed benzene enhancements above background.

Areas with enhanced concentrations of benzene and total alkanes were more commonly measured at the refinery fencelines than in the surrounding communities. Overall, enhancements of total alkanes were more frequently detected than benzene enhancements. This is consistent with alkanes being the major component of crude oil, while benzene is generally present in crude oil at levels <5% and thus emitted at much lower levels. Alkane enhancements tended to occur as broad sections distributed along refinery fencelines, while benzene enhancements were mainly observed as isolated areas along the fenceline.

Occasionally, enhancements of total alkanes and benzene were observed in communities away from the refinery fenceline. These enhancements were likely due to the presence of other sources of air pollution and not associated with refinery emissions. In most cases such enhancements occurred away from the refinery with no obvious plume traced back to the refinery fencelines, as would be expected if the refinery were the main source of pollution.

4. Optical Tent

Monitoring BTEX in large and complex refineries is a formidable challenge. The existing optical remote sensing fence-line monitoring systems, such as those implemented to satisfy the requirements of South Coast AQMD Rule 1180, are primarily designed as notification systems to detect and alert the public about elevated levels of air pollutants at the fence-line of refineries. To further explore the unique capabilities of modern ORS instruments, University of California Los Angeles (UCLA) was contracted by South Coast AQMD to develop a next generation BTEX monitoring system that provides near real-time BTEX observations over the entire refinery, both at the fence-line and within the facility. This project's objectives include substantiating the feasibility of long-term automated operation for this type of system, showcasing its capabilities and advantages in detecting elevated BTEX levels, and investigating whether providing spatial information to facility operators aids in promptly addressing the root causes of BTEX releases. The subsequent chapter provides a general description of the optical tent and discusses valuable insights gained from operating the optical tent over a span of 20 months.

4.1. Instrumentation and Setup

The optical tent utilizes open path UV absorption spectroscopy, employing a beam of UV light transmitted through the atmosphere. By analyzing the absorption of trace gases along this light path, it accurately identifies and quantifies BTEX compounds. For the deployment of such a system in a refinery, a setup was chosen that uses an active sending/receiving system on one end of an atmospheric path and a passive reflector on the other. This approach has the advantage that the deployment of passive reflectors inside the refinery is technically straightforward. To achieve comprehensive spatial coverage across the facility, multiple light paths were strategically positioned, taking into consideration the layout of the refinery.

The measurement and analysis approach of the optical tent are based on the DOAS method. The two sending/receiving systems, also called Long Path (LP)-DOAS, are based on a design published in Stutz et al., (2016). The LP-DOAS consists of a light source, a telescope, an array of quartz retroreflectors, and a spectrometer-detector combination (Figure 12). The telescope uses a fiber-based Newtonian telescope design and has a focal length of 120 cm, and a main mirror of 30 cm in diameter. Based on UCLA's earlier field work, this setup has proven to be highly stable and reliable. To allow for scanning over several reflectors and to properly aim the telescope, the telescope is mounted on horizontal and vertical stepper motor-controlled rotation stages. A dual UV light emitting diode (LED) setup, which is mounted in a thermally enclosed container, serves as the light source of the LP-DOAS. The inclusion of thermal stabilization for the LED has proven to be a major improvement of this system, compared to previous versions. A custom quartz fiber bundle (Figure 13) feeds the light from the LEDs into the telescope, collects the light reflected from the reflectors, and sends it into the spectrometer-detector combination. A 300 mm focal length imaging Czerny Turner spectrometer (Acton SpectraPro HRS 300) combined with a 1024 x 256 custom CCD detector array (Princeton Instruments PIXIS 256E) is the centerpiece of the LP-DOAS instrument. The spectrometer is thermally stabilized to within 0.1°C, while the CCD array detector is cooled to -70°C to reduce its dark signal.

An optical tent was developed and deployed at one of the refineries in the Basin. For this refinery, which is located on a hill side, the most practical setup was to place the sending/receiving systems in the southwest and northeast corners of the facility in elevated instrument shelters provided by the refinery

(labeled A & B in Figure 12). Ten reflectors were deployed, five for each sending/receiving system. Four of the reflectors were placed such that the optical tent is part of the refineries fenceline monitoring system (A1, A5, B1, B5), while the remaining six form internal light paths (A2, A3, A4, B2, B3, B4). The optical tent, therefore, consists of ten absorption paths with lengths ranging from 373m to 891m. Figure 12 illustrates the location of the ten paths and lists their respective lengths. Please note that the color code for the different paths in Figure 12 will be used throughout this report. Each sensing/receiving system aims sequentially at five reflectors. The time to scan all five reflectors can vary due to atmospheric conditions but is typically within 25-40 minutes.

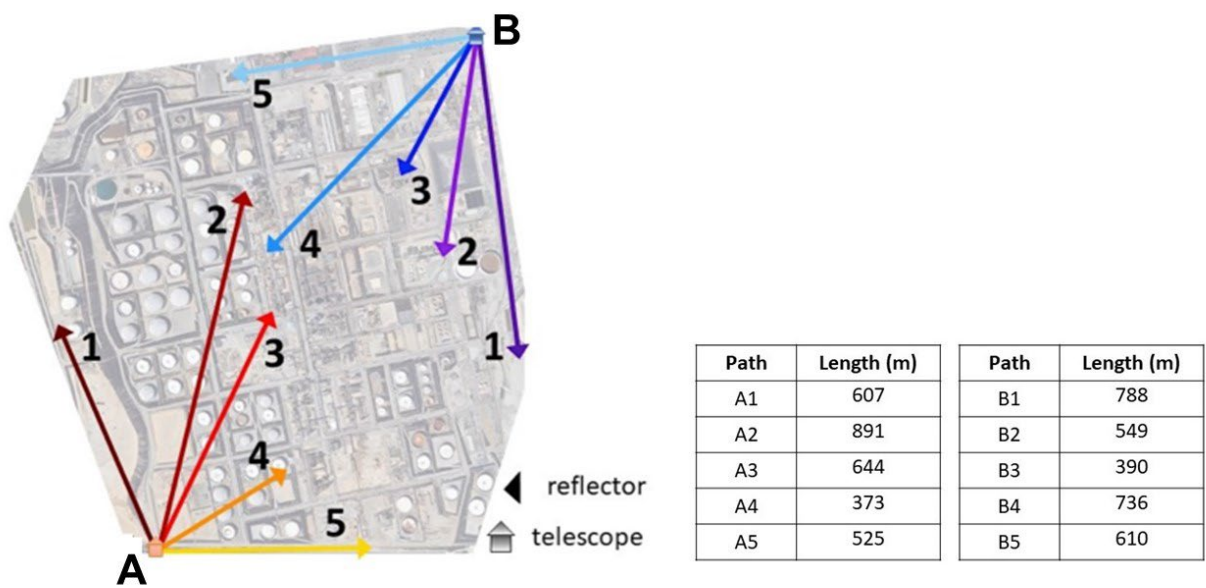


Figure 12. Setup and path length of the optical tent. Color convention for A and B paths will be maintained throughout this portion of the report.

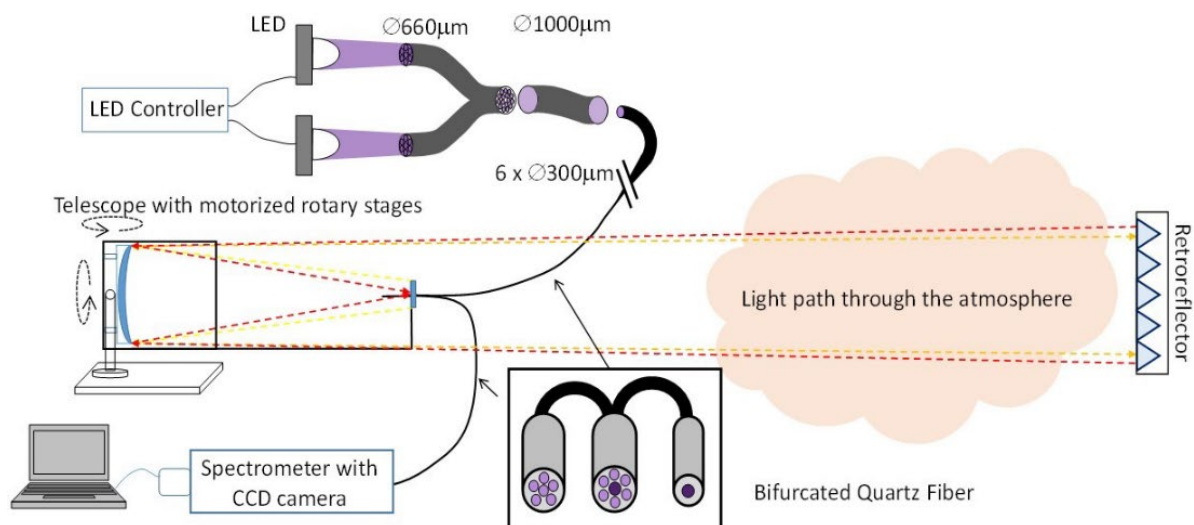


Figure 13. Schematic of the P-DOAS set-up.

An industrial personal computer controls the stepper motors as well as the data acquired by the spectrometer/detector system. The instrument software was adapted and optimized during the first 6 months of deployment to implement protocols on how the optical tent reacts to environmental conditions such as rain, fog, or smoke. The typical sequence of operation is to aim the LP-DOAS telescope on the reflectors in the following sequence: 1, 2, 4, 5, and 3. This pattern is then repeated continuously. After rotating the telescope onto a specific reflector, the aim of the telescope is optimized for maximum return light intensity. In this step the instrument also determines if the path is obstructed, for example by steam, or if atmospheric conditions allowing for the formation of fog have reduced the returned light intensity below acceptable levels. In both cases, the telescope will move on to the next reflector without taking a measurement. If sufficient light is returned from the reflector, an atmospheric absorption spectrum is recorded during a 3-minute-long period. This spectrum is stored on a cloud drive which also transmits it to UCLA for spectral data analysis. After the measurement, the system moves on to the next reflector. In addition, spectra of the LED light source are recorded every 3 hours by rotating a diffuser in front of the fiber. The LED spectra are used in the data analysis. Also, a quality check is performed on the LED spectra to ensure that the instrument is behaving normally. As a result of our optimization efforts, the optical tent typically operates unattended for weeks at a time.

An important aspect of the measurement of BTEX using UV open path remote sensing is the spectral retrieval of the trace gas absorption features in the measured atmospheric absorption spectra. The spectra from the optical tent are analyzed in near real-time using the DOAS technique (Platt and Stutz, 2008; Stutz et al, 2016). DOAS uses the narrowband absorptions of BTEX to identify and quantify each trace gas. The spectral retrievals are based on literature absorption cross sections for each BTEX compound, as well as those of O_2 , O_2O_2/O_2N_2 collisional complexes, and ozone, which also absorb in the same wavelength range. Absorption cross sections are unique for each compound and their absorption strength for a given wavelength are physical constants. Consequently, additional calibration of the instrument is not needed. The absorption cross sections are, however, adapted to the spectral response of the LP-DOAS instruments by convoluting them with the instrument response of a measured narrow mercury atomic emission line.

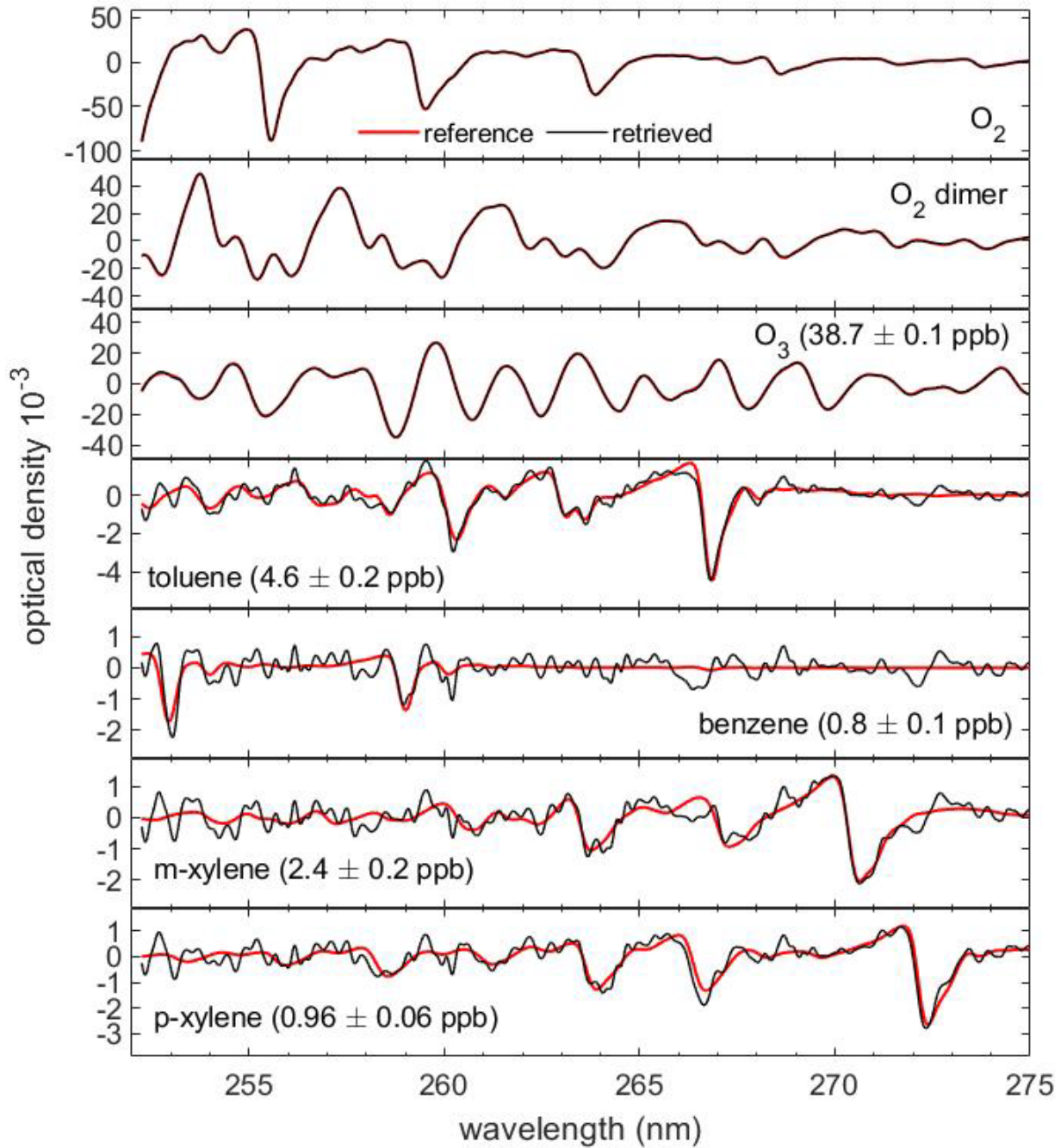


Figure 14. Example of a typical spectral retrieval of a measurement of the optical tent. Red curves are the calculated reference spectra. Black curves are the retrieved spectral structure from the measurement.

This convolution process yields a set of trace gas reference spectra for every light path of the optical tent. A spectral retrieval is then performed by fitting a linear combination of the reference spectra and a polynomial of degree five to the logarithm of the ratio of the atmospheric spectrum and the spectrum of the LED light source. The fitting algorithm is based on a combination of a linear and a nonlinear least squares method as described in detail in Platt and Stutz (2008). The result of the spectral retrieval are path-averaged trace gas concentration and their respective errors. Figure 14 shows the results of such a fitting procedure where the comparison of the reference spectra (red lines) and the retrieved spectral

structure (black lines) clearly shows the identification of BTEX compounds by the optical tent. The figure also shows the retrieved mixing ratios and the retrieval errors for this specific observation. It should be noted that this fitting approach determines the uncertainty of each measurement. The retrieval uses the DOASIS software, developed at the University of Heidelberg (Krause, 2006). It should be reiterated here that this approach allows first-principle absolute observations of BTEX, i.e., a calibration of the instruments, aside from a mercury emission lamp measurement during the setup phase, is not needed. Detailed technical evaluation of the performance of the optical tent is presented in Appendix 8.1.

The spectral retrieval has been set up for near real-time data analysis such that BTEX and ozone mixing ratios are determined as soon as a measured spectrum is uploaded to the designated cloud drive. The results of the real-time spectral retrievals from spectra observed on the fenceline paths of the optical tent (A1, A5, B1, B5) are sent to the fenceline contractor at the refinery and are publicly displayed. This data is also used to trigger public alerts in case mixing ratios exceed the Rule 1180 thresholds. The data for all optical tent paths are sent to the UCLA group operating the optical tent. A real-time display of the observations is then made available to refinery staff, South Coast AQMD staff, and UCLA. Figure 15 shows a flow schematic of the overall setup for the near real-time data analysis procedure.

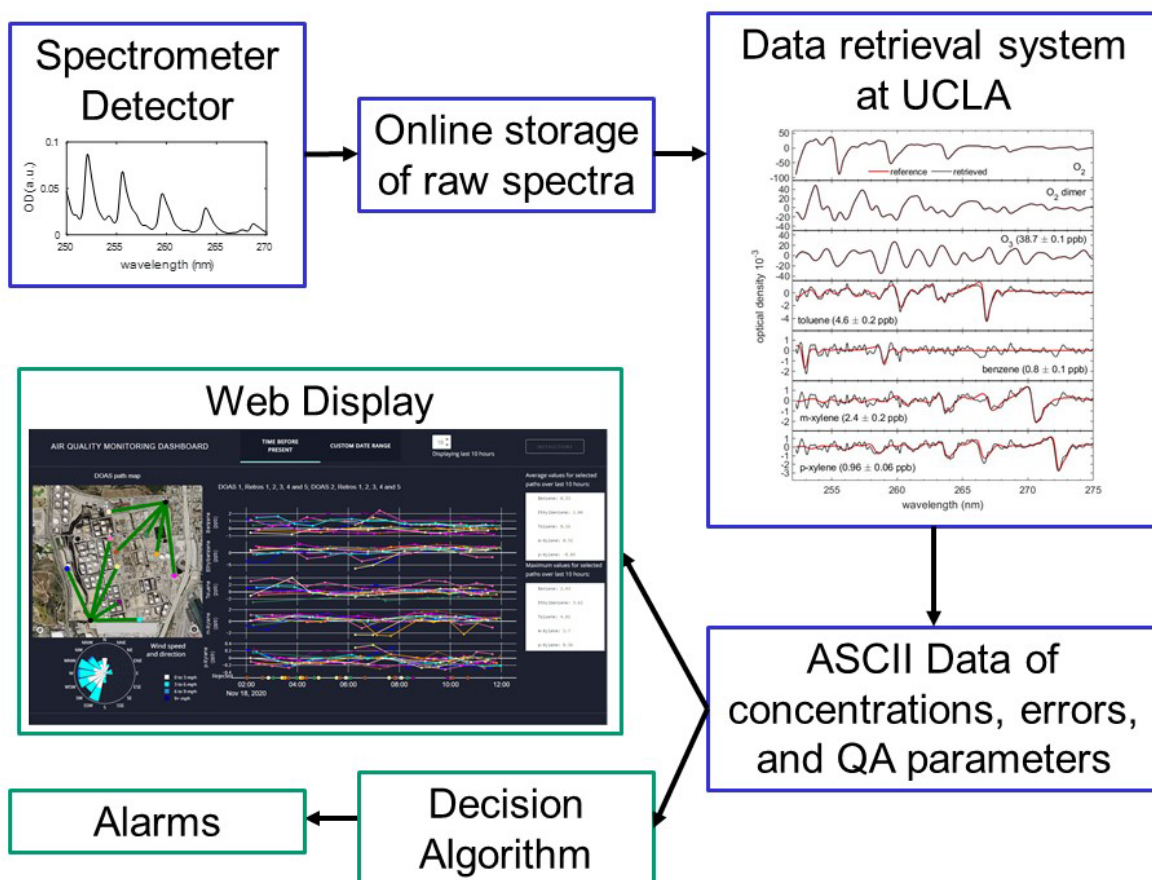


Figure 15. Schematic of the near real-time data analysis setup for the optical tent.

4.2. Optical Tent Performance Evaluation

The optical tent has been in operation since August 2020. During the time data was collected, from August 2020 through March 2022, the optical tent operated with a reliability rate greater than 99%; excluding data gaps due to maintenance, faulty light sources, and low atmospheric visibility due to fog. This data completeness percentage demonstrates the optical tent's reliability as an effective BTEX monitoring system. An unforeseen operational challenge encountered was the presence of frequent steam on path B4, which, under certain atmospheric conditions, hindered the successful measurement of BTEX. In future optical tent deployments, it is advisable to survey the refinery under a range of atmospheric conditions to avoid placing absorption paths directly over sources of steam.

The optical tent has maintained its sensitivity to BTEX compounds throughout its operational period (August 2020 – March 2022). In order to assess BTEX detection limits, the retrieval errors calculated during the spectral retrieval were analyzed. The BTEX retrieval errors from two fenceline paths of System A and B are presented in figures Appendix 8.1. Due to the influence of atmospheric conditions, the retrieval errors exhibit variations across different spectra, as depicted by the range of errors illustrated in the histograms. As a result, the system's detection limit is a dynamic value. For the purpose of the public data display of the refinery fenceline air monitoring data, and the quarterly data summary reports, a single detection limit for each pollutant was used. For the optical tent, three times the maximum error for a specific pollutant is used as the detection limit to account for most environmental conditions.

To assess the actual optical tent performance, the detection limit was determined by calculating the average of all retrieval errors and multiplying this value by a factor of two. Table 4 lists this average detection limit for the two LP-DOAS systems of the optical tent. The average detection limit for all BTEX compounds is below 1 ppb, thus confirming the sensitivity of the optical tent.

Table 4. Average detection limits for the two LP-DOAS systems of the optical tent. Detection limits were determined as twice the average retrieval error over the entire operational period on all light paths.

Compounds	Average Detection Limit (ppb)	
	System 1	System 2
Benzene	0.5	0.3
Ethylbenzene	0.9	0.6
Toluene	0.8	0.6
m-Xylene	0.75	0.5
p-Xylene	0.25	0.2

In summary, the performance of the optical tent throughout the first 20 months has performed as an effective BTEX monitoring system and has continuously operated at the desired sensitivity. From a practical standpoint, the optical tent has been efficiently optimized to operate fully automatically, requiring only occasional maintenance, primarily the replacement of LED light sources. Overall, this project successfully demonstrates the deployment and long-term operation of a fully automated, near real-time monitoring system for air toxics monitoring that encompasses an entire refinery.

4.3. Results

The optical tent observations provide unique insights into the frequency and levels of elevated BTEX observed inside the fenceline of a refinery. Figure 16 provides an overview of BTEX observations conducted over the refinery between August 2020 and March 2022. This data allows for an insight of how the optical tent can help a facility to rapidly identify and manage their unplanned releases. The comparison between internal and fenceline data from the optical tent also helps to highlight the advantage of monitoring inside a refinery. These points will be discussed in more detail in the following sections.

4.3.1. Characteristics of BTEX Detections

The data overview depicted in Figure 16 shows that, for most of the time, BTEX mixing ratios remain below the optical tent detection limits. For example, for benzene, optical tent detection limits typically ranged between 0.3 and 0.5 ppb, which were near the typical ambient benzene levels measured at MATES V fixed air monitoring sites (South Coast AQMD, 2021). However, elevated BTEX levels were sporadically detected within the facility. With only 0.8% of the time, hourly benzene levels exceeding 8 ppb, which is OEHHA Acute 1-hour Reference Exposure Level (REL) (OEHHA, 2008). Most instances of hourly benzene enhancements over 8 ppb were observed within the refinery, although three occurrences took place at the fenceline. Over nearly 20 months of operation, the number of hours when optical tent measured hourly concentrations of benzene in excess of 8 ppb were 20 and 149 for the refinery fenceline and internal paths, respectively.

Figure 17 shows a time series of BTEX during an emission event on December 18, 2020 that was quickly mitigated by the facility operator. The event was detected both on an internal light path (path A2) and at the fenceline of the refinery (path A1). This last event resulted in a Rule 1180 fenceline air quality notification to the public (South Coast AQMD Rule 1180 requires a notification to be issued when hourly fenceline concentrations of benzene exceed 8 ppb). With the assistance of the information from internal open paths, the facility operator promptly identified and addressed the leak, successfully mitigating it within an hour. As a result, the subsequent BTEX observations exhibited significantly lower BTEX mixing ratios.

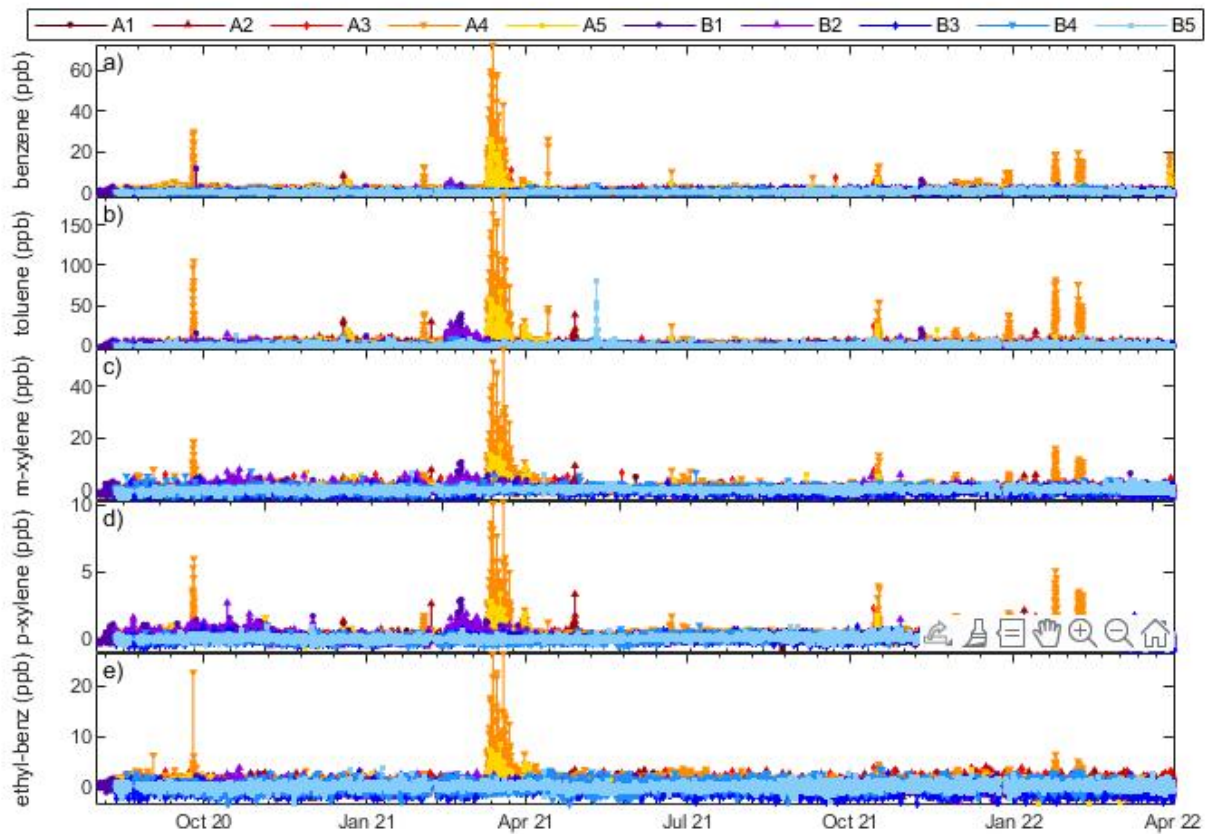


Figure 16. Optical tent data collected between August 2020 and March 2022.

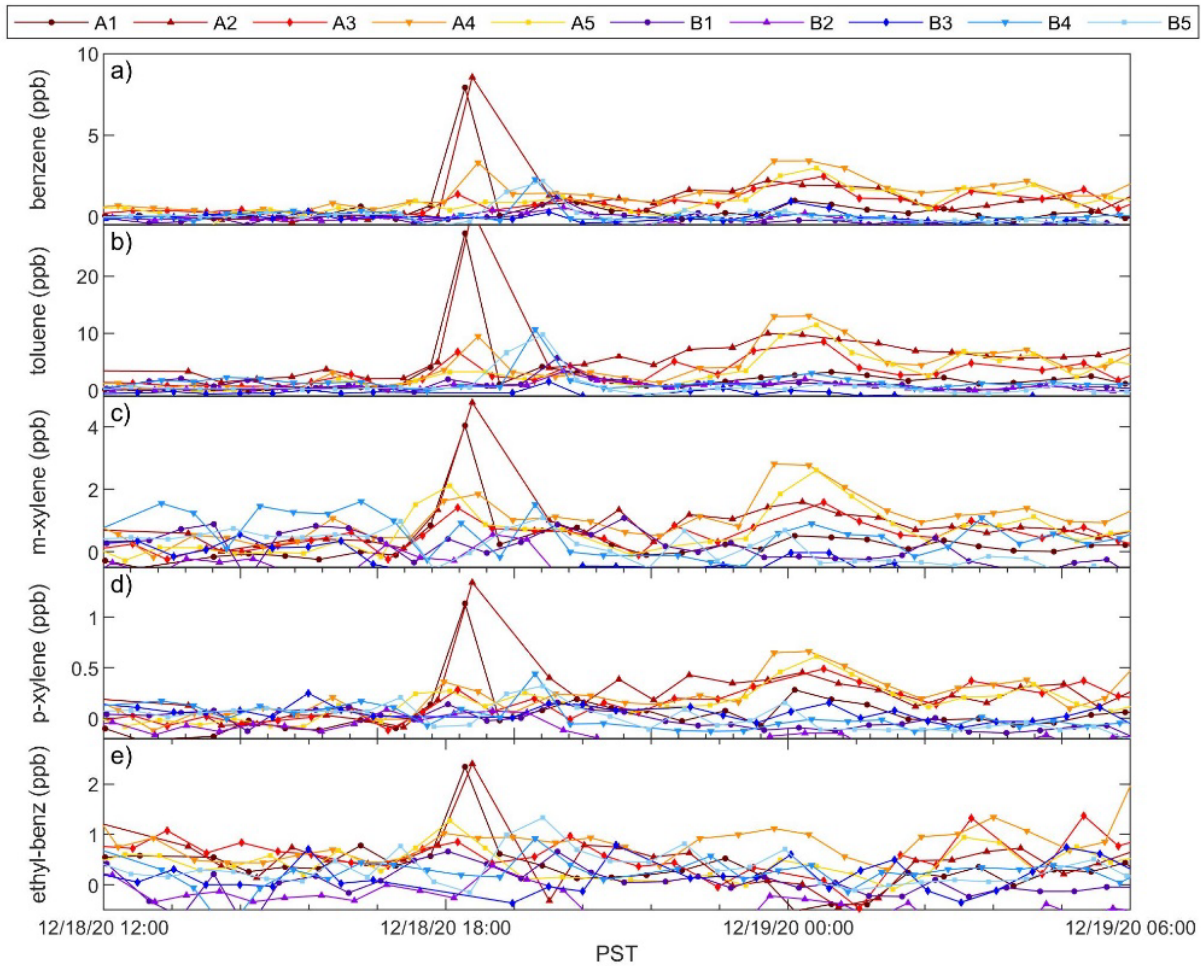


Figure 17. Example of a BTEX leak on December 18, 2020, that was quickly mitigated by the facility operator.

On March 9, 2021, the roof of a floating roof tank failed, exposing the underlying hydrocarbon mixture to the air causing a sustained BTEX emission event, that is illustrated by BTEX time series in Figure 18. Elevated BTEX levels (of about 5 ppb benzene) were initially detected during the night of March 9 – 10 on path internal A4 and, and subsequently, on fenceline path A5. Mitigating the equipment malfunction in this instance took over two weeks during which both internal path A4 and fenceline path A5 continued to register elevated BTEX measurements. Observations in Figure 20 also highlight the strong impact of meteorology on the recorded data, resulting in considerable diurnal variability of BTEX mixing ratios. Generally, BTEX levels observed during the night were higher than those during the day, potentially due to enhanced mixing during the day and variation in local wind. Lastly, Figure 18 also clearly shows the time when the event concluded on March 23, 2021.

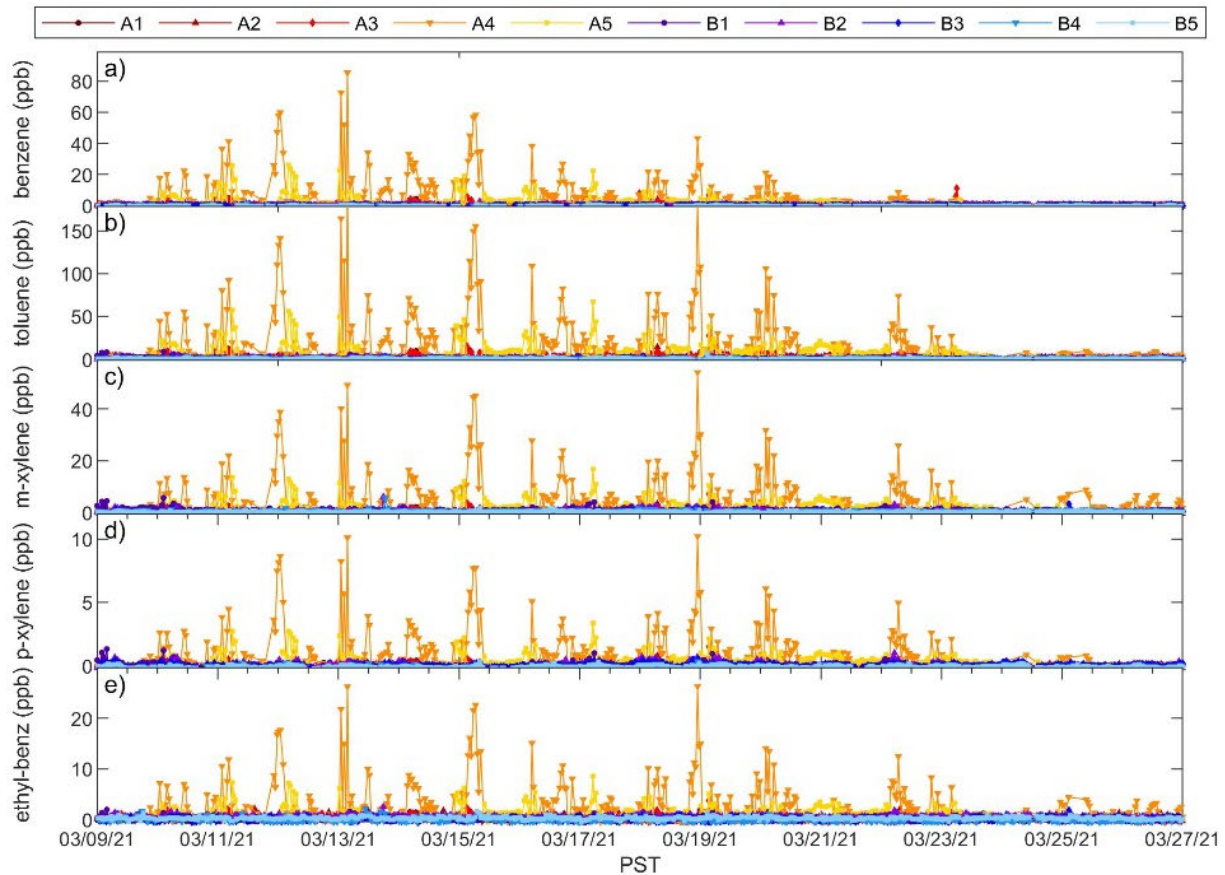


Figure 18. Time series of hourly BTEX concentrations measured March 09 – 27, 2021. Tank roof failure resulted in elevated BTEX concentrations measured by the optical tent on path A4 and A5.

It is worth noting that there were instances where BTEX detections were not associated with equipment failure but rather with known maintenance activities taking place within the refinery. For example, as part of the refinery’s maintenance operation, coating activities were performed underneath path B1 and B2, starting on February 14, 2021, and concluding around March 5, 2021. Figure 19 shows that during this period, BTEX levels on path B1 and B2 were elevated relative to other time-periods, although 1-hour average benzene levels remained well below OEHHA REL of 8 ppb.

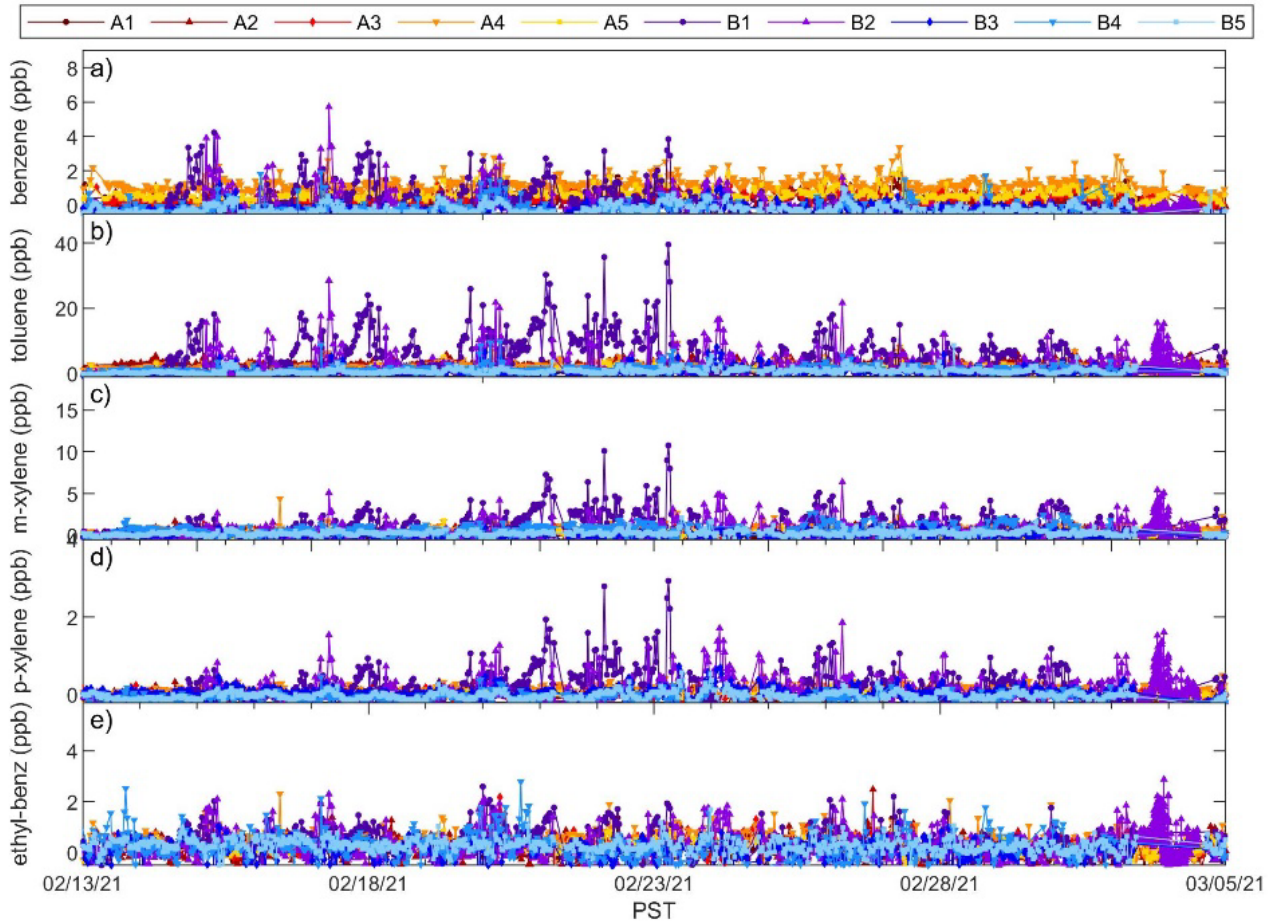


Figure 19. Time series of hourly BTEX concentrations measured February 13 – March 05, 2021. Coating activities directly below path B1 and B2 resulted in slightly elevated measured BTEX concentrations on these light paths.

With the exception of a few planned operational activities, the sporadic nature of the BTEX events suggests that the majority of the elevated BTEX occurrences can be attributed to primarily unplanned releases. With the optical tent’s capability to identify the locations where elevated BTEX levels are detected, the facility can swiftly pinpoint the source of the release and take remedial measures. Although challenging to quantify directly, there is anecdotal evidence suggesting a decrease in the time required to address and resolve unintended releases because of optical tent operations. These observations underscore the optical tent’s effectiveness in managing unforeseen BTEX releases within facilities.

4.3.2. Statistical Analysis of BTEX Detections

To gain insights into the probable location of BTEX releases, a statistical analysis was conducted using the optical tent dataset. The likelihood of a release was evaluated by counting the number of hours in which the average benzene mixing ratios exceeded an arbitrary threshold of 2 ppb. The results of this analysis are reported as percentage of hours above 2 ppb for each light path. It is worth noting that our findings remain consistent even when using higher thresholds. Furthermore, due to the limited frequency of measurements, the calculated averages often rely on just one or two data points.

Table 5. Percentage of hours benzene mixing ratios on a light path of the optical tent were above 2 ppb.

Path	% hours >2ppb	Path	% hours >2ppb
A1	0.09	B1	0.14
A2	0.16	B2	0.07
A3	0.30	B3	0.11
A4	5.7	B4	0.11
A5	1.0	B5	0.05

The southwestern corner of the refinery, specifically paths A3, A4, and A5, exhibited the highest number of releases. These paths are in close proximity to the refinery tanks. Based on these findings, the refinery tank farm is a probable source of unintended releases within the refinery. Consequently, it is crucial to conduct further in-depth studies regarding potential releases from the tank farms.

4.3.3. Influence of Local Meteorology on BTEX Observations

The optical tent data presents a unique opportunity to examine the influence of local transport effects on BTEX releases. Figure 20 depicts an event where elevated toluene levels were observed on paths A4 and A5. Notably, the mixing ratios of toluene exhibited high variability and demonstrated an inverse relationship between paths A4 and A5. Additionally, it is worth mentioning that mixing ratios were higher during nighttime when atmospheric conditions tend to be calmer compared to daytime when wind speeds and atmospheric mixing are greater.

Furthermore, we observed the impact of wind direction on toluene mixing ratios along the two paths. For wind directions of about 250 degrees, path A5 measured mixing ratios of about 10 ppb, whereas Path A4 measured toluene levels below the detection limit. Conversely, for wind directions between 160-220 degrees, the opposite pattern was observed, with path A4 detecting mixing ratios between 20-30 ppb and path A5 detecting very low toluene levels. We interpret these observations as a result of local transport effects that caused the movement of released toluene along different light paths.

This illustrates that despite spatial averaging over a single absorption path, observations remain sensitive to local meteorology. The combination of multiple paths in the optical tent helps to mitigate the influence of local meteorology, providing more comprehensive coverage and improved sensitivity to detect elevated BTEX levels (Figure 20).

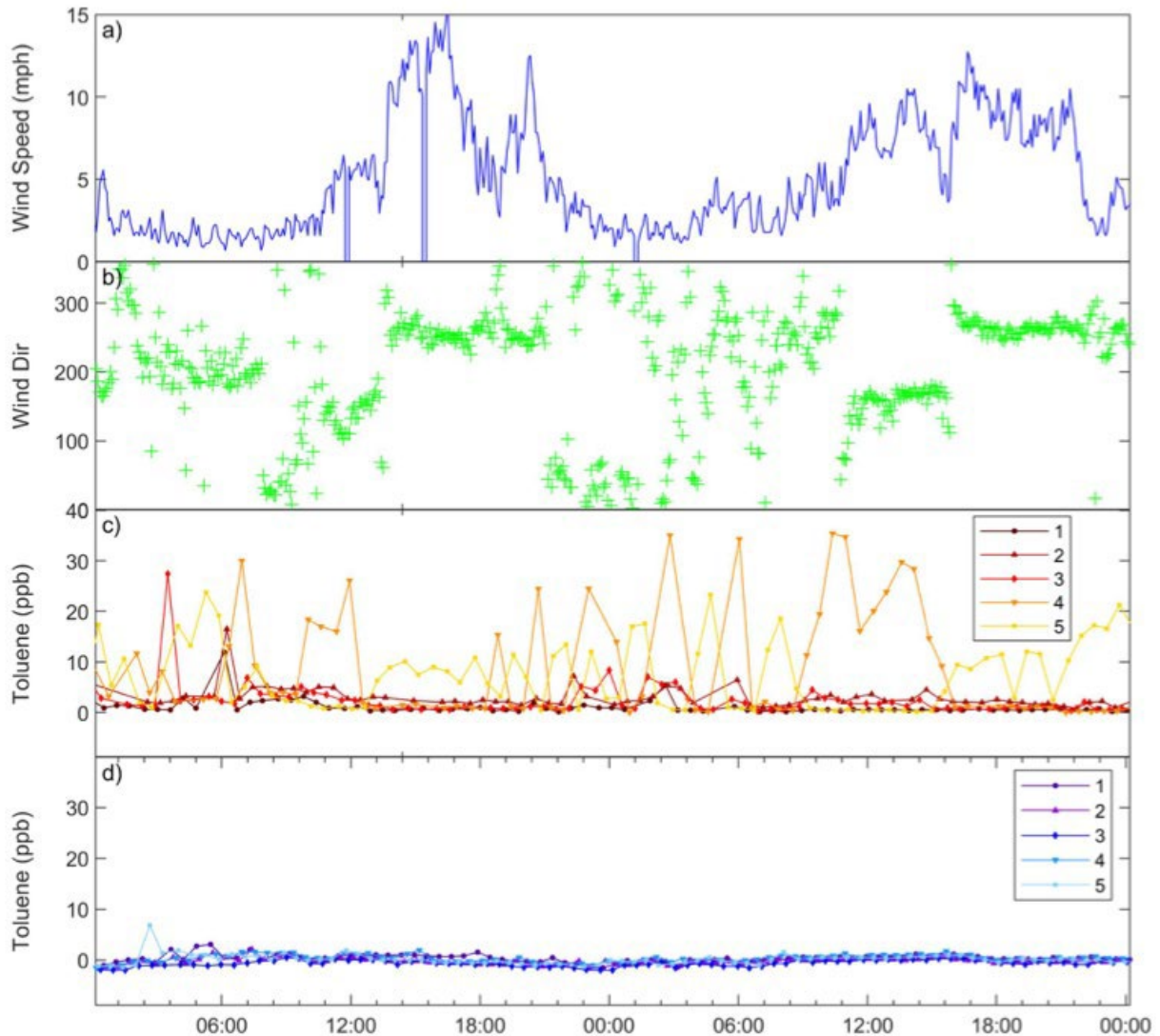


Figure 20. Toluene detection by the optical tent on March 19-20, 2021. Panels a) and b) show wind speed and wind direction, respectively; and panels c) and d) show toluene concentrations measured by systems A and B, respectively.

4.4. Advantages of the Optical Tent Compared to Fenceline Monitoring

Open path type monitoring is at the forefront of the field of air quality monitoring, with the optical tent approach representing an exciting new adaptation of the typical fenceline arrangement used so far. A statistical analysis of the optical tent observations (Table 5) indicates that elevated BTEX levels are more frequently detected on the internal paths of the optical tent compared to the fenceline paths. In Figure 21, for instance, elevated BTEX was observed over several days on the internal path A4, while nearby fenceline path A5 did not detect the event. This highlights the optical tent’s capability to enhance the probability of detecting unwanted releases within a refinery, therefore allowing the refinery personnel to identify and mitigate unwanted emissions and their causes quickly. Moreover, internal BTEX detections often exhibited higher mixing ratios than those at the fenceline (Figure 19, Figure 20, and Figure 21). This difference in mixing ratios makes it easier to identify elevated BTEX levels, thereby improving the efficiency of identifying unwanted releases. Although quantifying the advantage of the optical tent in detecting unwanted releases is challenging, Table 5 provides statistical data suggesting

that the optical tent is approximately six times more likely to detect an unwanted release compared to a fenceline-only system.

Although the advantages of an open path optical tent arrangement are apparent in this work, it must also be noted that adding such a system to an existing fenceline type arrangement may result in increased initial and ongoing costs of the monitoring efforts at a facility. Furthermore, while traditional open path fenceline monitoring systems are commercially available, at the time of this writing, optical tent systems have been offered by commercial providers.

Another advantage of the optical tent is its ability to provide real-time feedback on an approximate location of unforeseen BTEX releases by conducting open path measurements inside the facility. This aids the facility operators in quickly identifying malfunctioning equipment, reducing the time required to address the underlying cause of the release. Consequently, this capability should contribute to reducing overall BTEX emissions from the facility. Additionally, it offers a clear benefit to facility operators by streamlining the process of locating the source of an unwanted BTEX release and enabling near real-time mitigation efforts to determine their effectiveness.

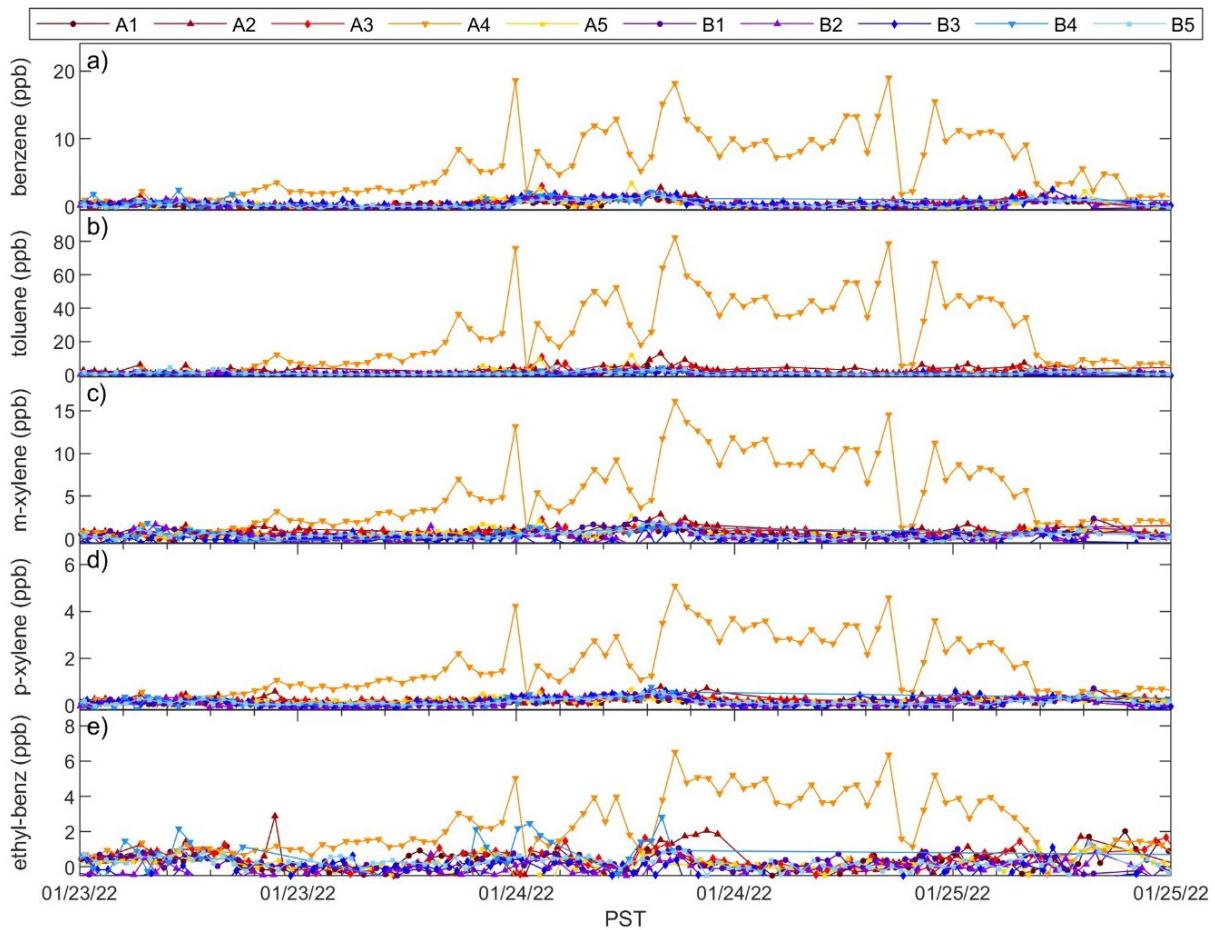


Figure 21. Example of a BTEX detection on internal path A4 that was not detected on the nearby fenceline path A5.

5. Hyperspectral Aerial Measurements

5.1. Instrumentation and Setup

In the summer of 2019, an Airborne Thermal Infrared Imaging Spectrometer (known as Mako) installed aboard a DHC-6 Twin Otter aircraft, was used by Aerospace Corporation (<https://aerospace.org/>) to conduct a series of aerial surveys of selected portions of the Los Angeles air basin. Mako is a 3-axis stabilized whiskbroom imager spanning the 7.5-13.2 μm spectral region in 128 contiguous channels, consisting of a cryogenically cooled high throughput longwave-infrared (LWIR) spectrometer coupled to a fast-readout focal plane sensor array. This combination allows high sensitivity measurements to be made with short dwell times, so that whiskbroom scanning can be implemented for areal acquisitions. Details on design, performance, and operation of Mako are described by Hall et al. (2016) and Buckland et al. (2017).

During data acquisition, the 128-pixel linear field-of-view is continuously scanned normal to the direction of flight (Figure 22) to build up an image (also referred as scene) by accumulating sequential cross-track scans (whisks) which are user programmable up to 3600 frames (pixels). The whiskbroom scanning approach permits areal coverage rates of up to 32 $\text{km}^2\text{min}^{-1}$ at a 2 m ground-sample distance (GSD) from an altitude of 12,000 ft (3,660 m) above ground level (AGL).

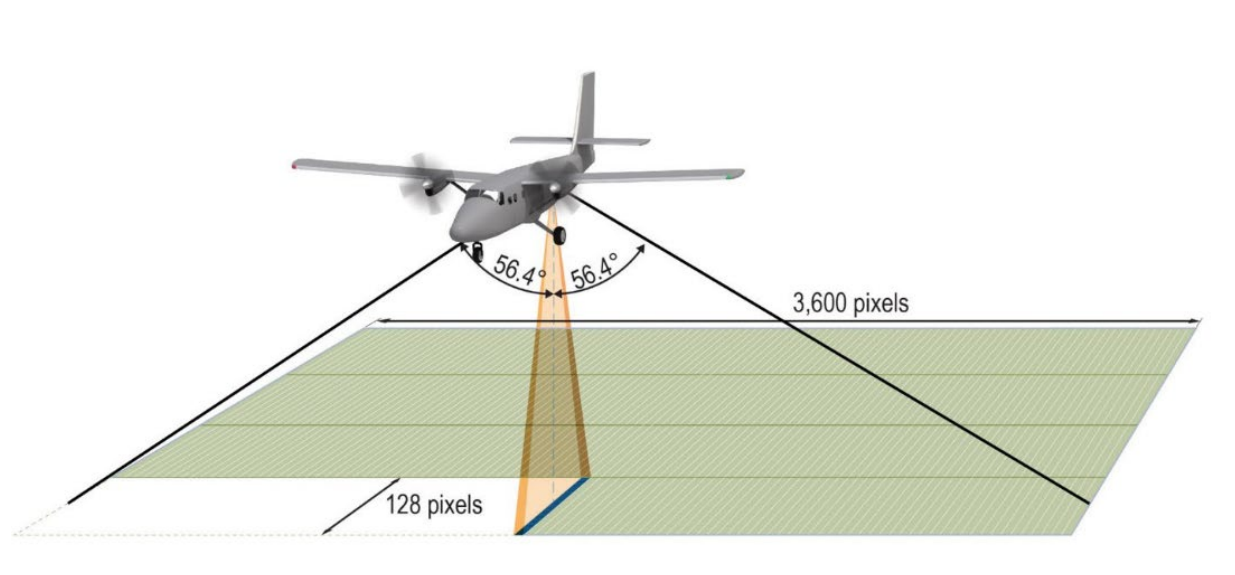


Figure 22. Mako operational concept, illustrating whiskbroom scanning geometry.

The spectro-radiometric performance of the Mako sensor is summarized in Table 6. An integrated scanning and flight planning tool provides the flexibility to acquire arbitrary polygons and enables multiple sequential looks at an area on the ground during overflight in order to resolve the temporal development of rapidly evolving phenomena such as the evolution of an emissions plume. The latter capability was invoked a few times for selected facilities of interest during the MATES V airborne campaign.

Table 6. Mako Operational Parameters

Parameter	Specification
Spectral coverage	7.57 – 13.16 μm
Spectral resolution (128 channels)	44 nm
Instantaneous field-of-view, IFOV	0.55 mrad
Along-track FOV (128 pixels per frame)	4°
Base frame rate	3255 Hz
Nominal operational frame rate (4 co-adds)	814 Hz
Cross-track pixels (user programmable)	400 – 3600
Cross-track field-of-regard, FOR (relative to nadir)	$\pm 56.4^\circ$ (max.)
Focal plane temperature	9.5 K
Noise-equivalent spectral radiance, NESR (10 μm, 4 co-adds)	$< 0.3 \mu\text{W cm}^{-2} \text{ sr}^{-1} \mu\text{m}^{-1}$
Noise-equivalent differential temperature, NEDT (10 μm, 300 K)	0.02 K

To extract spectral information from the LWIR imagery, a number of data calibration and correction steps are performed on the raw data, followed by a series of algorithms designed to compensate for background atmospheric contributions and detect and identify specified targets of interest within the scene. The flow chart in Figure 23 provides an overview of these data processing stages. The Open GIS Consortium, Inc. (OGC, 2022) was followed to denote the standard for imagery levels (color-coded in Figure 23). Processing steps include calibration (spectral and radiometric), bad-pixel mitigation, georeferencing, spectral-smile removal, atmospheric compensation, target detection, region-of-interest selection, target identification, and ultimately the automated generation of a tactical analysis report (TAR). Each step in this process is described in detail in Buckland et al. (2017). The Aerospace LWIR gas spectral library comprises approximately 700 species, with most deriving from the Pacific Northwest National Laboratory spectral database (Johnson et al., 2004).

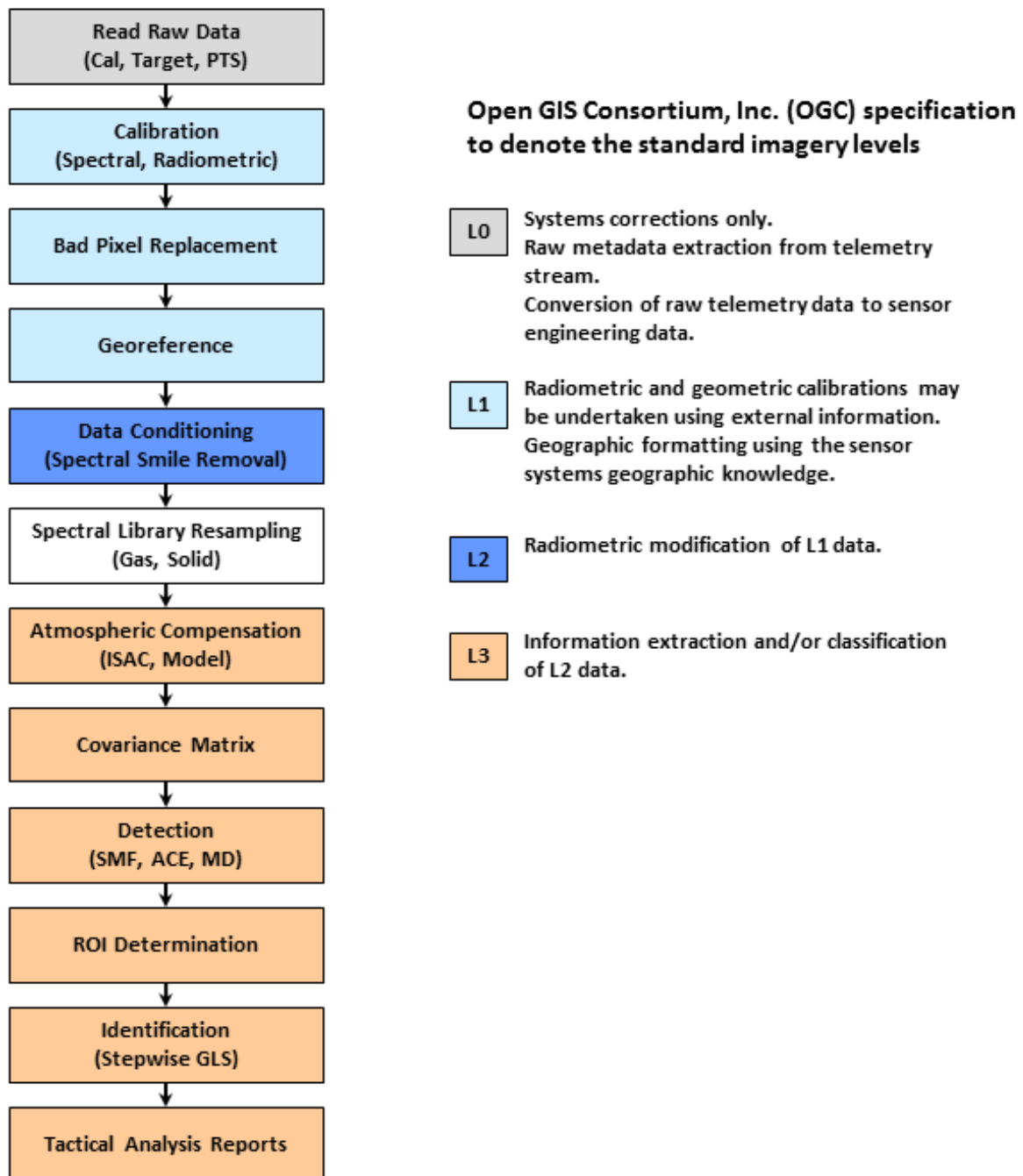


Figure 23. Overview flow diagram (top level) of the data processing stages.

5.2. Detection Limits of Aerial Hyperspectral Imaging

The sensitivity of the sensor to any given gas is dependent on spectroscopic properties of the gas, the prevailing atmospheric conditions, and the collection geometry. Using the procedure described by Buckland et al. (2017), the minimum detectable quantity (MDQ) was computed for each of South Coast AQMD’s compounds of interest (COIs), which included VOCs and other air toxics and pollutants relevant to this MATES V advanced monitoring project. These expected MDQ’s are listed in Appendix 8.2, where

a wind speed (u) of 5 ms^{-1} , thermal contrast (ΔT) of 5 K, and 2-m GSD have been assumed. The thermal contrast is defined by Equation 4:

$$\Delta T = |T_b - T_a| \quad \text{Equation 4}$$

in which T_a is the temperature of the air parcel containing the emission of interest and T_b is the brightness temperature of the underlying terrain. Unless dedicated measurements have been made, T_a and u must generally be drawn from meteorological archives such as MesoWest (Horel et al., 2002) or weatherunderground.com but these represent significant sources of error when computing emission fluxes (Buckland et al., 2017). Once these quantities have been ascertained, the MDQ value for the prevailing conditions can be estimated through a simple scaling relation:

$$MDQ = MDQ_{Table} \left(\frac{u}{\frac{5m}{s}} \right) \left(\frac{5K}{\Delta T} \right) \left(\frac{GSD}{2m} \right) \quad \text{Equation 5}$$

The MDQ_{Table} values are given in Appendix 8.2. Note, however, that MDQ values obtained this way do not adequately compensate for changes to the collection geometry or atmospheric parameters and should therefore be applied with caution. The MDQ_{Table} values provided in Appendix 8.2 are appropriate for the current incarnation of Mako. For the older archival data (see section below), they should be regarded as approximate.

5.3. Re-analysis of Historical Archive

Aerospace has been conducting flight-based measurements in the Basin since 2010, including in areas near the seven major petroleum refineries and environmental justice areas with facilities that are potential emitters of BTEX compounds. These historical acquisitions were reprocessed for this project with a focus on BTEX and other air toxics relevant to MATES V advanced monitoring project, and are summarized in Appendix 8.3. This exercise was conducted to further demonstrate the capabilities of Mako and to confirm its ability to successfully detect selected air pollutants that are relevant to this project.

Overall, the majority of detections were of ammonia and methane. The former is an extremely common observation through all Mako data sets since the MDQ is very low and this compound is emitted by many natural and industrial sources, such as petroleum refining, selective catalytic reduction (SCR) of NO_x, biomass burning, incinerators, agriculture, animal husbandry, and etc. Methane is similarly common throughout the Basin due to the prevalence of oil and gas production and distribution in the region. Ethene is the next commonly observed gas, that is normally produced as a byproduct of inefficient hydrocarbon (usually methane) combustion and as a fugitive emission from ethene production and storage equipment. Non-methane hydrocarbons such as propane, butane, isobutane, and styrene (frequently in association with acetone, which invariably traces back to plastics and fiberglass manufacturing businesses) were observed only occasionally.

The alcohol detected most frequently is methanol, but ethanol and isopropanol were also observed on occasion. Aerial measurements often observe co-emission of methanol and acetic acid from large piles of mulch at horticultural suppliers, for example garden centers. This is due to anaerobic fermentation within the mulch and is a well-known phenomenon (Buckland et al., 2017). More rarely, formic acid and ethanol (Hall et al., 2016) were also measured.

Emissions of m-xylene from a tank farm; sulfur dioxide from a ship at berth; dichloromethane from a hazardous waste handler, and tetrachloroethylene from a dry-cleaning business have been identified from the historical data and are shown in Figure 24. Each panel of this figure consists of a detection filter image pertaining to the named gas with the corresponding thermal scene image beneath. The red outlines show a region-of-interest (ROI) on the thermal image with pixels which contribute to the spectral identification of the given gas, whose source is marked by the red diamond in the filter image.

Only one instance of identification of the BTEX compounds that are of special interest in context of MATES V was found during the archival re-analysis. Figure 24(a) shows a m-xylene plume emitting from a pipeline at a tank farm. Of all the BTEX gases, m-xylene is the easiest to detect with Mako (see MQL for BTEX compounds in Appendix 8.2).

Figure 24(b) shows an example of sulfur dioxide being released from the exhaust stack of a container ship at berth in Long Beach Harbor, suggesting that it may have been burning high-sulfur fuel. Figure 24(c and d) show emissions of two different chlorinated hydrocarbon compounds (Appendix 8.2), which are infrequently found in aerial hyperspectral imaging surveys. The solvent dichloromethane seen in Figure 24(c) is likely emitted from a hazardous waste handling facility located in Long Beach. Tetrachloroethylene (PERC) is used as a dry-cleaning agent, as illustrated in the emission plume detected from a dry-cleaning business, depicted in Figure 24(d). (*Note: After December 31, 2020, PERC dry cleaning systems are no longer allowed to operate within the jurisdictional boundaries of South Coast AQMD*).

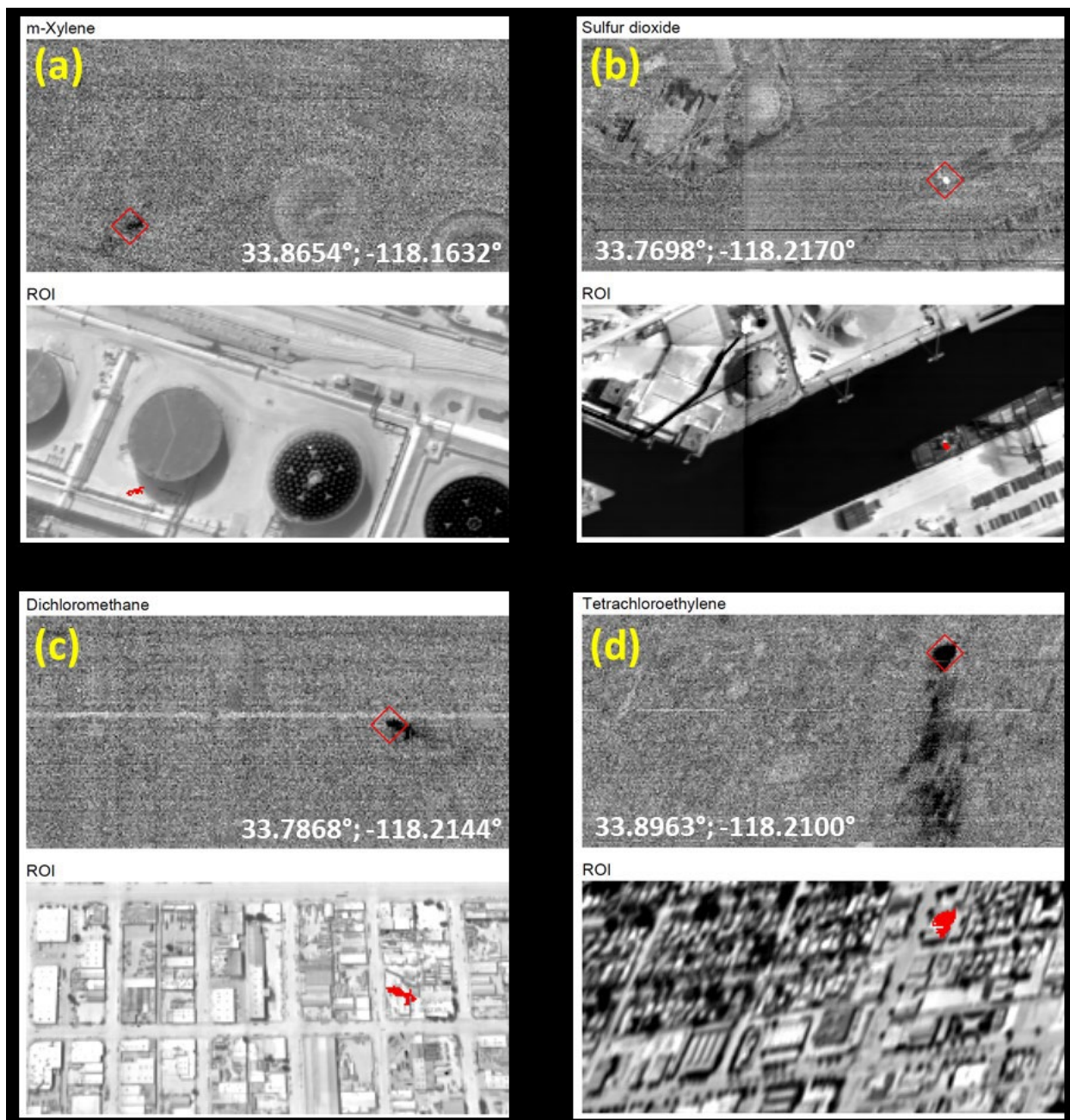


Figure 24. Examples of measurements of (a) m-Xylene emissions at a tank farm (acquisition date 2018-09-15); (b) sulfur dioxide released by a ship at berth (acquisition date 2016-05-11); (c) dichloromethane from a hazardous waste handler (acquisition date 2013-08-30); and (d) tetrachloroethylene from a dry-cleaning business (acquisition date 2011-08-24). Tetrachloroethylene is a chlorocarbon used for dry-cleaning; the California Air Resources Board (CARB) and California Office of Environmental Health Hazard Assessment (OEHHA) identified it as air toxic contaminant and a possible carcinogen (OEHHA, 2016).

5.4. Coordinated Flight Series

Dedicated flights for this MATES V advanced air monitoring project were conducted on July 9-12, 2019. The areas covered on each day are listed in Table 7. The Carson/Wilmington/Long Beach flights on July 11 were coordinated with ORS ML ground operations. The areas surveyed within the Basin included the cities of Carson, Wilmington, Long Beach, El Segundo, Manhattan Beach, and San Bernardino (Figure 25

and Figure 26). Some of the locations within each of the surveyed areas were scanned/imaged at higher resolution for improved measurement sensitivity. The full series of flight surveys is tabulated in Appendix 8.3.

Table 7. Airborne Study Domains and Acquisition Dates

Local Date	Domains of Operation
July 9, 2019	LAX/El Segundo/Manhattan Beach; Carson/Wilmington/Long Beach
July 10, 2019	San Bernardino
July 11, 2019	Carson/Wilmington/Long Beach
July 12, 2019	Central and east Los Angeles

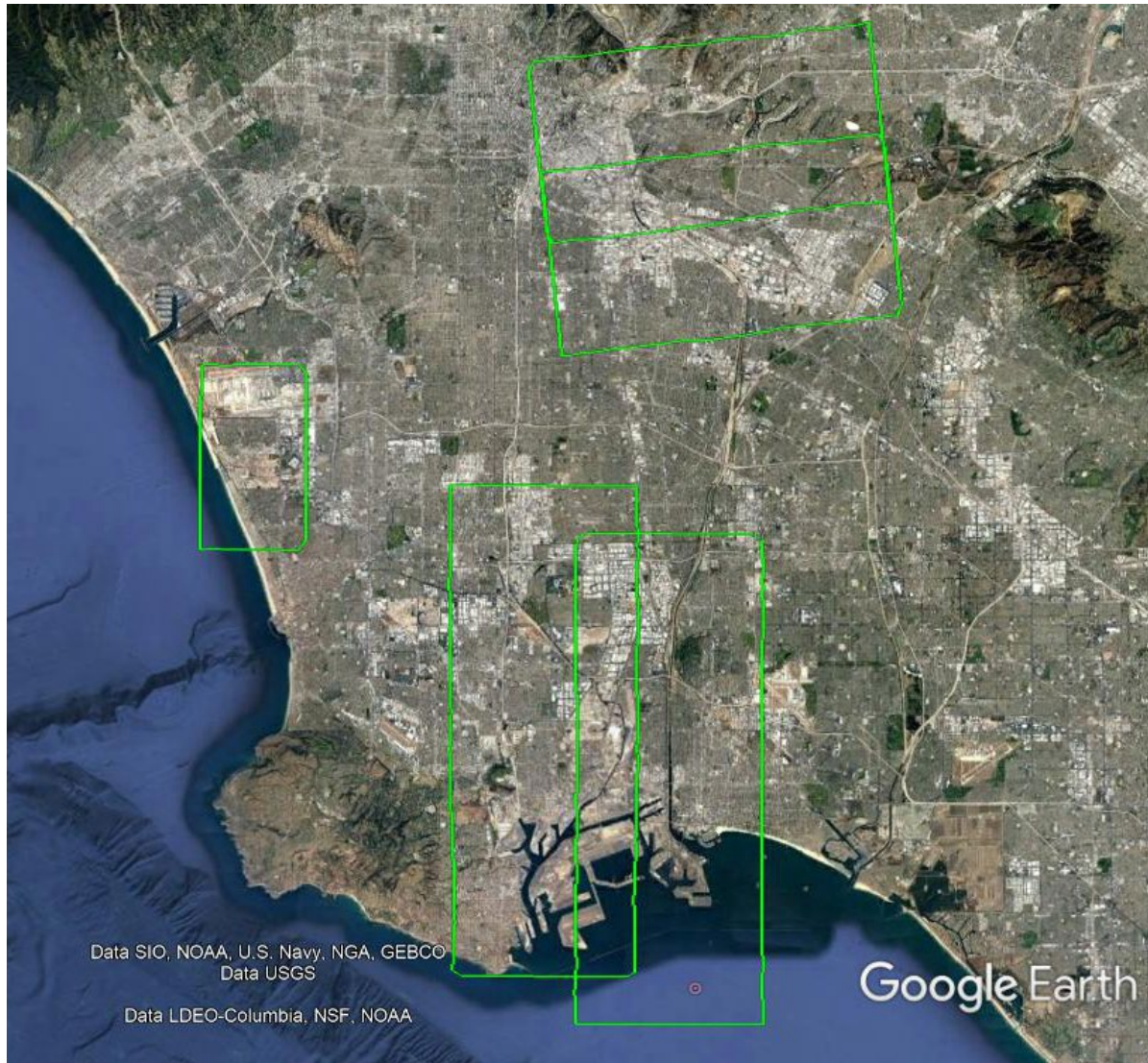


Figure 25. Mako survey areas (green boxes) in the western portion of the Basin.

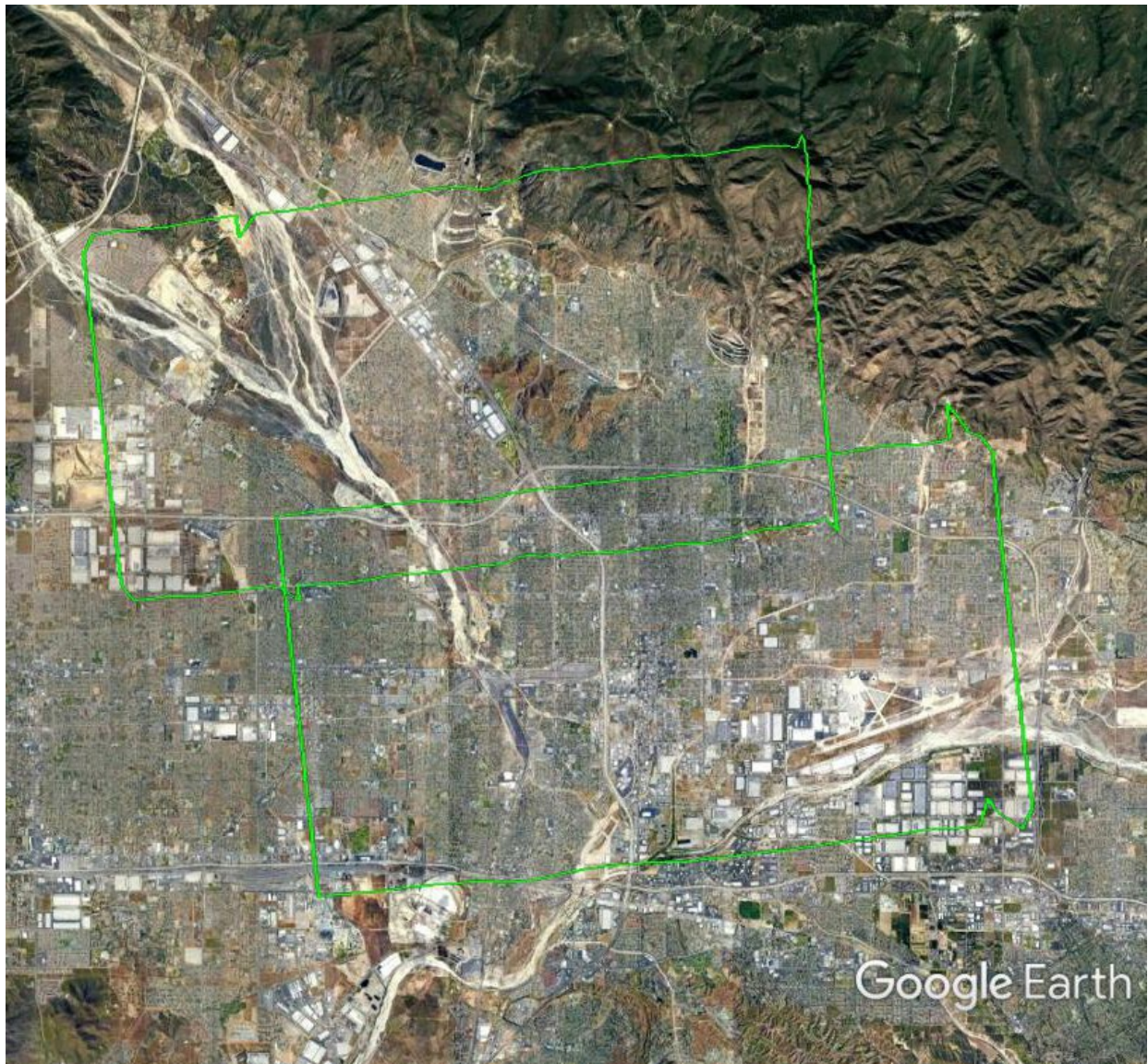


Figure 26. Mako survey areas (green boxes) in the San Bernardino area.

The paucity of detections of pollutants relevant to the MATES study observed in the archival data resulted in flights for MATES V to be conducted at lower altitudes to achieve lower MDQs (Equation 5). Hence, although the large-area survey lines were flown at the standard 2-m GSD, additional surveys were also flown at GSDs in the 0.4-1.0 m range (Appendix 8.4). In particular, a set of locations in central and east Los Angeles were surveyed at 0.4-m GSD. Operating at these low GSDs, and therefore low altitudes, dramatically reduces areal coverage rates from the $32 \text{ km}^2 \text{ min}^{-1}$ quoted in section 5.1, so that considerably more flight lines were required to completely cover all target areas.

5.4.1. LAX/El Segundo/Manhattan Beach Domain

The LAX/El Segundo/Manhattan Beach domain was surveyed on July 9, 2019. The principal target of relevance to MATES V in this domain (Figure 27) is Refinery E. Data from this location showed the

prevalence of ammonia and methane, but also included a weak detection of hydrogen sulfide. Detections of this hydrogen sulfide by Mako are rare due to a combination of its low detectivity in the LWIR (Appendix 8.2) and high degree of controls on emissions of this pollutant. The measured emissions were likely from a relatively small refinery flare stack where, although there was no flaring in progress, the thermal contrast was sufficient to produce measurements of quality above the MDQ. Figure 28(a) shows that hydrogen sulfide was detected at the exit of the refinery flare stack, before the plume temperature equilibrated with that of the ambient air. Figure 28(b) shows the same event, but for methane, with a discernable plume immediately downwind of the stack.

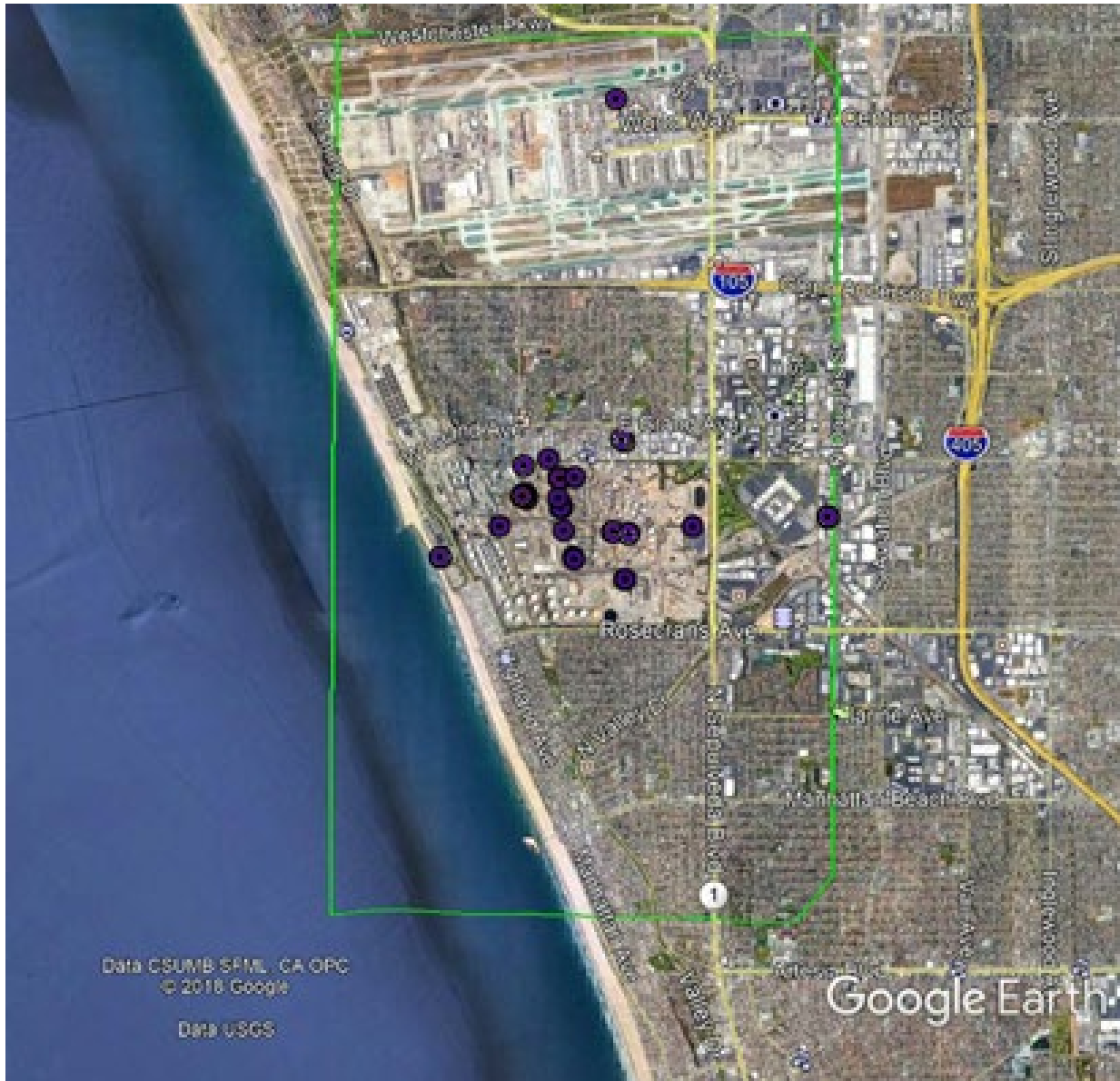


Figure 27. LAX/El Segundo/Manhattan Beach surveyed area (green box). The markers denote emission sites of single gases or mixtures located by Mako.

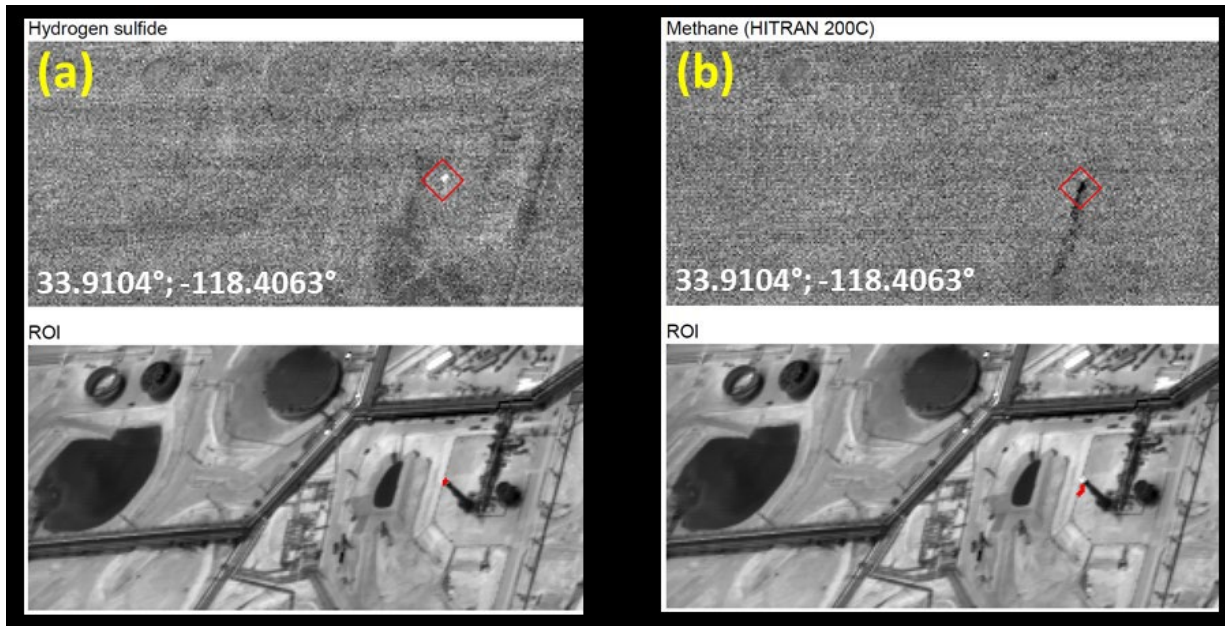


Figure 28. An example of a refinery flare stack emission: (a) hydrogen sulfide filter, and (b) methane filter (survey date: 2019-07-09).

5.4.2. San Bernardino Area

The San Bernardino area was surveyed on July 10, 2019. Measurement results show ubiquitous ammonia and a few methane plume occurrences with single detections of ethene and methanol plumes. No emissions were observed on that day at the Omnitrans facility, which was one of the facilities of interest in San Bernardino. The cluster of emission markers in Figure 29 represents the location of equestrian facilities mainly responsible for the ammonia and methane emissions measured by Mako. Methane emission was noted from the natural gas Generating Station in Redlands.

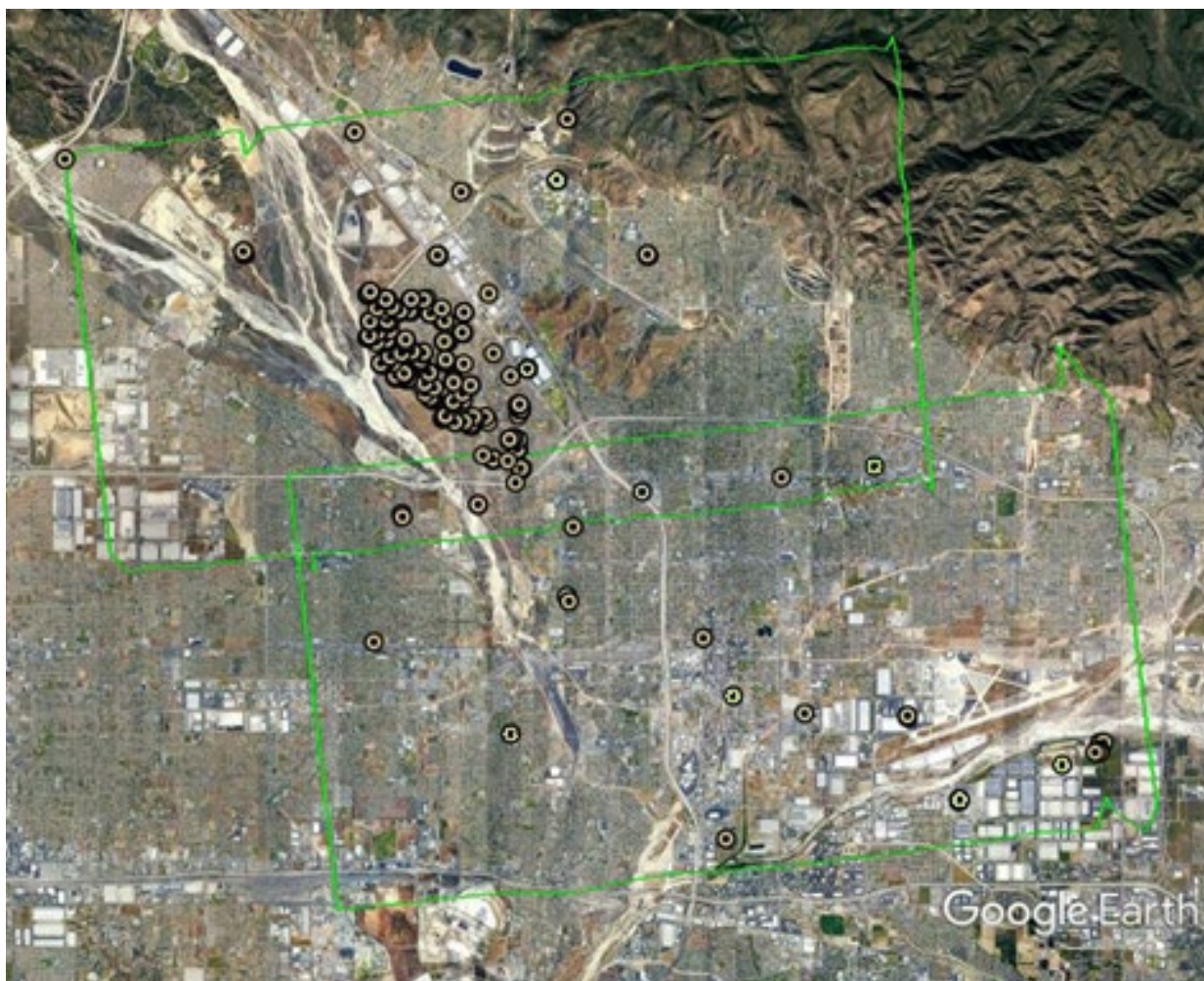


Figure 29. San Bernardino surveyed area (green boxes). The markers denote emission sites of single gases or mixtures (primarily of ammonia and methane) located by Mako.

5.4.3. Carson/Wilmington/Long Beach Area

The Carson/Wilmington/Long Beach area was surveyed on July 11, 2019. The number of emission plumes detected in the Carson/Wilmington/Long Beach industrial corridor attests to the intensity of industrial activity throughout this area (Figure 30). Measured emissions were dominated by ammonia, methane, and ethene emissions. Other COI emissions occasionally present were isobutane, methanol, ethanol, 2-butoxyethanol, 1,4-dichlorobenzene, dichloromethane, and styrene. The latter was often found mixed with acetone and these occurrences were frequently associated with plastics and/or fiberglass manufacturing operations. This commonly observed co-emission pattern constitutes a relatively robust signature for such processes.

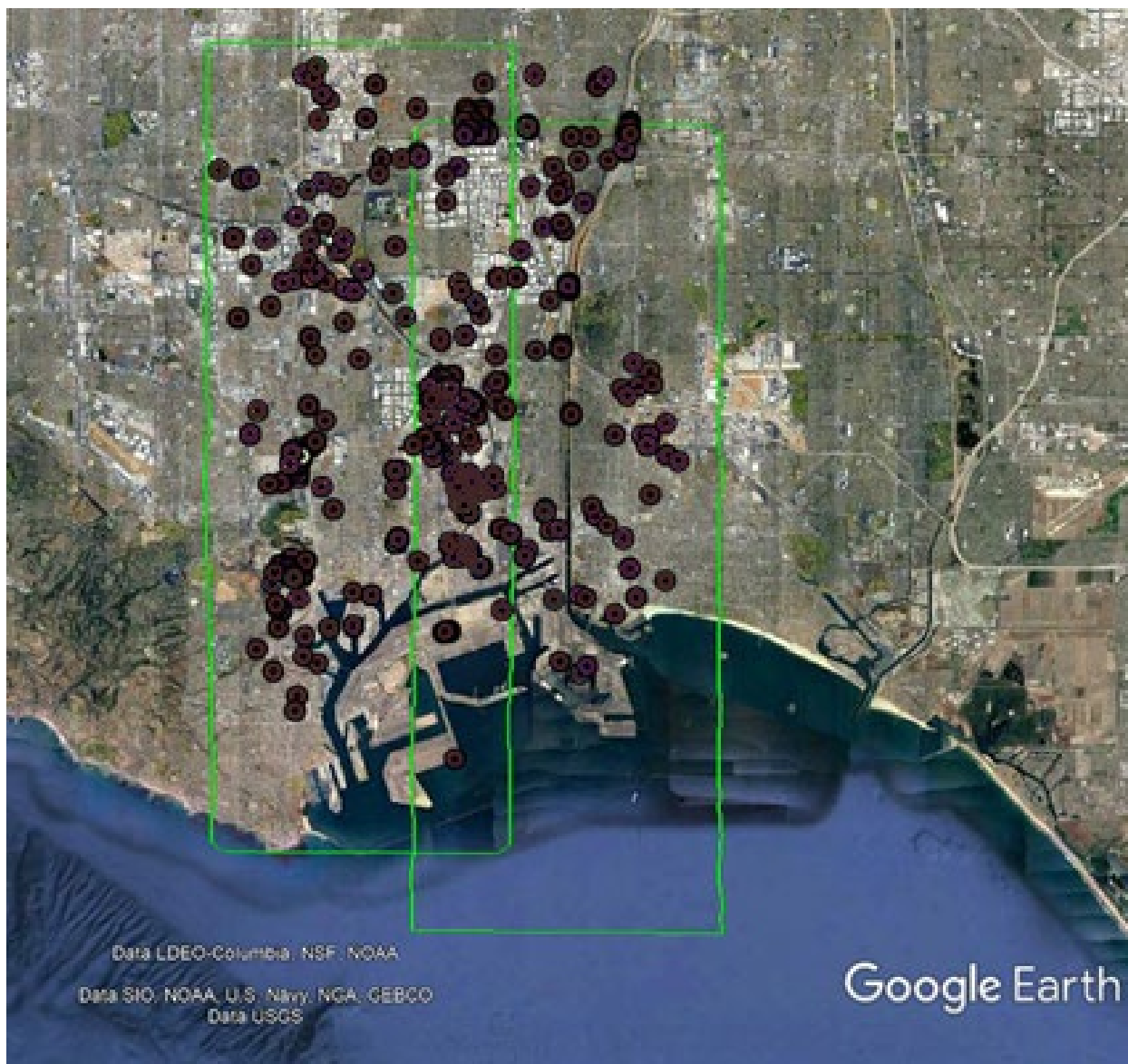


Figure 30. Carson/Wilmington/Long Beach surveyed area (green boxes). The markers denote emission sites of single gases or mixtures located by Mako.

An example of survey detections from the Carson/Wilmington/Long Beach flights is depicted in Figure 31. Figure 31(a) shows emissions of 1,4-dichlorobenzene from a textile manufacturing plant. Although used in the dyeing of fabrics, most apparel manufacturers have discontinued its use. Figure 31(b) shows a ship at berth in the Los Angeles Harbor that was found to be releasing sulfur dioxide from its dual exhaust stacks, possibly using high-sulfur fuel. The instance of styrene, shown in Figure 31(c), was a distributed source at the new I-710 connector under construction in Long Beach. Styrene is a byproduct of petroleum and natural gas processing and can be emitted from fugitive sources such as piping or valves. The major source of styrene is from manufacturing plastics and rubber. Commercial products containing styrene include insulation, fiberglass, plastic pipes, automotive parts, shoes, food containers, and carpet backing. Styrene also is present in motor vehicle exhaust and tobacco smoke. The source(s) of styrene emission presented in Figure 31(c) is unclear. Only one instance of the BTEX compounds was found during the dedicated flights, and it was classified as low confidence. Figure 31(d) shows a low-

confidence detection of benzene from a tank at a distribution complex in Carson. Several methane emission sources were recorded at the patch of waste ground adjacent to the I-405 in Carson. This site is a small privately-operated landfill that closed in 1965 (Gnerre, 2015).

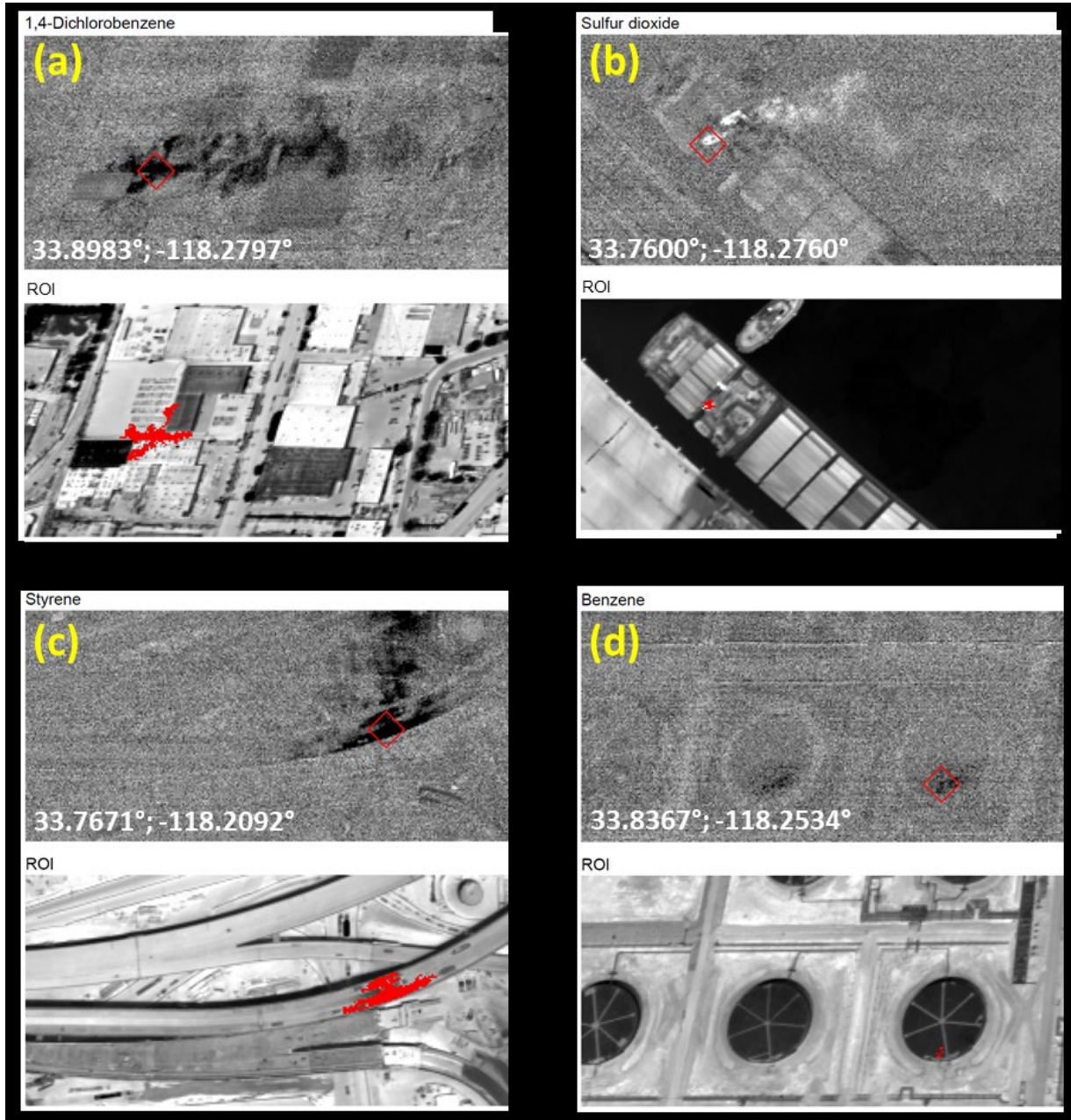


Figure 31. (a) 1,4-Dichlorobenzene from textile manufacturer (survey date 2019-07-09); (b) sulfur dioxide released by a ship at berth (survey date 2019-07-11); (c) styrene from a roadway under construction (survey date 2019-07-11); and (d) low-confidence benzene detection at a tank farm (survey date 2019-07-11).

5.4.4. Central and East Los Angeles Area

The Central and East Los Angeles area was surveyed on July 12, 2019, and is depicted in Figure 32. Predominant emission plumes of ammonia and methane, with some ethene, were detected during these flights. Other species detected were dichloromethane, methanol, ethanol, isopropanol, styrene, and sulfur dioxide. Table 8 summarizes the main emission sources identified in this region, and the main pollutants detected at each location.

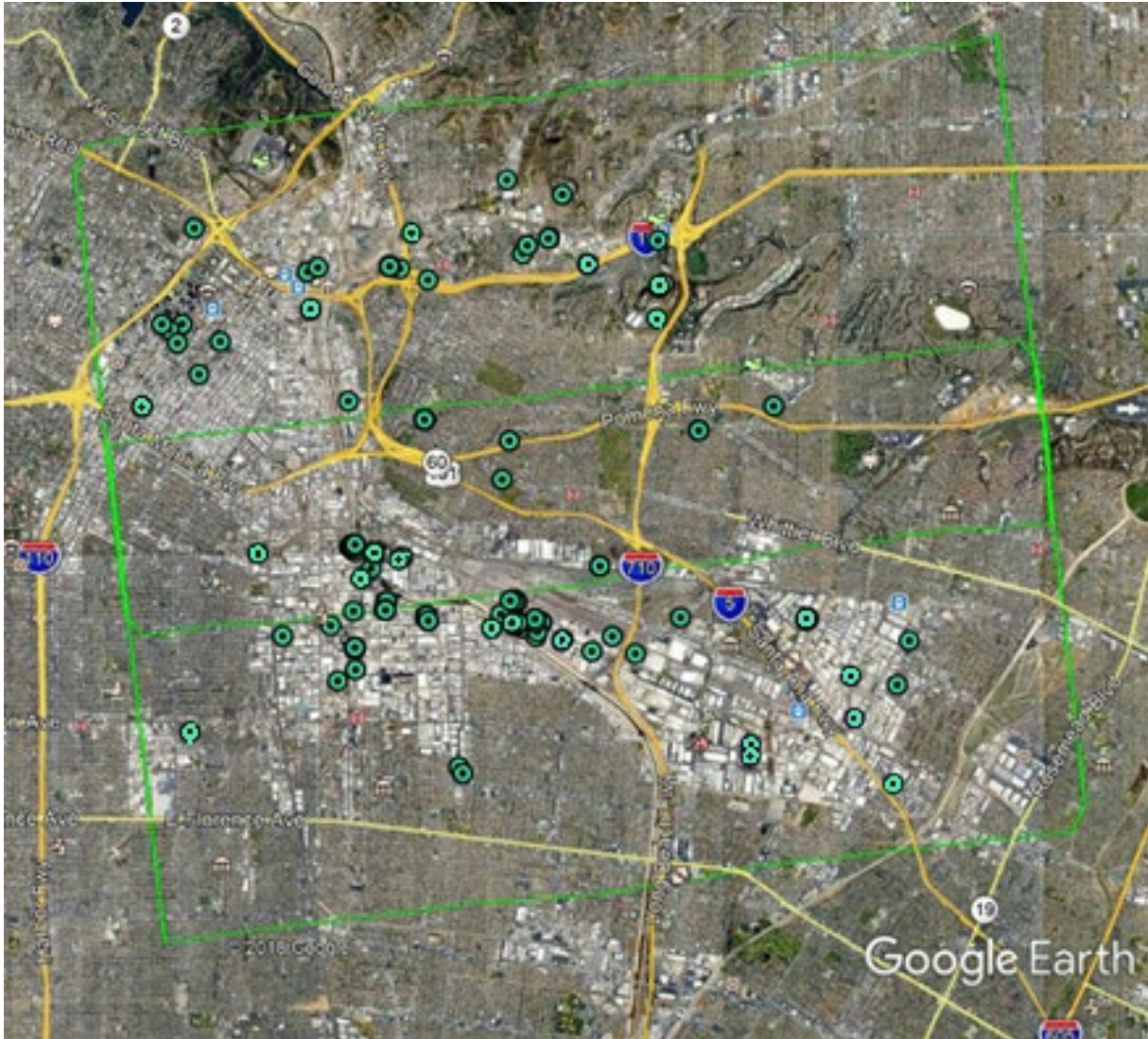


Figure 32. The green boxes represent the area surveyed in Central and East Los Angeles. The markers denote emission sites of single gases or mixtures listed in Table 7 located by Mako.

Table 8. Selected Sites of Special Interest in Central and East Los Angeles with Measured Emissions

Site	Emissions Observed
Rendering Plant (43)	Ammonia
Farmer John (55)	Ammonia
Darling Delaware (74)	Ammonia, Sulfur Dioxide
Baker Commodities (75)	Ammonia, Methane
West Coast Rendering (76)	Ammonia
D & D Cremation Services (77)	Ammonia

A noteworthy finding from the Central and East Los Angeles flights was a three-component plume of ammonia, methanol, and isopropanol, emitted by the Stericycle waste management service facility depicted in Figure 33. Multi-component emissions such as this are uncommon in Mako dataset.

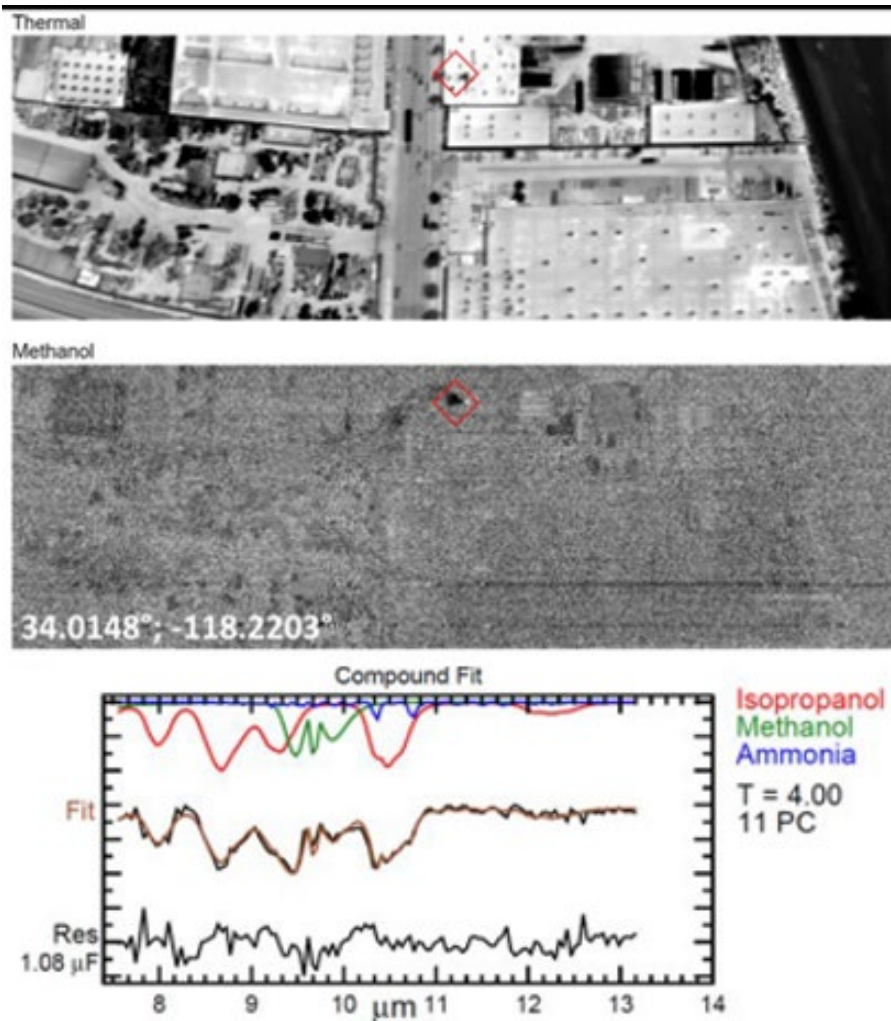


Figure 33. Visualization of three-component plume comprising isopropanol, methanol, and ammonia from a waste management facility, with upper panel showing a thermal image of the sampled area, middle panel showing a plume detection, and lower panel showing spectral fitting identifying these pollutants (survey date 2019-07-12).

5.5. Vehicular Emissions

The MATES V flights showed a number of ammonia emissions from vehicles, with source types ranging from sedans to heavy trucks. Figure 34(a) shows a prominent ammonia plume emitted by an articulated heavy truck, while the sedan about to exit the frame in Figure 34(b) emitted a much smaller, but still detectable, ammonia plume.

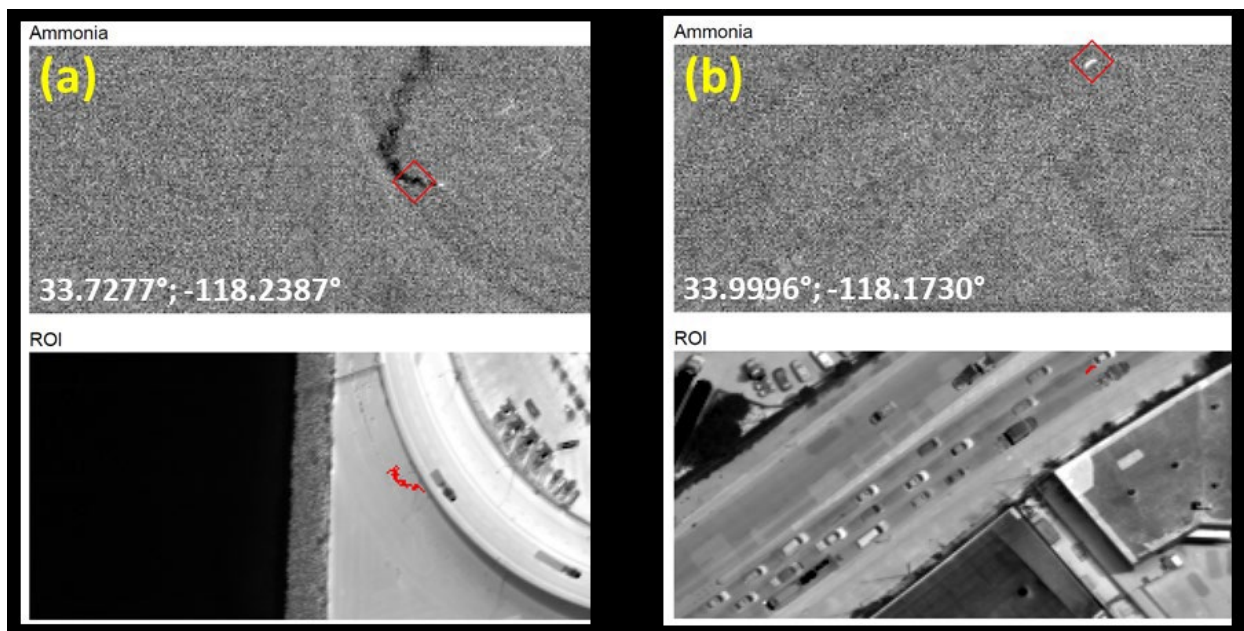


Figure 34. Ammonia emitted by vehicles in motion: (a) articulated truck (survey date 2019-07-11), and (b) sedan (survey date 2019-07-12).

These emissions might have resulted from the use of diesel exhaust fluid, which is a fuel additive that generates ammonia in SCR systems to lower NO_x content in tailpipe exhaust. Although mobile emitters were not a focus of this project, it seems appropriate to mention this trend to highlight the measurement capabilities of the Mako. The MATES V flight data also include a few instances of methanol and ethene being emitted by moving vehicles, which also have not been observed before.

6. Conclusions

Three advanced ORS air monitoring approaches/technologies, namely 1) mobile monitoring surveys using ORS on a mobile platform, 2) an open path optical tent covering a section of a petroleum refinery, and 3) aerial based hyperspectral thermal-infrared imaging, were used in different parts of the South Coast Basin for monitoring of selected air toxic emissions from refineries and other industrial sources; and for assessing potential community impact(s) of these emissions. These measurements were primarily carried out in communities near petroleum refineries with the goal of better assessing certain air toxic concentrations within the most impacted communities, while evaluating the strengths and limitations of the above-mentioned technologies and measurement strategies.

An ORS ML was used to successfully derive emission estimates of total alkanes from six refineries in the Basin. The resulting data was consistent with previous estimates of total alkanes collected during a 2015 pilot study. Ground level concentration data of total alkanes and benzene from the ORS ML show that enhancements above background were primarily observed at refinery fencelines. Enhancements within communities adjacent to refinery communities were observed less frequently, and were usually localized near other sources of air pollution such as vehicle traffic, oil wells, gas stations, and other local sources. The observations conducted during this project demonstrated ORS ML as a powerful tool for leak detection at the fenceline of petroleum facilities for community monitoring and air monitoring applications. As the mobile monitoring dataset expands in the future, a relationship between air pollution measurements made at fencelines of refineries or other industrial facilities and air quality within the community will be further explored.

An optical tent including 10 paths was designed and developed at one of the major refineries in Los Angeles. Since its deployment in August 2020, the optical tent has been operating continuously with a data recovery of over 99%. The main advantage of an open path system with path length arranged in a tent-like configuration is the ability to quickly identify pollution source locations and mitigate emission within the refinery. Highest average BTEX, and most frequent benzene observations above 2 ppb, from normal operation (excluding coating operations) was found near the refinery tanks. Observations inside the refinery identified unforeseen releases due to equipment failure earlier and more clearly than fenceline observations. In many cases, fenceline observations missed BTEX releases observed inside the facility. Realtime optical tent observations have provided the refinery with data to rapidly identify and mediate equipment failures that lead to BTEX releases. The shortened remediation time, therefore, would lead to an overall decrease of BTEX emissions from the facility.

The new optical tent points the way to expanding fenceline BTEX monitoring as a notification tool, to a system that helps the refinery operator to identify and locate BTEX releases, and thus to speed up mitigation efforts. Continuous operation of the optical tent, with nearly 99% data capture, demonstrates feasibility and readiness of this technology for wider use. Although research-grade open path systems were used in this project, commercially available technologies that would allow implementation of optical tents or similar air monitoring approaches at petrochemical facilities already exist. Savings from lost product and personnel hours cost for mitigation of large releases over the lifetime of an optical tent system, may offset capital investment for its installation.

An aerial based hyperspectral thermal IR imaging system was used to measure the concentration of multiple air pollutants over the Basin refineries. This system was able to successfully detect ammonia

and methane, but air toxics levels were below the detection limit of this technique, which is limited compared to other measurement tools. The ability of this imaging system to measure over large areas quickly and the associated advantages over ground-based measurement are appealing, but the lower sensitivity to air toxics, in addition to the high cost of operating an aerial based measurement platform, are critical trade-offs that may not align with many air toxics evaluation measurement goals and purposes.

Overall, all three monitoring approaches were successful in detecting air pollution emissions from multiple sources. The air measurement technologies and methods presented here are cutting edge within the field of air quality monitoring and the use of such strategies is likely to expand in the future. The value of this study lies in the assessment of the strengths and weaknesses of these approaches and their feasibility for implementation.

The airborne hyperspectral imaging approach has a clear advantage in spatial coverage and is a suitable approach for surveying gases typically present at high concentrations (i.e., methane, ammonia, etc.). However, detections of air toxics (benzene, toluene, etc.) were rare, likely because these compounds are typically present at levels below the detection limit of system used. Additionally, there are high costs associated with this monitoring approach that will likely limit the frequency at which such measurements can be made. The two ground-based ORS approaches were effective at detecting air toxics and are more cost-effective options for ongoing air toxic monitoring. South Coast AQMD has implemented an approach that includes the installation of open path systems for continuous ongoing fenceline monitoring at all major refineries in the South Coast Basin as a part of Rule 1180 implementation (South Coast AQMD, 2017b), as well as routine or on-demand mobile air monitoring in environmental justice and other communities (e.g., AB 617 program). Such an arrangement allows for both continuous monitoring of air toxics at refinery fencelines and the ability to respond to air pollution events with community monitoring and/or facility wide emission estimation.

7. References

- Bogumil, K., Orphal, J., Homann, T., Voigt, S., Spietz, P. & Fleischmann, O. et al. (2003). Measurements of molecular absorption spectra with the SCIAMACHY pre-flight model. Instrument characterization and reference data for atmospheric remote-sensing in the 230–2380 nm region. *Journal of Photochemistry and Photobiology A: Chemistry*, 157, 167–184.
- Börjesson, G., Samuelsson, J., Chanton, J., Adolfsson, R., Galle, B. & Svensson, B.H. (2009). A national landfill methane budget for Sweden based on field measurements, and an evaluation of IPCC models. *Tellus B*, 61, 424–435.
- Buckland, K. N., S. J. Young, E. R. Keim, B. R. Johnson, P. D. Johnson, and D. M. Tratt (2017), “Tracking and quantification of gaseous chemical plumes from anthropogenic emission sources within the Los Angeles Basin,” *Remote Sensing of Environment*, 201, 275-296, doi:10.1016/j.rse.2017.09.012.
- Burrows, J., Richter, A., Dehn, A., Deters, B., Himmelmann, S. & Voigt, S. et al. (1999). Atmospheric remote-sensing reference data from GOME-2. Temperature-dependent absorption cross sections of O₃ in the 231-794 nm range. *Journal of Quantitative Spectroscopy and Radiative Transfer*, 61, 509–517.
- Etzkorn, T., Klotz, B., Sørensen, S., Patroescu, I.V., Barnes, I. & Becker, K.H. et al. (1999). Gas-phase absorption cross sections of 24 monocyclic aromatic hydrocarbons in the UV and IR spectral ranges. *Atmospheric Environment*, 33, 525–540.
- Fally, S., Carleer, M. & Vandaele, A.C. (2009). UV Fourier transform absorption cross sections of benzene, toluene, meta-, ortho-, and para-xylene. *Journal of Quantitative Spectroscopy and Radiative Transfer*, 110, 766–782.
- Galle, B., Samuelsson, J., Svensson, B.H. & Borjesson, G. (2001). Measurements of methane emissions from landfills using a time correlation tracer method based on FTIR absorption spectroscopy. *Environmental science & technology*, 35, 21–25.
- Gnerre, S. (2015), “Tracing the history of a very important South Bay vacant lot,” *The Daily Breeze*, 29 August 2015, <http://blogs.dailybreeze.com/history/2015/08/29/tracing-the-history-of-a-very-important-south-bay-vacant-lot>.
- Griffith, D. (1996). “Synthetic Calibration and Quantitative Analysis of Gas-Phase FT-IR Spectra” *Applied Spectroscopy* 50,1
- Hall, J. L., R. H. Boucher, K. N. Buckland, D. J. Gutierrez, E. R. Keim, D. M. Tratt, and D. W. Warren (2016), “Mako airborne thermal infrared imaging spectrometer – performance update,” *Proceedings of SPIE*, 9976, 997604, doi:10.1117/12.2239245.
- Horel, J., M. Splitt, L. Dunn, J. Pechmann, B. White, C. Ciliberti, S. Lazarus, J. Slemmer, D. Zaff, and J. Burks (2002), “MesoWest: Cooperative mesonets in the western United States,” *Bulletin of the American Meteorological Society*, 83(2), 211-225, doi:10.1175/1520-0477(2002)083<0211:MCMITW
- Johnson, T. J., R. L. Sams, and S. W. Sharpe (2004), “The PNNL quantitative infrared database for gasphase sensing: a spectral library for environmental, hazmat and public safety standoff detection”, *Proceedings of SPIE*, 5269, 159-167, doi:10.1117/12.515604.

Kraus, S. (2006). DOASIS: a framework design for DOAS, PhD Thesis, Technische Informatik, Univ. Mannheim, Shaker, Aachen, 2006.

Mellqvist, J. (1999). Application of infrared and UV-visible remote sensing techniques for studying the stratosphere and for estimating anthropogenic emissions. PhD, Göteborg, Sweden.

Mellqvist, J., Johansson, J., Samuelsson, J. & Offerle, B. (2008a). Emission Measurements of Volatile Organic Compounds with the SOF method in Normandy 2008.

Mellqvist, J., Johansson, J., Samuelsson, J., Rivera, C., Lefer, B. & Alvarez, S. (2008b). Comparison of Solar Occultation Flux Measurements to the 2006 TCEQ Emission Inventory and Airborne Measurements for the TexAQ5 II. Project No. 582-5-64594-FY08-06, TCEQ report., Texas.

Mellqvist, J., Samuelsson, J., Johansson, J., Rivera, C., Lefer, B. & Alvarez, S. et al. (2010). Measurements of industrial emissions of alkenes in Texas using the solar occultation flux method. *J. Geophys. Res.*, 115.

Mellqvist, J., Samuelsson, J., Offerle, B., Salberg, H., Johansson, J. & Jakkola, S. (2009). Emission Measurements of Volatile Organic Compounds with the SOF method in the Rotterdam Harbor 2008.

Office of Environment Health Hazard Assessment (OEHA), 2016, Tetrachloroethylene, <https://oehha.ca.gov/chemicals/tetrachloroethylene>, accessed 10-07-2022.

Office of Environment Health Hazard Assessment (OEHA), 2008, Appendix D. Individual Acute, 8-Hour, and Chronic Reference Exposure Level Summaries, page 140, <https://oehha.ca.gov/media/downloads/crn/appendixd1final.pdf>, accessed 09/11/23.

Open GIS Consortium, Inc. (OGC), <https://www.ogc.org/>, accessed September 2022.

Platt, U. and Stutz, J. (2008) Differential Optical Absorption Spectroscopy Principles and Applications. Springer-Verlag. Rothman, L.S., Barbe, A., Chris Benner, D., Brown, L.R., Camy-Peyret, C. & Carleer, M.R. et al. (2003). The HITRAN molecular spectroscopic database. Edition of 2000 including updates through 2001. *Journal of Quantitative Spectroscopy and Radiative Transfer*, 82, 5–44.

Sharpe, S.W., Johnson, T.J., Sams, R.L., Chu, P.M., Rhoderick, G.C. & Johnson, P.A. (2004). Gas-phase databases for quantitative infrared spectroscopy. *Applied spectroscopy*, 58, 1452–1461.

South Coast Air Quality Management District (2021), MATES V Multiple Air Toxics Exposure Study in the South Coast AQMD, Final Report, August 2021, <http://www.aqmd.gov/docs/default-source/planning/mates-v/mates-v-final-report-9-24-21.pdf?sfvrsn=6> (accessed September 2023).

South Coast Air Quality Management District (2019), Rule 1180 Community Air Monitoring Plan, https://www.aqmd.gov/docs/default-source/fenceline_monitroing/r1180_draft_community_monitoring_plan_rev_2_04022020_final_use_updated1.pdf?sfvrsn=8 (accessed September 2023).

South Coast Air Quality Management District (2017a), Emission Measurements of VOCs, NO₂ and SO₂ from the Refineries in the South Coast Air Basin Using Solar Occultation Flux and Other Optical Remote Sensing Methods, Final Report, April 2017, <http://www.aqmd.gov/docs/default->

[source/fenceline_monitoring/project_1/fluxsense_scaqmd2015_project1_finalreport\(040717\).pdf?sfvrsn=10](https://www.aqmd.gov/source/fenceline_monitoring/project_1/fluxsense_scaqmd2015_project1_finalreport(040717).pdf?sfvrsn=10) (accessed September 2022).

South Coast Air Quality Management District (2017b), Rule 1180 – Refinery Community and Fenceline Air Monitoring, <http://www.aqmd.gov/home/rules-compliance/rules/support-documents/rule-1180-refinery-fenceline-monitoring-plans> (accessed September 2022).

Stutz, J., Hurlock, S.C., Colosimo, S.F., Tsai, C., Cheung, R., Festa, J., Pikelnaya, O., Alvarez, S., Flynn, J.H., Erickson, M.H., Olaguer, E.P. (2016). A novel dual-LED based long-path DOAS instrument for the measurement of aromatic hydrocarbons. *Atmospheric Environment*, 147, 1352–2310.

8. Appendices

8.1. Histograms of Optical Tent BTEX Retrieval Errors

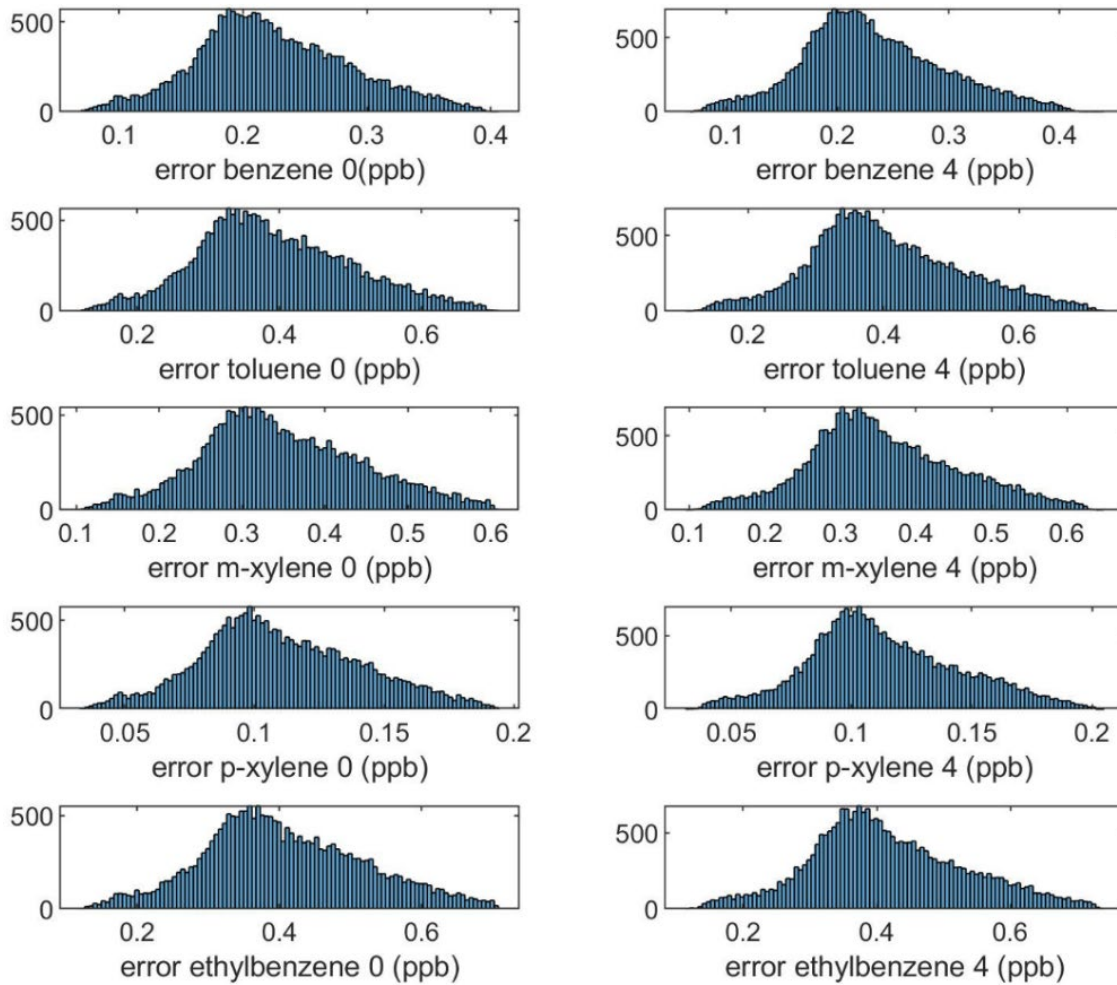


Figure 8.1. Histogram of retrieval errors of BTEX compounds along the two fenceline paths (Path 1 on left, Path 5 on right) of System 1 during the entire operation period of the optical tent.

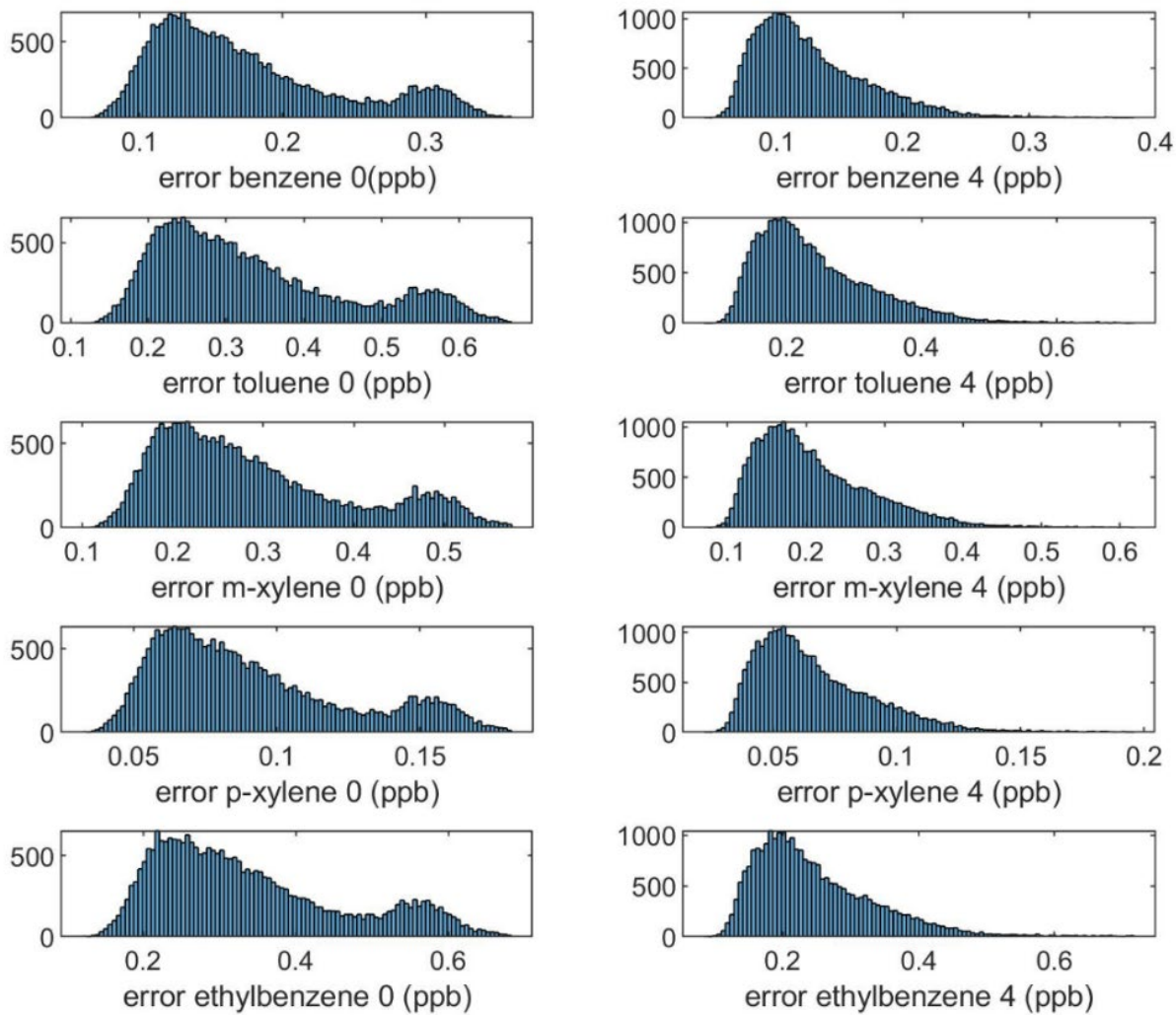


Figure 8.2. Histogram of retrieval errors of BTEX compounds along the two fenceline paths (Path 1 on left, Path 5 on right) of System 2 during the entire operation period of the optical tent. The double peak in the left figures is likely due to two very specific conditions on this path that sometimes lead to higher errors.

8.2. COIs and Associated Mako MDQs

Gas	CAS*	NECL** (ppm-m K)	MDQ*** (kg/h)
1,1-Dichloroethane	75-34-3	74.00	6.47
1,2-Dichloroethane	107-06-2	124.11	10.85
1,2-Dibromoethane	106-93-4	33.45	5.55
1,3-Butadiene	106-99-0	46.64	2.23
1,3-Dichlorobenzene	541-73-1	19.12	2.48
1,4-Dichlorobenzene	106-46-7	11.83	1.54
Acetaldehyde	75-07-0	429.67	16.72
Acetylene	74-86-2	138.09	3.18
Acrolein	107-02-8	87.68	4.34
Ammonia	7664-41-7	14.91	0.22
Benzene	71-43-2	424.03	29.26
Butane	106-97-8	1583.28	81.29
Carbon tetrachloride	56-23-5	4.86	0.66
Carbonyl sulfide	463-58-1	348.81	18.51
Chloroform	67-66-3	7.78	0.82
Dichloromethane	75-09-2	37.52	2.81
Ethane	74-84-0	2161.53	57.42
Ethanol	64-17-5	153.31	6.24
Ethene	74-85-1	33.20	0.82
Ethylbenzene	100-41-4	389.33	36.51
Formaldehyde	50-00-0	685.05	18.17
Hexane	110-54-3	2008.21	152.88
Hydrogen cyanide	74-90-8	798.47	19.06
Hydrogen sulfide	7783-06-4	37887.40	1140.48
Isobutane	75-28-5	496.69	25.50
Methane	74-82-8	669.21	9.48
Methanol	67-56-1	59.85	1.69
Naphthalene	91-20-3	16.60	1.88
Nitrogen dioxide	10102-44-0	1433.40	58.25
Nitrogen dioxide and dimer	10544-72-6	N/A	N/A
Octane	111-65-9	1402.29	141.50
Pentane	109-66-0	1209.83	77.11
Propane	74-98-6	2249.93	87.64
Propene	115-07-1	95.41	3.55
Styrene	100-42-5	56.68	5.22
Sulfur dioxide	7446-09-5	312.00	17.66
tert-Butyl methyl ether	1634-04-4	29.91	2.33
Tetrachloroethylene	127-18-4	8.85	1.30
Toluene	108-88-3	680.43	55.38
Trichloroethylene	79-01-6	15.71	1.82
Vinyl chloride	75-01-4	70.07	3.87
m-Xylene	108-38-3	56.53	5.30
o-Xylene	95-47-6	356.73	33.46
p-Xylene	106-42-3	74.03	6.94

*Chemical Abstract Service (CAS) numbers are listed for unambiguous chemical specification.

**NECL = Noise Equivalent Concentration Length (Buckland et al., 2017).

***MDQs are listed for a light industrial clutter type with $\Delta T = 5$ K, $u = 5$ m/s and pressure of 1 atm at 2-m GSD.

Refer to Section 1.4 for conversion to other conditions.

8.3. Summary of Historical Data Over L.A. Refineries and Related Sites

AGL = Above Ground Level

GSD = Ground-Sample Distance

Location	Local Date	Sessions	AGL (ft)	GSD (m)	Comments
Binary Starfire					
Anaheim St. refinery, Long Beach	2018-09-11	180911_184539	6,000	1.0	
Chevron Refinery	2018-09-14	180914_173308 180914_174258 180914_175249 180914_181252 180914_182246 180914_183257 180914_184304	5,000	0.8	
Torrance Refinery	2018-09-14	180914_184935 180914_185635 180914_190129	5,000	0.8	
Carson tank farm	2018-09-14	180914_190623 180914_191052 180914_191531	5,000	0.8	
Carson BP Refinery	2018-09-14	180914_191937 180914_192349 180914_192821 180914_193313 180914_193743 180914_194239 180914_194802	5,000	0.8	
Kinder Morgan tank farm, Long Beach	2018-09-15	180915_184854	5,000	0.8	
Refinery and tanks, LB Port	2018-09-15	180915_185343 180915_211323 180915_211815	5,000	0.8	
Tesoro Refinery	2018-09-15	180915_212521	5,000	0.8	
San Pedro Refinery	2018-09-15	180915_213143	5,000	0.8	
Tesoro Refinery and Praxair	2018-09-15	180915_215023	5,000	0.8	
Tesoro Refinery and Praxair	2018-09-15	180915_215952 180915_220453 180915_220953	5,000	0.8	
San Pedro Refinery	2018-09-15	180915_213644 180915_214114 180915_214547	5,000	0.8	
Paramount Petroleum and residences	2018-09-15	180915_221400	5,000	0.8	
N. Long Beach tank farm	2018-09-15	180915_221753 180915_222229	5,000	0.8	
Paramount Refinery	2018-09-15	180915_223309	5,000	0.8	
Chevron Refinery	2018-09-15	180916_013718 180916_014358	5,000	0.8	

Torrance Refinery	2018-09-15	180916_014917 180916_015436 180916_015906	5,000	0.8	
Carson BP Refinery	2018-09-15	180916_020801 180916_021833 180916_022224	5,000	0.8	
Urban Vigil					
El Segundo Refinery	2017-06-21	170621_221414	6,000	1.0	
El Segundo Refinery	2017-06-21	170621_233348	12,000	2.0	
El Segundo Refinery	2017-06-21	170621_235532	12,000	2.0	
Torrance Refinery	2017-06-21	170622_001304	12,000	2.0	
Port of Long Beach/refineries	2017-06-21	170622_002655	12,000	2.0	
El Segundo Refinery	2017-06-27	170627_220020	6,000	1.0	
Devils Gulch					
El Segundo Refinery	2017-05-04	170504_191500	12,000	2.0	Cloud contamination
J2M					
El Segundo Refinery	2017-04-09	170410_000334	12,000	2.0	First flight with new FPA ("Mako-2")
Torrance Refinery	2017-04-09	170410_005624	12,000	2.0	First flight with new FPA ("Mako-2")
Port of Long Beach/refineries	2017-04-09	170410_011501	12,000	2.0	First flight with new FPA ("Mako-2")

Location	Local Date	Sessions	AGL (ft)	GSD (m)	Comments
New Dawn					
Torrance Refinery	2016-08-15	160816_001210	12,000	2.0	
Port of Long Beach/refineries	2016-08-15	160815_234925 160816_000130	12,000	2.0	
Mystic Jewel					
El Segundo Refinery	2016-05-10	160511_003534	12,000	2.0	INS / PTS issues this mission; use w/caution

El Segundo Refinery	2016-05-11	160511_224502	12,000	2.0	INS / PTS issues this mission; use w/caution
Torrance Refinery	2016-05-11	160511_230152	12,000	2.0	INS / PTS issues this mission; use w/caution; no georeferencing
Port of Long Beach/refineries	2016-05-11	160511_231634 160511_233322	12,000	2.0	INS / PTS issues this mission; use w/caution
El Segundo Refinery	2016-05-14	160514_214722	12,000	2.0	INS / PTS issues this mission; use w/caution
Torrance Refinery	2016-05-14	160514_224436 160514_225821 160514_231246	12,000	2.0	INS / PTS issues this mission; use w/caution
Obsidian Dawn					
El Segundo Refinery	2015-09-23	150923_194126	12,000	2.0	
Port of Long Beach/refineries	2015-09-23	150923_195243	12,000	2.0	
Carson Refinery	2015-09-23	150923_205217	6,000	1.0	
El Segundo Refinery	2015-09-25	150926_050045	12,000	2.0	Nighttime collect
Torrance Refinery	2015-09-25	150926_051110	12,000	2.0	Nighttime collect
Port of Long Beach/refineries	2015-09-25	150926_052234	12,000	2.0	Nighttime collect
Carson Refinery	2015-09-25	150926_054417	6,000	1.0	Nighttime collect
El Segundo Refinery	2015-09-29	150929_182737	12,000	2.0	Wide-angle scan over El Segundo including LAX
El Segundo Refinery	2015-09-29	150929_183349	12,000	2.0	Wide-angle scan over El Segundo including LAX
Terminal Frost					
El Segundo Refinery	2015-04-21	150421_213721	12,000	2.0	Broken cloud
Torrance Refinery	2015-04-21	150421_215252	12,000	2.0	Broken cloud
Port of Long Beach/refineries	2015-04-21	150421_220707	12,000	2.0	Broken cloud
Port of Long Beach/refineries	2015-04-22	150422_113920	12,000	2.0	Broken cloud; nighttime collect
Radiant Gray					
El Segundo Refinery	2014-07-22	140722_172729	12,000	2.0	
Torrance Refinery	2014-07-22	140722_180401	12,000	2.0	
Port of Long Beach/refineries	2014-07-22	140722_182048	12,000	2.0	
Port of Long Beach/refineries	2014-07-22	140722_184416	12,000	2.0	

Open Road					
El Segundo Refinery	2013-08-26	130826_190629 130826_193755 130826_194750	4,000	0.7	
Torrance Refinery	2013-08-26	130826_215830	12,000	2.0	
Port of Long Beach/refineries	2013-08-26	130826_221236	12,000	2.0	
El Segundo Refinery	2013-08-28	130828_182348	12,000	2.0	
Port of Long Beach/refineries	2013-08-28	130829_020748	12,000	2.0	
Torrance Refinery	2013-08-28	130829_022845	12,000	2.0	
El Segundo Refinery	2013-08-29	130830_025746	12,000	2.0	
Port of Long Beach/refineries	2013-08-30	130830_212703	12,000	2.0	
Rampant Shark					
El Segundo Refinery	2011-08-24	110824_205854	12,000	2.0	Caution: FPA issues
El Segundo Refinery	2011-08-24	110824_211450	12,000	2.0	Caution: FPA issues
El Segundo Refinery	2011-08-24	110824_213000	12,000	2.0	Caution: FPA issues
El Segundo Refinery	2011-08-24	110824_232323	12,000	2.0	Caution: FPA issues
El Segundo Refinery	2011-08-24	110824_220145	12,000	2.0	Caution: FPA issues
Port of Long Beach/refineries	2011-08-24	110824_224447	12,000	2.0	Caution: FPA issues
Port of Long Beach/refineries	2011-08-24	110824_225408	12,000	2.0	Caution: FPA issues
Torrance Refinery	2011-08-24	110824_230208	12,000	2.0	Caution: FPA issues
Torrance Refinery	2011-08-24	110824_231135	12,000	2.0	Caution: FPA issues
Anaheim St. refinery, Long Beach	2011-08-28	110828_213048	12,000	2.0	Caution: FPA issues
Test Flight-1					
El Segundo Refinery	2010-09-15	100916_014933	12,000	2.0	~3x the NESR design point; no georeferencing

8.4. Summary of Data Collected During MATES V Flights

Location	Local Date	Sessions	AGL (ft)	GSD (m)	Comments
Mates Five					
El Segundo Refinery	2019-07-09	190709_202255	4,000	0.7	
El Segundo survey	2019-07-09	190709_204138	6,000	1.0	
LAX/El Segundo/Manhattan Beach survey	2019-07-09	190709_210516	12,000	2.0	
Carson/Wilmington/Long Beach survey	2019-07-09	190709_211646 190709_213354	12,000	2.0	
Phillips 66 Wilmington Refinery	2019-07-09	190709_214637	12,000	2.0	Multilook; no georeferencing
Tesoro Calciner, Long Beach	2019-07-09	190709_215413	12,000	2.0	Multilook
Tesoro Carson Refinery	2019-07-09	190709_215913	12,000	2.0	Multilook
Tesoro Wilmington Refinery	2019-07-09	190709_220528	12,000	2.0	Multilook
San Bernardino survey	2019-07-10	190710_203717 190710_210700 190710_211713	12,000	2.0	190710_203717: No georeferencing
San Bernardino survey	2019-07-10	190710_213035 190710_213725 190710_214609 190710_215353 190710_220200 190710_221322 190710_222300	6,000	1.0	
San Bernardino survey	2019-07-10	190710_223233 190710_224039 190710_224922 190710_225858 190710_230732 190710_231621 190710_232441 190710_233232 190710_234038	4,000	0.7	190710_224922: No georeferencing
Omnitrans facility, San Bernardino	2019-07-10	190710_234836	4,000	0.7	Multilook
Carson/Wilmington/Long Beach survey	2019-07-11	190711_192553 190711_193513 190711_194622 190711_195834 190711_200857 190711_201907 190711_202857	6,000	1.0	
Carson/Wilmington/Long Beach survey	2019-07-11	190711_204218 190711_204936 190711_205719 190711_210507 190711_211256 190711_212038 190711_212754 190711_213538 190711_214322 190711_215126 190711_215900 190711_220618 190711_221404 190711_222149 190711_222938 190711_223732 190711_224541 190711_225342 190711_230125 190711_230841 190711_231600	4,000	0.7	

Light industries and recycling, Central L.A.	2019-07-12	190712_205418	12,000	2.0	
Light industries and recycling, East L.A.	2019-07-12	190712_210012	12,000	2.0	
Light industries, recycling, railyard, Vernon	2019-07-12	190712_210624	12,000	2.0	
East L.A. survey	2019-07-12	190712_211441 190712_212423 190712_213330 190712_214239 190712_215231 190712_220133	7,000	1.2	
Republic Services (Waste Transfer Station), East L.A.	2019-07-12	190712_221246	2,000	0.4	
Southland Disposal, GU's Recycling, East L.A.	2019-07-12	190712_221819	2,000	0.4	
Toxic waste handlers/recyclers, Central L.A.	2019-07-12	190712_222226	2,000	0.4	
Darling Delaware Co., Vernon	2019-07-12	190712_222732	2,000	0.4	
Exide Technologies/Rendering and Cremation/Baker Commodities, Vernon	2019-07-12	190712_223225	2,000	0.4	
Preferred Freezer Services, Vernon	2019-07-12	190712_223800	2,000	0.4	

8.5. Technical Reports Addendum Asset Summaries (TRAAS)

All Aerospace deliverable reports containing measurements generated with the assistance of technical measurement and test equipment must provide a summary report indicating that the equipment met all calibration and maintenance requirements during the period in which the data were gathered, in accordance with Corporate practice.

The following TRAAS reports concern equipment used to certify integrity of the data products used to support MATES V and are provided in fulfillment of Aerospace Corporate policy. Because the policy was enacted in 2011, no TRAAS report is available for the 2010 data collect. However, the absence of a TRAAS report does not signify any deficiency in QA/QC practices at the working level.

Technical Reports Addendum Asset Summary #2019071517111421892			
Report Name: Mako Mates Five July 2019			
First Aerospace Author / PI: Dr. Eric R Keim			
Created By: Dr. Eric R Keim			
NON Aerospace MTE: <i>No assets reported.</i>			
<hr/>			
ACX389	LAKESHORE CRYOTRONICS INC 218	Usage Dates: 07/09/2019 - 07/13/2019	
Calibration Date	Calibration Due Date	Certificate Number	Certificate Notes
10/31/2017	09/29/2019	FD9AD68A-4595-4820-95A7-21D7C8987 B02	TMT-NORMAL
<hr/>			
ADI688	SANTA BARBARA INFRARED DDB-06-A-06-A-L-25-ES-P	Usage Dates: 07/09/2019 - 07/13/2019	
Calibration Date	Calibration Due Date	Certificate Number	Certificate Notes
07/02/2019	01/31/2021	62743D2D-5535-48A6-B1E0-A89DBC2C B318	TMT-NORMAL
<hr/>			
page 1 / 1			

Technical Reports Addendum Asset Summary #2019010316312521892

Report Name: Mako Binary Starfire September 2018
First Aerospace Author / PI: Dr. Eric R Keim
Created By: Dr. Eric R Keim

NON Aerospace MTE: *No assets reported.*

ACA970 SANTA BARBARA INFRARED DDB-06-A-06-A-L-25-ES-X Usage Dates: 09/10/2018 - 09/16/2018

Calibration Date	Calibration Due Date	Certificate Number	Certificate Notes
08/02/2017	07/28/2019	2DD0BD11-070D-4242-B1C0-347ADB5A C848	TMT-NORMAL

ACI696 SORENSEN COMPANY XTS60-1MRA Usage Dates: 09/10/2018 - 09/16/2018

Calibration Date	Calibration Due Date	Certificate Number	Certificate Notes
06/20/2017	06/16/2019	A02508CA-1AAF-43B6-BB28-2EEEE75F CFF7	TMT-NORMAL

ACX389 LAKESHORE CRYOTRONICS INC 218 Usage Dates: 09/10/2018 - 09/16/2018

Calibration Date	Calibration Due Date	Certificate Number	Certificate Notes
10/31/2017	09/29/2019	FD9AD68A-4595-4820-95A7-21D7C8987 B02	TMT-NORMAL

Technical Reports Addendum Asset Summary #2017070610251621892

Report Name: Mako Urban Vigil June 2017

JO: 837600

First Aerospace Author / PI: Dr. Eric R Keim

Created By: Dr. Eric R Keim

NON Aerospace MTE: *No assets reported.*

ACA970 SANTA BARBARA INFRARED DDB-06-A-06-A-L CONTROLLER, BLACKBODY Usage Dates: 06/21/2017 - 06/30/2017

Calibration Date	Calibration Due Date	Certificate Number	Certificate Notes
12/28/2015	08/27/2017	1cd6593045eb574491d05467a2ef3ba2	TMT-NORMAL

ACI696 SORENSEN COMPANY XTS60-1MRA POWER SUPPLY, PROGRAMMABLE Usage Dates: 06/26/2017 - 06/30/2017

Calibration Date	Calibration Due Date	Certificate Number	Certificate Notes
06/20/2017	06/16/2019	5298d55e28bde94595805c84e7b871ad	TMT-NORMAL

ACX389 LAKESHORE CRYOTRONICS INC 218 MONITOR, TEMPERATURE Usage Dates: 06/21/2017 - 06/30/2017

Calibration Date	Calibration Due Date	Certificate Number	Certificate Notes
03/21/2016	10/15/2017	d331fd3d7e887c4f841670e6b35eae89	TMT-NORMAL

Technical Reports Addendum Asset Summary #2017051512314821892

Report Name: Mako Devils Gulch May 2017

JO: 837600

First Aerospace Author / PI: Keim, Eric R

Created By: Keim, Eric R

NON Aerospace MTE: *No assets reported.*

ACA970 SANTA BARBARA INFRARED DDB-06-A-06-A-L CONTROLLER, BLACKBODY Usage Dates: 05/01/2017 - 05/04/2017

Calibration Date	Calibration Due Date	Certificate Number	Certificate Notes
12/28/2015	08/27/2017	1cd6593045eb574491d05467a2ef3ba2	TMT-NORMAL

ACI696 SORENSEN COMPANY XTS60-1MRA POWER SUPPLY, PROGRAMMABLE Usage Dates: 05/01/2017 - 05/04/2017

Calibration Date	Calibration Due Date	Certificate Number	Certificate Notes
09/24/2015	05/21/2017	78e6a95d01d23e41b413cb2fbc8ccb8a	TMT-NORMAL

ACJ073 LAKESHORE CRYOTRONICS INC 218 MONITOR, TEMPERATURE Usage Dates: 05/01/2017 - 05/04/2017

Calibration Date	Calibration Due Date	Certificate Number	Certificate Notes
04/06/2017	06/25/2017	4d943cec2fb443429ecd08d53072d851	Extension

Technical Reports Addendum Asset Summary #2017041808230121892

Report Name: Mako J2M April 2017

JO: 894100

First Aerospace Author / PI: Keim, Eric R

Created By: Keim, Eric R

NON Aerospace MTE: *No assets reported.*

ACA970 SANTA BARBARA INFRARED DDB-06-A-06-A-L CONTROLLER, BLACKBODY Usage Dates: 04/07/2017 - 04/10/2017

Calibration Date	Calibration Due Date	Certificate Number	Certificate Notes
12/28/2015	08/27/2017	1cd6593045eb574491d05467a2ef3ba2	TMT-NORMAL

ACJ073 LAKESHORE CRYOTRONICS INC 218 MONITOR, TEMPERATURE Usage Dates: 04/07/2017 - 04/10/2017

Calibration Date	Calibration Due Date	Certificate Number	Certificate Notes
04/06/2017	06/25/2017	4d943cec2fb443429ecd08d53072d851	Extension

Technical Reports Addendum Asset Summary #2016082508522321892

Report Name: Mako New Dawn August 2016

JO: 812100

First Aerospace Author / PI: Keim, Eric R

Created By: Keim, Eric R

NON Aerospace MTE: *No assets reported.*

ACA970 SANTA BARBARA INFRARED DDB-06-A-06-A-L CONTROLLER, BLACKBODY Usage Dates: 08/07/2016 - 08/17/2016

Calibration Date	Calibration Due Date	Certificate Number	Certificate Notes
12/28/2015	08/27/2017	1cd6593045eb574491d05467a2ef3ba2	TMT-NORMAL

ACJ073 LAKESHORE CRYOTRONICS INC 218 MONITOR, TEMPERATURE Usage Dates: 08/07/2016 - 08/17/2016

Calibration Date	Calibration Due Date	Certificate Number	Certificate Notes
07/31/2015	03/26/2017	346caa67907296499b92e57d607b4573	TMT-NORMAL

Technical Reports Addendum Asset Summary #2016051713083321892

Report Name: Mako Mystic Jewel May 2016

JO: 894100

First Aerospace Author / PI: Keim, Eric R

Created By: Keim, Eric R

NON Aerospace MTE: *No assets reported.*

ACA970 SANTA BARBARA INFRARED DDB-06-A-06-A-L CONTROLLER,BLACKBODY Usage Dates: 05/09/2016 - 05/15/2016

Calibration Date	Calibration Due Date	Certificate Number	Certificate Notes
12/28/2015	08/27/2017	1cd6593045eb574491d05467a2ef3ba2	TMT-NORMAL

ACJ073 LAKESHORE CRYOTRONICS INC 218 MONITOR,TEMPERATURE Usage Dates: 05/09/2016 - 05/15/2016

Calibration Date	Calibration Due Date	Certificate Number	Certificate Notes
07/31/2015	03/26/2017	346caa67907296499b92e57d607b4573	TMT-NORMAL

Technical Reports Addendum Asset Summary



TRAAS ID #: 2015043016594621892

Report Name: Terminal Frost

Aerospace Report Number:

Start Date of Test: 2015-04-20

Created By: 21892 Keim, Eric R

JO: 802300

End Date of Test: 2015-04-27

First Aerospace Author / PI: 21892 Keim, Eric R

Program:

Description: Mako sensor airborne collect

Keywords:

Asset:	Manufacturer:	Model:	Usage Start Date:	Usage End Date:	Asset Comment:
ACA970	SANTA BARBARA INFRARED	DDB-06-A-06-A-L	2015-04-20	2015-04-27	
Date:	Calibration Due Date:	Comment:	Certificate Number:		
2014-05-13	2015-10-11	TMT-NORMAL	b05fe9489b19b4891f9d7cb7a7bbdb2		
Asset:	Manufacturer:	Model:	Usage Start Date:	Usage End Date:	Asset Comment:
ACX389	LAKE SHORE CRYOTRONICS INC	218	2015-04-20	2015-04-27	
Date:	Calibration Due Date:	Comment:	Certificate Number:		
2014-08-12	2015-12-06	TMT-NORMAL	6f444fd534954846b89bc77ba4ea2b1		

*Support and Auxiliary Equipment are not calibrated.

Technical Reports Addendum Asset Summary



TRAAS ID #: 2014080813111121892

Report Name: Radiant Gray

Aerospace Report Number:

Start Date of Test: 2014-07-22

Created By: 21892 Keim, Eric R

JO: 802100

End Date of Test: 2014-07-25

First Aerospace Author / PI: 21892 Keim, Eric R

Program:

Description: Mako sensor airborne collect

Keywords:

Asset:	Manufacturer:	Model:	Usage Start Date:	Usage End Date:	Asset Comment:
ACA970	SANTA BARBARA INFRARED	DDB-06-A-06-A-L	2014-07-22	2014-07-25	
Date:	Calibration Due Date:	Comment:	Certificate Number:		
2014-05-13	2015-10-11	TMT-NORMAL	b05fe9489b19b4891f9d7cb7a7bbdb2		
Asset:	Manufacturer:	Model:	Usage Start Date:	Usage End Date:	Asset Comment:
ACX389	LAKESHORE CRYOTRONICS INC	218	2014-07-22	2014-07-25	
Date:	Calibration Due Date:	Comment:	Certificate Number:		
2013-07-03	2014-08-03	TMT-NORMAL	4d3b59c30fe1454fb11ac54e6f3036ad		

*Support and Auxiliary Equipment are not calibrated.

Technical Reports Addendum Asset Summary



TRAAS ID #: 2014030608563227598

Report Name: Open Road

Aerospace Report Number: N/A

Start Date of Test: 2013-08-25

Created By: 27598 Tratt, David M

JO: 8877-00

End Date of Test: 2013-08-30

First Aerospace Author / PI: 27598 Tratt, David M

Program: IR&D

Description: Mako sensor airborne collect executed 26-30 August, 2013.

Keywords:

Asset:	ACA970	Manufacturer:	SANTA BARBARA INFRARED RES	Model:	DDB-06-A-06-A-L	Usage Start Date:	2013-08-25	Usage End Date:	2013-08-30	Asset Comment:	Asset comprises hot and cold blackbody sources and blackbody temperature controller.
--------	--------	---------------	----------------------------	--------	-----------------	-------------------	------------	-----------------	------------	----------------	--

Date:	2013-04-26	Calibration Due Date:	2014-06-22	Comment:	TMT-NORMAL	Certificate Number:	191e3d08f8413b48826041dbe6c26185
-------	------------	-----------------------	------------	----------	------------	---------------------	----------------------------------

Asset:	ACX389	Manufacturer:	LAKESHORE CRYOTRONICS INC	Model:	218	Usage Start Date:	2013-08-25	Usage End Date:	2013-08-30	Asset Comment:	Temperature diode controller. Calibration due date: 08/03/2014.
--------	--------	---------------	---------------------------	--------	-----	-------------------	------------	-----------------	------------	----------------	---

Date:	2013-07-03	Calibration Due Date:	2014-08-03	Comment:	TMT-NORMAL	Certificate Number:	4d3b39e30fe1454b11ac54e6f3036ad
-------	------------	-----------------------	------------	----------	------------	---------------------	---------------------------------

*Support and Auxiliary Equipment are not calibrated.

Technical Reports Addendum Asset Summary



TRAAS ID #: 2012121114181127598

Report Name: Default Addendum Name 2012121114181127598

Aerospace Report Number: N/A

Start Date of Test: 2011-10-01

Created By: 27598 Tratt, David M

JO: 8877-00

End Date of Test: 2012-09-30

First Aerospace Author / PI: 27598 Tratt, David M

Program: IR&D

Description: Blackbody calibration sources and associated controller. Report references flight data acquired in 2011, at which time the calibration due date was 01/25/2012.

Keywords:

Asset: ACA970 Manufacturer: SANTA BARBARA INFRARED Model: DDB-06-A-06-A-L-25-ES-X Usage Start Date: 2011-10-01 Usage End Date: 2012-09-30 Asset Comment: Current due date is 03/24/2013.

Date:	Calibration Due Date:	Comment:	Certificate Number:
2011-07-20	2200-01-01	SAE	ACA970:1311120000
2012-01-25	2013-03-24	NORMAL	e27e1fac3c54274692bc4d57b67d3ed1

*Support and Auxillary Equipment are not calibrated.

8.6. Controlled Release

The lack of air toxics COI relevant to MATES V detected during the archival re-analysis phase of this study prompted the need to conduct controlled experiments to confirm the detectability of sample COIs before starting the airborne data acquisition phase of the study. This section and the discussion herein focuses on BTEX compounds, especially benzene, because of its health effects concerns. From the re-analysis of historical data, m-xylene was detected once (Figure 8.3(a)). Ethylbenzene was also detected (on a few occasions) in other similar aerial surveys conducted in the past using the Mako (Tratt et al, 2018), but never from refineries. This controlled release, therefore, focused on toluene and benzene because these compounds had not been observed in prior airborne surveys of the Basin.

The releases were carried out using Aerospace's portable plume generator (PPG). The PPG system uses Coriolis mass flow controllers to set the flux rate, and auxiliary instrumentation is used to record air temperature and humidity, wind speed and direction, ground and sky radiometric temperature, and solar irradiance (Westberg and Matic, 2016). The PPG is then programmed to release the selected chemical at the desired flow rate while the airborne sensor is flown overhead. Release rates were specified to be three to five times the MDQ to ensure that the emission would be detected under varying test conditions. The release altitude was 10 m AGL.

8.6.1. Toluene Test Release

The toluene releases were carried out at Aerospace's El Segundo campus on March 29, 2019. Figure 8.3 displays a detection image from one pass over the release site at 12,000 ft AGL (2-m GSD), showing a plume of toluene. The measurements at this time were used to compute the prevailing toluene MDQ of 8.7 kg/h (Table 8.1).

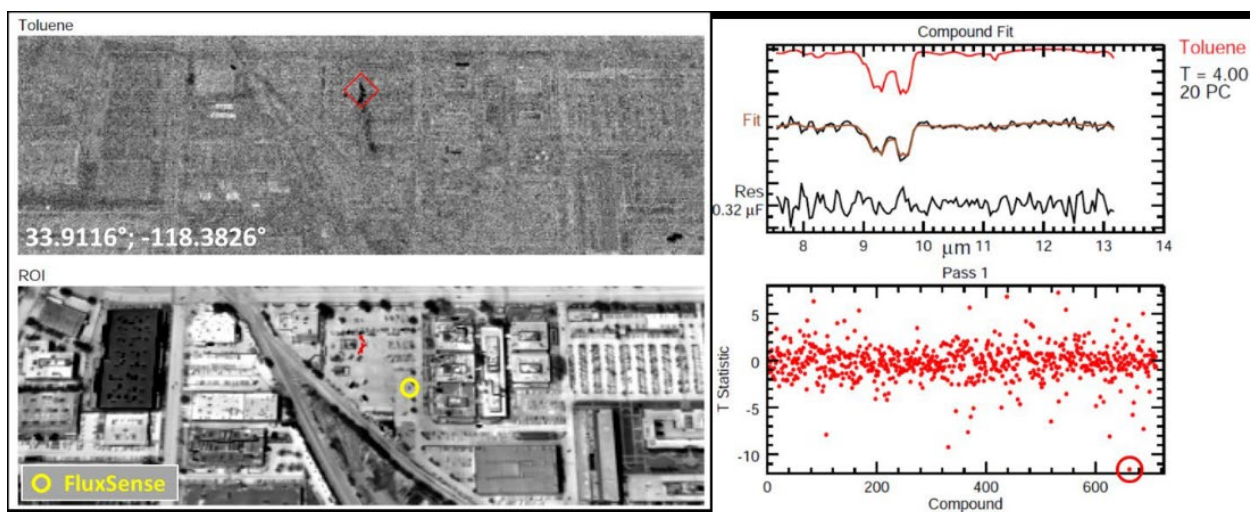


Figure 8.3. Controlled toluene release detected by Mako (acquisition date 2019-03-29).

Table 8.1. Experimental Parameters During Controlled Toluene Release

Parameter	Value
Toluene flow rate	45.3 kg/h
Air temperature, T_a	18.9 °C
Wind speed, u (average of 5.7-m and 10-m values)	3.3 m/s
Ground temperature, T_b (average of locations 1 and 2)	39.6 °C
ΔT	20.7 °C
GSD	2 m
Local MDQ (Equation 5)	8.7 kg/h
Planned release rate	5.0 x MDQ
Release rate at 21:25:18 UTC	5.2 x MDQ

8.6.2. Benzene Test Release

The benzene releases were carried out at El Mirage Dry Lake on April 2, 2019. Figure 8.4 displays a detection image from one pass over the release site at 12,000 ft AGL (2-m GSD), showing a plume of benzene. These were used to compute the prevailing benzene MDQ, which was found to be 9.2 kg/h (Table 8.2). This MDQ values for benzene under desert clutter conditions is 50% of the light industrial clutter value given in Appendix 8.2.

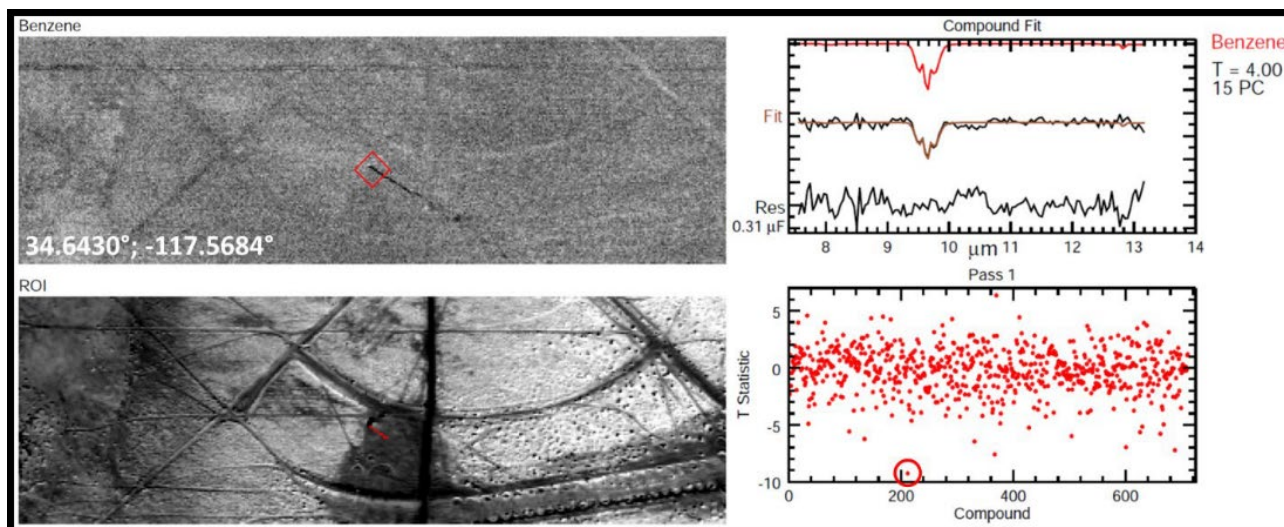


Figure 8.4. Controlled benzene release detected by Mako (acquisition date 2019-04-02).

Table 1. Experimental Parameters During Controlled Benzene Release

Parameter	Value
Benzene flow rate	30.0 kg/h
Air temperature, T_a	20.4 °C
Wind speed, u (average of 5.7-m and 10-m values)	10.8 m/s
Ground temperature, T_b (average of locations 1 and 2)	37.6 °C
ΔT	17.2 °C
GSD	2 m
Local MDQ (Equation 5)¹	9.2 kg/h
Planned release rate	4.0 x MDQ
Release rate at 20:05:36 UTC	3.3 x MDQ